DOE/MC/11076-2455
(DE88009106)

Energy

FOSSIL

ANNUAL TECHNICAL PROGRESS REPORT FOR THE PERIOD OCTOBER 1986—SEPTEMBER 1987

Work Performed Under Contract No. FC21-86MC11076

For
U. S. Department of Energy
Office of Fossil Energy
Morgantown Energy Technology Center
Laramie Project Office
Laramie, Wyoming

By
Western Research Institute
Laramie, Wyoming

DISCLAIMER

DOE/MC/11076-2455
(DE88009106)
Distribution Categories UC-109 and UC-123

WESTERN RESEARCH INSTITUTE

ANNUAL TECHNICAL PROGRESS REPORT

October 1986-September 1987

On Research Performed for the

U.S. Department of Energy

Under Cooperative Agreement No. DE-FC21-86MC11076

October 1987

TABLE OF CONTENTS

FOREWORD

This report describes the technical progress made by the Western Research Institute of the University of Wyoming Research Corporation on work performed for the U.S. Department of Energy under Cooperative Agreement number DE-FC21-86MC11076 for the period October 1, 1986, through September 30, 1987. This research involves five resource areas: oil shale, tar sand, underground coal gasification, advanced process technology, and advanced fuels research. Under the terms of the cooperative agreement, an annual project plan has been approved by DOE. The work reported herein reflects the implementation of the research in the plan and follows the structure used therein.

DISCLAIMER

Mention of specific brand names or models of equipment is for information only and does not imply endorsement by the Western Research Institute or the U.S. Department of Energy.

EXECUTIVE SUMMARY

1.0 Oil Shale

The first pair of reference oil shales have been characterized by material balance Fischer assay and related gas composition, organic carbon conversion, ^{13}C NMR on the shales and oils, heating value, oxygen by neutron activation, analyses of oil shale concentrates, the mineralogy of raw and retorted shales, and trace element distributions.

Shale oils have been produced from each reference oil shale by multiple retort runs. The oils have been demulsified and composited. Each composite has been distilled by three ASTM methods, and the viscosity, density, molecular weight, and elemental composition have been determined for the whole oils and one complete set of distillate fractions. The analytical data for the whole oils and the distillate fractions have been used to perform API correlation calculations. Field ionization mass spectra and thermal conductivities have been determined for both whole oils. Dielectric property data have been acquired for each composite oil and for the western shale. The eastern reference shale could not be cored appropriately to determine its dielectric properties.

A series of isothermal pyrolysis experiments have been conducted to study the decomposition of kerogen in the reference oil shales. Considerably more bitumen was extractable from the western oil shale residue, which indicates that bitumen formation during pyrolysis may be related to the carbon structure of the kerogen. The amount of bitumen formed also appeared to increase with increasing temperature. The rate of formation of saturates plus olefins for western oil shale appeared to fit a first-order rate equation quite well. The rate of formation of aromatics may require a more complex model.

Two retorting experiments have been conducted to determine the effect of pillars on in situ retorting production. In the base experiment, a small column of oil shale rubble was retorted. A similar rubble column and a surrounding wall of oil shale were used in the second test to simulate pillars in an in situ retort. The results showed that the amount of rubble column combusted was affected greatly by the pillar walls. Production of oil and gas from the pillars was also found to be significant.

To evaluate the potential for external fuel to improve yields from nonuniform retort beds, three experiments have been run in the 10-ton retort. Propane was mixed with the injection air in test S81. In test S82, coal dust was placed in the rubble bed using air injection before ignition. In test S83, coal fines were injected into the high permeability zone of the retort during retorting. Preliminary results indicate that test S83 was the most successful in creating a secondary combustion front and in yield.

Two radio-frequency retorting tests on oil shale have recently been completed. In the first test, a 915 MHz generator applying 1,000 watts and, subsequently, a 2,450 MHz generator applying 1,500 watts were used

on a 612-pound block of oil shale. In the second test, the 915 MHz generator was used to fracture a block of oil shale and retort adjacent rubble. Evaluation of the results has just begun.

Study of trace elements on spent oil shales from several retorting processes indicates that these elements predominantly reside in iron sulfide phases. Oxidation of reduced sulfur would thus solubilize trace elements. Results of equilibrium solubility tests suggest the presence of mineral phases for strontium, barium, fluoride, molybdenum, and arsenate. Adsorption isotherm data and saturation index values suggest that adsorption controls leachate chemistry for arsenite and selenite.

Several geochemical models have been evaluated for application to solid waste piles. However, the models lack sufficient thermodynamic data for minerals and solution complexes. Development of more reliable thermodynamic data bases is required.

Chemical analyses and toxicological studies have been conducted on groundwater samples from in and around Rio Blanco's retort 1 at lease tract C-a in Colorado. Comparison of results from samples taken in October 1986 with results of earlier sampling indicates improvement of the water quality within the retort.

2.0 Tar Sand

Tar sand deposits in the United States were evaluated as possible sources of reference tar sand for in situ and hot oil extraction research. An initial screening identified 20 deposits; however, for logistical reasons they were reduced to 9. Three of the nine, Asphalt Ridge and Sunnyside in Utah and Arroyo Grande in California, were selected as reference resources. Samples from the two Utah deposits have been obtained, and arrangements have been made for acquisition of a sample from the California deposit.

Mass balance Fischer assay analyses were performed on tar sand samples from the Asphalt Ridge and Sunnyside deposits. In general, fairly good elemental balances were obtained; however, this was only the case after the use of cryogenic grinding was instituted. Mineral carbon was only detected and measured in the sample from the Sunnyside deposit. The bitumen was removed from the sand by solvent extraction using toluene and pyridine. Numerous chemical and physical properties of the bitumen were measured, and it was concluded that the properties are similar to others that have been reported.

A study was also conducted that will lead to a better understanding of the interaction between the bitumen and the mineral matrix. A microcalorimeter was used to measure the various interactions. The strength of the interaction (bonding energy) between the bitumen and the mineral matrix was found to be very low (0.01 cal/g). It was proposed that this information should be considered during the development of surface recovery methods.

Three one-dimensional simulations of the in situ forward combustion process were conducted to evaluate its effectiveness for recovering oil

from the Sunnyside (Utah) tar sand deposit using steam-oxygen, air-oxygen or air injection. Some unexpected plugging problems were experienced in all experiments; however, the development of ignition and operation procedures that produce a sharp combustion front may eliminate the plugging problem.

Western Research Institute is developing a new pyrolysis process called ROPE© (recycle oil pyrolysis and extraction) for production of product oil that requires a minimum of upgrading to produce a finished, marketable fuel. Ten experiments were conducted using Utah tar sands from the Asphalt Ridge and Sunnyside deposits. Results obtained to date demonstrate the feasibility of the ROPE© concept. Future research to develop the process will require longer experiments in a 6-inch bench-scale unit that will allow steady-state operations and more reliable product yield evaluations.

Three one-dimensional and one three-dimensional simulations of forward combustion with steam-oxygen injection were conducted using Asphalt Ridge (Utah) tar sand. Results from these experiments indicate fuel deposition decreases while product oil yield and combustion front velocity increase as the steam-to-oxygen ratio increases. Channeling of the combustion front increases fuel consumption and oxygen demand while decreasing oil yield, but the oil quality is improved because of secondary cracking and pyrolysis of the product oil.

Research on kinetics and stoichiometry of bitumen pyrolysis has been concentrated on development of a procedure for removing highly volatile components from the tar sand bitumen before isothermal kinetic analyses. Because of difficulties with vacuum distillation of bitumen, a series of experiments were performed in which whole tar sand was heated to preselected isothermal temperatures and allowed to soak. The residual material was cooled and analyzed using a standard nonisothermal thermogravimetric method. A detailed analysis of the thermogravimetric analysis data showed that, although the light hydrocarbon material could be removed, some low-volatility material was being formed even at low temperatures. A 300°C (572°F) thermal pretreatment was selected as the best compromise for preparing samples for isothermal pyrolysis experiments.

The capabilities of the tar sand reservoir simulator (TSRS) have been extended to include two-dimensional areal sweep geometry as well as one-dimensional geometry. Several additional enhancements made to the model account for nonadiabatic boundary conditions, gravity effects, and the effect of coke laydown on bed porosity. Kinetic expressions and stoichiometry describing the pyrolysis of Asphalt Ridge bitumen have been improved based on the results from this research.

Results from preliminary numerical simulations of the Asphalt Ridge tube reactor combustion experiments showed good agreement with respect to measured temperatures, front velocities, and oil yield; however, large pressure response discrepancies were observed. These discrepancies

were eliminated by increasing the apparent viscosities of the oil phase. It remains uncertain what chemical or physical changes are responsible for this apparent decrease in oil phase mobility observed during the Asphalt Ridge tests.

A series of wet forward combustion tests were conducted in a tube reactor on Asphalt Ridge and Sunnyside tar sand. Four oil samples were collected during each of the three Asphalt Ridge tests. These represented the different stages of operation for each of the tests. The first stage was the injection of steam to confirm the presence of a communication path. The oil that was produced during this phase was improved in quality relative to the original bitumen in part because of the increase in distillate in the 204-316°C (400-600°F) boiling range. The increase in this component is the result of steam distillation. However, the majority of this oil sample was produced by the production mechanisms of thermal expansion and viscosity reduction. The next stage of the test was the injection of steam and oxygen. The three oil samples collected during this stage were also improved in quality relative to the bitumen. This improvement was due to thermal cracking of the molecules to lower-molecular-weight species.

A series of wet forward combustion tests was also planned for Sunnyside tar sand; however, plugging of the tube reactor was encountered. Consequently, the injectant was changed from steam-oxygen to nitrogen-oxygen. A partially successful test was performed only after a modified reactor heating schedule was adopted. The tube reactor was heated to 232-260°C (450-500°F) in front of the pyrolysis and combustion zones. Because of the difficulties encountered during the operation of this series of tests, a detailed discussion of the oil products was not considered appropriate. A preliminary investigation of the plugging problem was initiated. It was tentatively concluded that the problem was due to increased amounts of very viscous bitumen near the bottom of the tar sand core.

A composite of the oil produced during the wet forward combustion of a block of Asphalt Ridge tar sand was evaluated for potential end use. The oil was vacuum distilled to produce a distillate and a residue. The ambient-to-412°C (775°F) distillate was evaluated as a potential hydrogenation feedstock to produce aviation turbine fuels. The properties of the distillate were improved with respect to not only the bitumen but also the thermally produced oil. Combined gas chromatographic/mass spectrometric analysis was conducted on a neutral fraction from the distillate. It was determined that the sample is composed of predominantly tricyclic alkanes and two- and three-ring aromatics. The presence of these compound classes indicates that the distillate has potential to be a hydrogenation feedstock for the production of advanced aviation turbine fuels.

The vacuum distillation residue (+412°C [+775°F]) was evaluated as a pavement binder. The residue met all of the requirements for a lower-grade binder and all but one for a higher-grade binder. Performance prediction tests were also conducted on the residue. The thin-film accelerated aging test showed that the residue has a very low aging index, indicating it may not harden properly. However, results from the

water susceptibility test indicate that when coated on appropriate aggregates the residue performs as well as or better than some petroleum asphalts.

WRI is investigating the environmentally significant effects associated with in situ combustion of tar sand. The approach involves characterization of the raw material and each of the product streams. The resulting information can be used to identify, and subsequently mitigate, potential environmental hazards.

Three combustion tests were conducted in the tube reactor and one in the block reactor. The effluents were sampled and analyzed for selected environmentally significant substances. Elemental closure generally varied between 50 and 100%.

Laboratory experiments were conducted to assess the mineralogical changes that occur in tar sand as a result of exposure to process water. Preliminary results indicate an increase in porosity and permeability.

3.0 Underground Coal Gasification

Western Research Institute (WRI) has developed and maintains a water quality data base for the Department of Energy (DOE). It contains data from the Hanna, Hoe Creek, and Rocky Mountain 1 (RM1) underground coal gasification (UCG) sites. The accuracy of data entry and the overall quality of the data are evaluated using several programs developed by WRI. Site characteristics and the impact of UCG are determined using the data as input to site assessment programs.

A total of 30 drill and coreholes were completed and geophysically logged to characterize the Rocky Mountain 1 site and surrounding area. Evaluation of data obtained from the field program indicated that the selected site is amenable to UCG. Structural analyses indicated the coal seam dips gently to the northeast with no major structural discontinuities within the proposed module areas. Examination of core indicated little tectonic fracturing and small-scale faulting, but cleating was well formed. Stratigraphic analyses indicated a fairly homogeneous, hard, and nearly impermeable overburden section immediately above the coal.

Thirty-day batch equilibration tests were conducted on samples obtained during excavation of the Tono I UCG cavity to simulate leaching. Five different materials were represented: ash, slag, altered overburden, and two types of char. The major constituents in the leachates were calcium, magnesium, sodium, sulfate, and total dissolved solids and they were generated predominantly from char and ash. Minor constituents in the leachates included boron, ammonia, and total organic carbon and they were generated predominantly from char. These results indicated that the majority of potential groundwater contamination resulting from leaching of UCG-affected material will be derived from char and ash. Char and ash are predominantly located around the perimeter of a UCG cavity. Therefore, test operation and shutdown procedures should allow for maximum influx of groundwater through the perimeter into the main cavity area.

A laboratory simulator has been developed to study postburn UCG coal pyrolysis and groundwater contamination. To date, 30 simulation tests have been completed. The first 24 experiments were funded by the Gas Research Institute (GRI) and the last six tests were funded by DOE. The results of the contamination control research indicated that cooling of the rubble-coal char interface is needed to minimize postburn pyrolysis. This cooling is best achieved by reducing the cavity pressure to promote natural groundwater intrusion. A gradual reduction in cavity pressure from gasification to postburn venting phase is recommended to prevent coal spalling, which can cause contaminants to be deposited in the roof rock.

Two block tests were conducted to study the removal of residual contaminants from Illinois Herrin #6 coal cavities. Application of a transient diffusion model for a semi-infinite wall allowed the determination of phenolic species concentrations in the coal pores. These results agreed well with known solubilities of phenolic compounds in water. It is concluded that removal of contaminants from the cavity sidewall can be hastened by prompting water influx from the coal seam aquifer into the UCG cavity.

Groundwater at the Hanna UCG test site was affected by test operations and required restoration. The groundwater restoration project at the Hanna UCG sites consisted of cleanup of two UCG cavities. In order to complete this task, an evaporation pond and a portable carbon adsorption system were constructed. The results of the test have not been analyzed at this time.

Two million gallons of contaminated groundwater, pumped from wells adjacent to the Hoe Creek II underground coal gasification cavity, were treated and then injected into the gasification cavity. Treatment consisted of suspended solids removal and carbon adsorption, which reduced phenol concentration to below detectable limits (less than 20 parts per billion [ppb]). Phenol concentrations in the untreated water pumped from WS-10 decreased from 974 ppb when treatment began on July 2, 1987, to about 200 ppb by the time treatment ended on August 29. Phenol concentrations in groundwater pumped from well WS-22 were more erratic during the course of the tests, but they did decrease to the 150-to-200 ppb range by the time treatment was terminated.

4.0 Advanced Process Technology

Advanced exploratory research (AER) at the Western Research Institute was structured for activities that cut across multiple domestic fossil energy resources. Two task areas were investigated: (1) advanced extraction processes, and (2) advanced mitigation concepts. The research was designed to increase knowledge of exploration, extraction, and alternate fuels production to enhance the long-term availability of liquid and gaseous fuels from domestic fossil resources. The WRI AER part of the DOE APT program focus involves experiments that explore extraction and advanced instrumentation to develop concepts for exploration, recovery, and utilization.

Contaminant control and new technology activity for extraction processes have been researched. Experimental procedures are being developed in these activities as a result of many years of experience with oil, gas, and oil shale research.

The specific objective for contaminant control activity has been focused on the reduction of pyrolysis contaminant production from in situ thermal extraction processes. Physical simulation of underground coal gasification has been performed. Physical and mathematical models were developed first for UCG to study the migration and control of contaminants from in situ thermal extraction. Results of this research are being used for the Rocky Mountain 1 field study being conducted by DOE and the Gas Research Institute.

The objective of new technology research is to investigate promising new concepts to improve extraction efficiency and product quality, and to improve waste management control. Research has been designed to investigate the simultaneous operation of underground coal gasification and indirect oil shale extraction technologies. The potential for significant increases in energy efficiency, favorable economics, and environmental benefits has been investigated.

The objective of research on advanced mitigation concepts is to develop an approach to identify research needs for exploration, production, and conversion from fundamental results in the extraction of oil and gas from fossil materials. Metal complexes in oil shale, tar sand, and coal have been investigated to develop research recommendations and advance any needed concept development for utilization and environmental control. Research that applies to multiple fossil materials is being conducted to determine the source and concentration of contaminants associated with thermal extraction processes for many resources and extraction concepts. Other new procedures are being developed to identify heteroatom compounds in liquid products from advanced extraction research.

5.0 Advanced Fuels Research

Advanced fuels, also referred to as high-density fuels, are fuel mixtures composed mainly of alicyclic and aromatic hydrocarbons. These mixtures are more dense than conventional fuel mixtures which typically contain high proportions of low-density aliphatic components. Coal-derived liquids, which are highly aromatic, are viewed as a promising source of advanced fuels. Processing coal liquids to remove undesirable compounds of sulfur, nitrogen, and oxygen and to partially saturate aromatics could, in theory, yield fuels of almost any desired density and composition.

One of the largest commercial sources of coal liquids is the Great Plains Gasification Plant near Beulah, North Dakota. Gasification of lignite coal at this plant yields synthetic natural gas as the primary product, and three liquid by-products--tar oil, crude phenols, and naphtha. These by-products are produced at the nominal levels of 3,300, 900, and 750 barrels per day, respectively. Although these by-products are currently burned to produce process steam, the Department of Energy

is interested to determine if these liquids could serve as a source of more valuable products. The U.S. Air Force shares this interest, specifically regarding the production of aviation turbine fuel for nearby Minot Air Force Base.

This investigation was funded to evaluate the potential of producing military aviation turbine fuels, grades JP-4, JP-8, and JP-8X (high-density), from Great Plains by-products. Drum samples of each by-product were provided to WRI by Air Force Wright Aeronautical Laboratories (AFWAL). Analyses of the drum samples were compared with by-product analyses performed at the plant, and it was concluded that the drum samples represented typical production. Continuous hydrogenation screening experiments were then conducted on each by-product.

Initial experiments performed with whole tar oil resulted in reactor plugging because of accumulation of fine inorganic particulate matter in the top sections of the catalyst bed. To remove particulates, the tar oil was distilled to produce a -232°C (-450°F) light distillate and a 232-399°C (450-750°F) heavy distillate. Particulates were rejected in the distillation residue.

Hydrogenation of the heavy distillate reduced concentrations of nitrogen, sulfur, and oxygen to acceptable levels of less than 35 parts per million (ppm). However, none of the intermediate products were sufficiently saturated to yield an acceptable jet fuel.

The light distillate was extracted with caustic solution to remove phenols. The raffinate liquid was blended with heavy distillate to form an upgraded feedstock for further hydrogenation experiments. Hydrogenation of the raffinate-distillate blend yielded several intermediates which were suitable for fuels preparation. A specification grade JP-8 test fuel was distilled from a blend of two of these intermediates. In addition, a high-density test fuel was prepared from one intermediate that met all JP-8X specifications except the freezing point. Hydrogen consumption levels to achieve fuel-quality process intermediates exceeded 3,400 standard cubic feet per barrel (scfb).

Hydrogenation of crude phenols to levels sufficient to eliminate oxygen yielded process intermediates composed mainly of cyclohexanes and paraffins. Hydrogen consumption exceeded 4,300 scfb, and yielded low-boiling mixtures which could make a minor contribution to JP-4 production but not to production of JP-8 or JP-8X.

Hydrogenation of naphtha under mild conditions demonstrated that it could be easily desulfurized to yield a low-boiling mixture of cycloalkanes, benzene, and alkylbenzenes at a hydrogen consumption level of about 700 scfb. The products were too low boiling to contribute to jet fuel production.

It is concluded that the tar oil by-product is the only significant source of jet fuels, and that the crude phenols could make only a minor contribution to JP-4 production. However, the high level of hydrogen

consumption necessary to deoxygenate the phenols, and the unavoidable loss of hydrogen to water production makes the process uneconomical. Hydrodesulfurization of naphtha yields a product unsuited for jet fuel; however, this product might be useful as a gasoline blending component.

WESTERN RESEARCH INSTITUTE

ANNUAL TECHNICAL PROGRESS REPORT

OCTOBER 1986-SEPTEMBER 1987

OIL SHALE

1.0 OIL SHALE

TABLE OF CONTENTS

1.0 OIL SHALE

1.1 Chemical and Physical Characterization of Reference Shales

1.1.1 Chemical Characterization

Chemical measurements were made on the first pair of DOE reference shales (obtained in 1986). The western reference shale is a Mahogany zone, Parachute Creek Member, Green River Formation oil shale obtained from the Exxon Colony mine located near Parachute, Colorado. The eastern reference shale is a Clegg Creek Member, New Albany shale obtained from the Knieriem quarry, which is located approximately 16 miles south of the Ohio river at Louisville, Kentucky. Material balance Fischer assay (MBFA) results for the reference shales are reported in Table 1-1. Gas compositional data are given in Table 1-2. The conversion of organic matter to gas, oil and residue products can be determined from these data (Table 1-3). The greater conversion of organic carbon to oil for the western reference shale is clearly evident from the data in Table 1-3. The differences in conversion of organic carbon to oil, gas and residue products are related to the carbon structure of the original organic matter.

Table 1-1. Material Balance Fischer Assay Results for Reference Shales

Product Spent Shale	wt %	Gal/ton	Specific Gravity	% Ash	Mineral Carbon, wt %	C, wt %	H, wt %	N, wt %	S, wt %
Western Reference Oil Shale									
Oil	10.24	27.50	0.8927	-	-	83.2	12.2	1.7	0.7
Gas	4.60	-	-	-	-	41.4	7.0	-	4.8
Spent shale	83.50	-	-	78.63	4.9	8.8	0.2	0.5	1.1
Water	1.62	3.88	-	-	-	-	11.1	-	-
Raw shale	100.00	-	-	66.90	4.2	18.0	1.9	0.6	1.3
% Recovery	99.96	-	-	98.14	97.42	98.8	101.4	89.7	94.1
Eastern Reference Shale									
Oil	5.67	14.38	0.9448	-	-	84.5	10.6	1.2	1.6
Gas	3.16	-	-	-	-	39.5	12.4	-	40.5
Spent shale	89.54	-	-	87.12	0.22	8.7	0.4	0.9	4.5
Water	1.20	2.87	-	-	-	-	11.1	-	-
Raw shale	100.0	-	-	78.38	0.25	13.9	1.4	0.4	5.8
% Recovery	99.57	-	-	99.52	78.8	99.7	104.9	114.1	92.6

Table 1-2. Results of Material Balance Fischer Assay Gas Analyses

Component	Weight %	
	Western Shale	Eastern Shale
H_2	0.73	0.060
CO	0.166	0.057
CH_4	0.236	0.343
CO_2	2.829	0.285
C_2H_4	0.050	0.045
C_2H_6	0.148	0.213
H_2S	0.234	1.356
C_3H_6	0.082	0.067
C_3H_8	0.089	0.104
C_4+	0.693	0.630

Table 1-3. Organic Carbon Conversion in Reference Shales

Product	% Conversion	
	Western	Eastern
Oil	61.7	35.1
Gas	13.8	9.1
Residue	23.7	55.8

Solid-state ^{13}C NMR measurements were made on the reference shales, and liquid-state ^{13}C NMR measurements were made on the MBFA shale oils (Table 1-4). The carbon aromaticity values of the shales are compatible with the conversion data in Table 1-3. In addition, the shale oil aromaticity values are similar to results of previous work for similar shales (Netzel and Miknis 1982; Miknis et al. 1986).

Determinations of the amount of oxygen present were made by neutron activation analysis in triplicate for the raw western shale and both spent shales. Duplicate analyses were done for the raw eastern shale. Single samples of oils were analyzed and the values are reported in Table 1-5 for total oxygen and include contributions from organic and inorganic sources. The amount of organic oxygen for the raw and spent shales cannot be determined. However, the oxygen values for the shale oils are organic oxygen values, and these can be compared with the values obtained by subtracting the sum of the carbon, hydrogen, sulfur, and nitrogen weight percentage values in each oil (Table 1-1) from 100% (i.e., calculating oxygen by difference).

Table 1-4. Heating Values of Oil Shales and Product Oils and Molecular Weights of Shale Oils

Property	Western	Eastern
Heating Value, Btu/lb		
Raw shale	2607	2859
Spent shale	370	1587
Shale oil[a]	18650	18100
Molecular weight - shale oil[b]	295	275
Carbon aromaticity		
Raw shale	0.259	0.450
Shale oil	0.236	0.420
Proton aromaticity		
Shale oil	0.043	0.110

[a] Calculated from the Boie equation,
H_g(Btu/lb) = 151.2 (C) + 499.7 (H) + 27 (N) + 45 (S) -47.7 (O)

[b] Vapor phase osmometry in chloroform

Table 1-5. Summary of Neutron Activation Analyses for Oxygen (Wt %)

		Oxygen wt %		
	Sample	Raw Shale	Spent Shale	Shale Oil[a]
Western	1	33.9	36.9	2.30[b]
	2	35.8	37.8	2.2[c]
	3	35.9	37.4	
	Avg	35.2	37.4	
Eastern	1	33.6	36.6	1.60[b]
	2	34.3	36.9	2.10[c]
	3	--	36.5	
	Avg	34.0	36.7	

[a] Composite of the three samples
[b] Measured value
[c] Calculated difference from Table 1-1.

Kerogen concentrates were prepared using hydrochloric acid (HCl) and hydrogen fluoride (HF) following the procedures of Durand and Nicaise (1980) and Orr (1986). A concentration procedure not involving successive attack on mineral species was also attempted for purposes of comparison with orthodox procedures. In this procedure (Siskin et al. 1987), kerogen is desorbed from mineral surfaces by a hot ammonium sulfate solution while carbonates are decomposed. The desorbed kerogen is then concentrated by flotation.

Results for the debitumenized, decarbonated shales are fairly consistent. The western shales lose significant amounts of material from HCl extraction and bitumen removal. Hence, residual materials are relatively rich in organic carbon compared with the parent shale (Table 1-6). Mineral carbon is absent, which shows that the HCl procedure is effective for removing carbonate minerals. There is little acid-soluble material present in the eastern reference shale, so little enrichment of organic carbon content in the decarbonated-debitumenized shales is observed.

Table 1-6. Yields and Elemental Composition of Oil Shale Concentrates

Sample	Shale	Treatment	Yield, Wt % of Starting Shale	Mineral C, wt %	Total C, wt %	H, wt %	N, wt %	S, wt %
1	Western	Raw Shale	100	4.2	18.0	1.9	0.6	1.3
2	Eastern	Raw Shale	100	0.3	13.9	1.4	0.4	5.8
3	Western	HCl	53.02	<0.1	27.4	3.6	0.8	1.4
4	Western	HCl	53.27	<0.1	26.0	3.3	0.9	1.5
5	Eastern	HCl	89.41	<0.1	15.2	1.5	0.3	--
6	Eastern	HCl	89.89	<0.1	14.2	1.4	0.3	6.0
7	Western	HCl/HF	20.5	<0.1	64.4	8.2	2.3	3.5
8	Eastern	HCl/HF	29.6	<0.1	36.3	3.6	1.4	--
9	Eastern	HCl/HF	32.4	<0.1	43.4	4.0	1.4	19.7
Float	Western	NH_4SO_4	32.3	1.0	36.1	4.8	2.4	3.5
Sink	Western	NH_4SO_4	65.1	1.7	6.5	1.4	1.4	7.8

For the western reference shale, the yields of kerogen and pyrite correspond well with the organic carbon content and pyrite content of the original shale. The eastern shale is known to have large amounts of pyrite. Pyrite and some other minerals may have escaped exhaustive reaction with HF.

The ammonium sulfate procedure of Siskin et al. (1987) was used to obtain a kerogen concentrate of the western reference shale. This procedure yielded float and sink fractions, both of which were analyzed (Table 1-6). Both fractions probably contained some residual ammonium sulfate. The organic carbon was greatly concentrated into the float fraction by this procedure.

Gross heating values were measured for the reference shales using ASTM procedure D-3286 (Table 1-4). Measurements were made on the raw shales and the spent shales from the MBFA tests. The heating value for the western shale is slightly less than that of the eastern shale, probably because of the contribution from the endothermic carbonate decomposition of the western shale. The heating value of the spent shale is greater for the eastern shale because of the greater residue carbon on the spent shale. Heating values for the shale oils were calculated using the Boie equation (Ringen et al. 1979).

The bulk and clay mineralogies of the raw and retorted reference shales were determined by x-ray diffraction (XRD). Since this technique is qualitative rather than quantitative, peak height data provided in this report should be used as estimates of relative abundance of minerals within a given sample. Minerals present in minor amounts may be difficult to identify because of the mineralogic complexity of oil shales and the presence of one or more dominant mineral phases. In order to minimize problems related to sample complexity, slow scans were used to improve accuracy, and multiple runs were performed to increase precision.

Minerals identified in western reference shale are listed in Table 1-7. Dawsonite, Mg-siderite, and pyrite were present only in raw western reference shale, whereas augite, pyrrhotite, akermanite/gehlenite, and periclase were minerals generated during the Fischer assay. Mineralogical changes caused by retorting included decomposition of carbonates, alteration of sulfides, and formation of higher-temperature silicates and oxides. A more detailed summary of mineral reactions occurring during the retorting of oil shale is given by Mason et al. (1984).

Minerals identified in eastern reference shale are listed in Table 1-8. Pyrrhotite, augite, and akermanite/gehlenite are minerals generated as a result of increased temperatures and are present only in the spent shales. The major changes observed from retorting were decreased relative amounts of calcite, alteration of sulfides, and formation of high-temperature silicates. Silicate minerals are the dominant mineral phases in eastern reference shales. Clay mineral identification procedures showed the presence of illite, illite-smectite mixed layer clay, kaolinite, and chlorite.

Eastern reference shales are dominated by silicate minerals, especially clay minerals and quartz, while western reference shales contain both carbonate and silicate minerals in moderate abundances. However, in western reference shales, clay minerals constitute only a minor fraction of the total mineral assemblage. Clay minerals contained in the eastern reference shales are abundant and diverse in type, while

Table 1-7. Minerals Identified in Western Reference Shale by X-ray Diffraction[a]

	Quartz	Ankerite	Calcite	Dawsonite	Na-Feldspar	K-feldspar	Mg-siderite	Pyrite
Raw Western Reference Shale								
JCPDS Value[b]	26.65	30.80	29.40	15.62	27.94	27.68	32.00	33.04
Mean	NM[c]	30.76	29.48	15.62	27.96	27.61	32.11	33.00
Minimum	NM	30.76	29.48	15.61	27.94	27.58	32.10	33.01
Maximum	NM	30.77	29.50	15.64	27.97	27.65	32.14	33.10

	Quartz	Ankerite	Calcite	Na-Feldspar	K-feldspar	Augite[d]	Pyrrhotite[d]	Akermanite/ gehlenite[d]	Illite
Spent Western Reference Shale									
JCPDS	26.65	30.80	29.40	27.94	27.68	29.82	43.65	31.12/ 31.28	8.84
Mean	NM	30.76	29.51	27.96	27.62	29.91	43.52	31.22	8.83
Minimum	NM	30.74	29.49	27.95	27.55	29.84	43.39	31.17	8.66
Maximum	NM	30.77	29.52	27.87	27.67	30.00	43.66	31.27	8.93

[a] Minerals are ranked in general order of decreasing abundance
[b] Joint Committee for Powder Defraction standards
[c] Not measured
[d] Augite, akermanite/gehlenite and pyrrhotite are formed during retorting.

Table 1-8. Minerals Identified in Eastern Reference Shale by X-ray Diffraction[a]

	Quartz	Illite	Smectite	Pyrite	Na-feldspar	Kaolinite/ Chlorite	K-feldspar	Calcite
Raw Eastern Reference Shale								
JCPDS[b] Value	26.65	8.84	19.84	33.04	27.94	12.51	27.68	29.40
Mean	NM[c]	8.83	19.85	33.05	27.94	12.51	27.75	29.46
Minimum	NM	8.81	19.82	33.04	27.88	12.47	27.68	29.45
Maximum	NM	8.84	19.88	33.06	27.97	12.56	27.79	29.47

	Quartz	Illite	Pyrrhotite[d]	Augite[d]	Na-feldspar	Smectite	Kaolinite/ Chlorite	Pyrite	K-feldspar	Akermanite[d]
Spent Eastern Reference Shale										
JCPDS Value	26.65	8.84	43.65	29.82	27.94	19.84	12.51	33.04	27.513	1.12-31.28
Mean	NM	8.83	43.85	29.93	27.93	19.81	12.51	33.04	27.52	31.24
Minimum	NM	8.82	43.83	29.91	27.88	19.79	12.49	33.02	27.46	31.19
Maximum	NM	8.84	43.87	29.95	29.95	19.85	12.52	33.08	27.57	31.29

[a] Minerals ranked in general orders of decreasing abundance
[b] Joint Committee for Powder Defraction standards
[c] Not measured
[d] Augite, akermanite, and pyrrhotite are formed during retorting.

clay minerals in western reference shales are limited in abundance and type (only illite was detected). Western reference shale contained abundant ankerite (ferroan dolomite isotype), calcite, Mg-siderite, and dawsonite, while calcite was the only carbonate mineral detected in the eastern reference shale. Particle sizes for both references shale types are very small; however, only the eastern reference shale could be considered a true shale. Western reference shale should be considered a kerogenaceous marlstone.

The raw oil shales, spent shales, and shale oils generated from the MBFA were analyzed for major and minor trace elements (Table 1-9). These data reaffirm previous observations that all the elements of interest remain in the spent shale (see for example Johnson 1986). Differences in the major trace elements in the shales simply reflect their differences in mineralogy. For example, the high calcium and magnesium values of the western shale reflect its carbonate mineralogy, while high silicon and iron values for the eastern shale reflect the silicate mineralogy and high pyrite contents of these shales. The eastern shales also have greater concentrations of the minor trace elements than the western shales. It has been suggested (Leventhal and Kepferle 1981; Spiewek et al. 1981) that strategic metals could be obtained through the leaching of these elements from the spent shale in a retorting operation. A report by Miknis and Robertson (1987) provides greater detail on the results of this characterization work.

The objectives of research on kerogen decomposition are to obtain a better understanding of kerogen decomposition in relationship to kerogen structure and to ascertain the importance of soluble intermediates in the overall decomposition of kerogen. By understanding these relationships it may be possible to improve the efficiency of conversion processes or develop novel approaches for greater conversion of kerogen to oil.

Isothermal pyrolysis experiments have been conducted on the western and eastern reference oil shales in the temperature range of 375° to 440°C (707° to 824°F). The pyrolysis experiments were conducted using a fluidized sand bath reactor system developed at WRI (Conn et al. 1984). With this system, large samples of oil shale (~20 g) are used so that sufficient quantities of pyrolysis products are generated for detailed chemical analyses. Material balances for the system are 100 ± 0.1 wt % for oil shales.

The thermal decomposition of the western and eastern reference oil shales gives results analogous to those reported previously for western (Miknis et al. 1985a) and eastern (Miknis et al. 1985b) oil shales. That is, the western oil shale, having a higher aliphatic carbon fraction than the eastern oil shale, generates more oil during pyrolysis. For example, at 425°C (797°F) for a reaction time of 480 minutes, 61% of the western oil shale kerogen is converted to oil, while only 35% of the eastern oil shale kerogen is converted to oil under the same experimental conditions.

Table 1-9. Major and Minor Trace Elemental Distributions

Element	Western Reference Shale			Eastern Reference Shale		
	Raw	Spent	Oil	Raw	Spent	Oil
Major[a]						
Al	4.16	4.99		6.11	6.37	
Ca	8.87	10.20		0.86	0.91	
Fe	2.45	2.94	<1.5 ppm	6.66	6.96	<23.4 ppm
K	1.58	1.86	<400 ppm	2.91	3.04	<423 ppm
Mg	2.56	2.99		0.80	0.82	
Mn	0.03	0.04	<1.6 ppm	0.03	0.03	<1.8 ppm
P	0.14	0.18	<0.8 ppm	0.04	0.03	<84 ppm
Na	1.68	2.01		0.35	0.37	
Si	14.8	17.67		28.47	29.4	
Ti	0.16	0.19		0.38	0.39	
Ba	0.04	0.05	<1.6 ppm	0.04	0.04	<1.7
Sr	0.06	0.07	<0.4 ppm	0.09	0.09	<1.4 ppm
Minor[b]						
Be	<2.2	<1.9	<0.8	<2.2	<1.8	<0.83
Cd	0.82	0.75	<0.8	0.43	0.74	<0.83
Co	14.0	16.0	<0.8	43.4	46.1	<0.83
Cr	35.6	40.5	11.0	76.4	79.1	20.7
Cu	75.0	83.7	1.8	89.9	96.0	2.8
Li	145.0	159.0	<1.4	35.2	35.7	<1.3
Mo	21.0	23.1	<0.8	178.0	194.0	<0.84
Ni	24.8	28.2	1.8	103.0	110.0	5.0
Pb	3.5	50.0	<0.4	74.0	93.0	<0.5
V	117.0	137.0	<1.6	199.0	212.0	<1.8
Zn	84.2	103.4		127.0	147.0	

[a] All values are percentages unless shown otherwise.
[b] All values are ppm.

The amount of benzene-soluble intermediate (bitumen) differs substantially between the two types of oil shale. For all times and temperatures, more bitumen is extractable from the western oil shale residue product than from the eastern oil shale residue product. For example, at 425°C (797°F) a maximum of 49% of the kerogen in the western reference oil shale is extractable as soluble bitumen, whereas only 15% of the eastern oil shale kerogen is extractable. The fraction of kerogen that forms bitumen during pyrolysis appears to be related to the original kerogen structure, but other shales having different aromatic and aliphatic carbon structures need to be investigated to confirm this observation.

Evaluation of the pyrolysis data for the bitumen indicates that, for both shales, the maximum amount of extractable bitumen increases with increasing temperature and also shifts to shorter reaction times with increasing temperature. This observation is important because it indicates that the temperature at which the kerogen decomposition is rate-controlling is lower than previously thought. The results indicate that for western oil shale this temperature is about 390°C (734°F), instead of 482°C (900°F) deduced by Braun and Rothmann (1975) from the data of Hubbard and Robinson (1950) for Colorado oil shale. Moreover, activation energy of the kerogen decomposition appears to be greater than that for the bitumen decomposition, which is also in disagreement with previous work (Braun and Rothmann 1975).

Evaluation of molecular weight data for the produced oils indicates that the molecular weights are fairly constant at all times and temperatures. The average molecular weights of the produced oils are 260 ± 40, and 250 ± 30 for the western and eastern shale oils, respectively. Molecular weights of the bitumen vary with time at each temperature and for each shale. In all cases, the molecular weight of the bitumen reaches a maximum value and then decreases. Maximum values occur sooner at higher temperatures. The atomic hydrogen-to-carbon ratio of the oil remains constant during pyrolysis, whereas that of the bitumen decreases with time and temperature (Figure 1-1). These data, along with the molecular weight data, show that the composition of the bitumen changes during pyrolysis. Therefore, bitumen is not a suitable entity to use as a kinetic intermediate in an oil shale decomposition model. Instead, the bitumen must be considered to be composed of subcomponents that decompose to form oil, gas, and residue products.

Work is continuing to understand the nature of the oils and bitumen produced during oil shale pyrolysis. A liquid chromatographic technique is under development for analysis of these types of materials. Sequential alumina and silica gel separations are used to obtain compound class separations. For the oils, the compound classes are saturates plus olefins, aromatics, and polars.

The rate of formation of these fractions in the western reference shale oils has been fit to a first-order model using a nonlinear least-squares analysis of the separation data (Table 1-10). A better fit is obtained for the saturate plus olefin fraction than for the aromatics fraction. This indicates that the generation of the saturates plus olefins during pyrolysis of western oil shale can be modeled using a simple first-order rate equation whereas the generation of aromatics may require a more complicated model. The activation energy and frequency factors for the saturates plus olefins are very close to those obtained in a previous study (Miknis et al. 1985a) in which a variety of analytical methods and species were used to obtain the Arrhenius parameters for the thermal decomposition of a 52 gallons-per-ton (gpt) Colorado oil shale.

The bitumen from the western shale pyrolysis experiments has been separated into a hydrocarbon and a polar fraction. These fractions have been fit to a first-order model in which each fraction is considered to behave as an intermediate. Good fits to the separation data have been

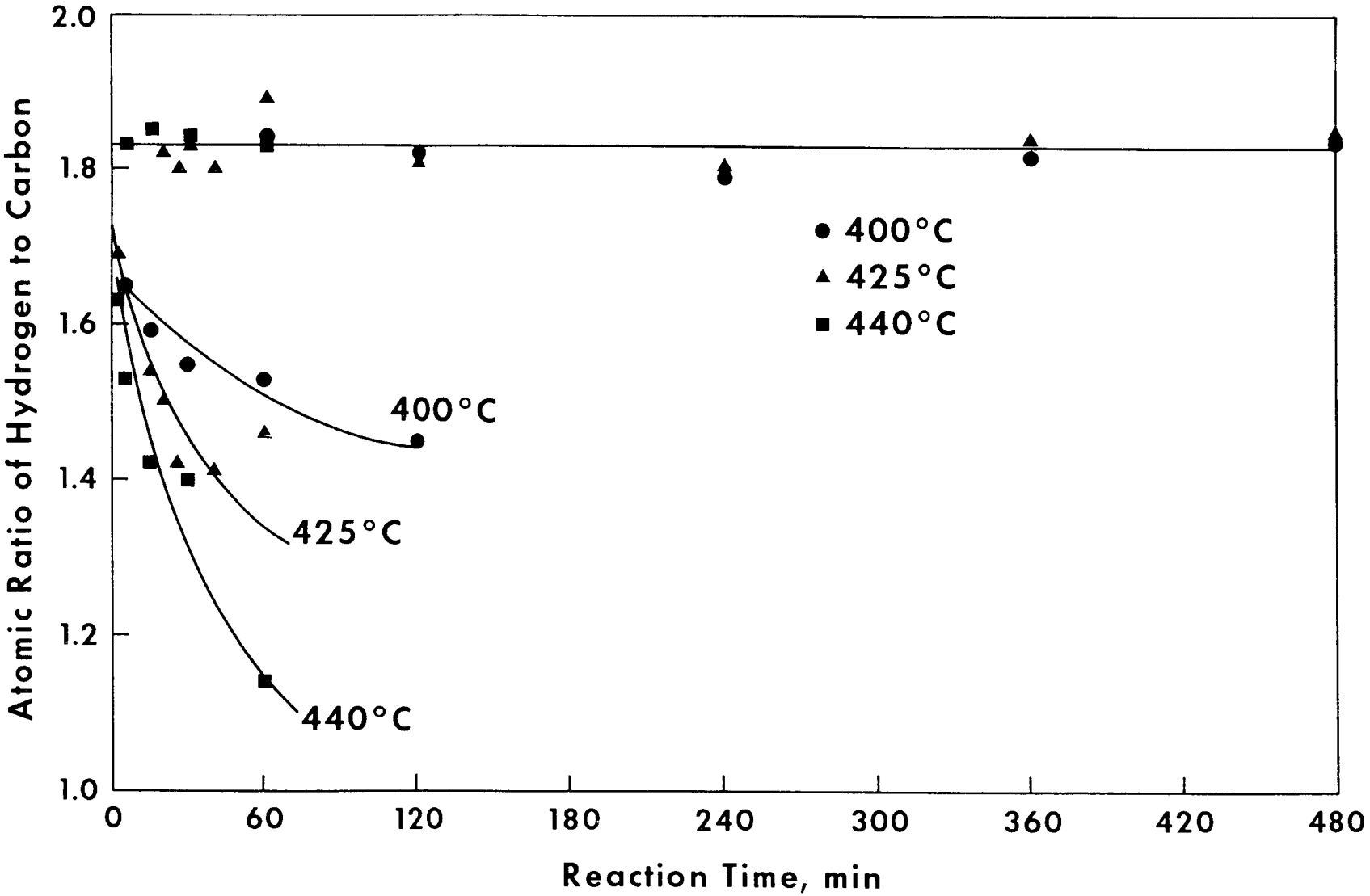

Figure 1-1. Hydrogen-to-Carbon Ratio in Oil and Bitumen vs. Time, Western Reference Oil Shale Products

Table 1-10. Kinetic Parameters for Formation of Oil Fractions

Fraction	Frequency Factor, min^{-1}	Activation Energy, kcal/mol	Index of Determination, r^2
Saturates plus olefins	$6.47 \cdot 10^{14}$	52.3	0.999
Aromatics	$2.20 \cdot 10^{17}$	59.81	0.887

obtained (Figures 1-2 and 1-3). When the curves for the polar and aromatic fractions are summed to form the total bitumen curves a good fit is also obtained between the generated bitumen curves and the experimental data (Figure 1-4). These preliminary results suggest that there is merit in studying the bitumen in greater detail.

1.1.2 Physical Characterization

One eastern and one western reference shale oil were prepared by compositing material from multiple retorting experiments in which the reference shales were used. The oils were mostly from directly fired experiments; each composite contained oil from one indirectly fired run. The retorting conditions have been described by Merriam et al. (1987). The crude emulsions were demulsified as described by Robertson (1983) and composited into a single sample of eastern oil and a single sample of western oil.

Each oil was produced in quantities such that ASTM D-86, D-1160, and D-2892 distillations could be performed as described by ASTM Annual Standards (1984). Each oil was distilled by the appropriate ASTM method.

Each whole oil and each of the TBP fractions was subjected to elemental analysis, and the viscosity and molecular weight (by vapor phase osmometry and density determination) of each fraction were determined.

A series of American Petroleum Institute (API) correlation calculations was performed using the data for the whole oils and data for the ASTM D-2892 fractions. These calculations were performed as described by Raizi and Daubert (1980), Kessler and Lee (1976), Twu (1984), Brule et al. (1982), Reid et al. (1977), and by the API Technical Data Book (1978) to acquire information for use in the ASPEN computer model. The properties that were calculated were molecular weight, critical temperature, critical pressure, critical volume, critical compressibility, Benedict-Webb-Rubin orientation parameter, Watson characterization factor, acentric factor, liquid molar volume, enthalpy, fugacity, liquid vapor pressure, solubility parameter, heat of combustion, and heat of vaporization.

The field ionization mass spectrometry (FIMS) data were acquired for each of the whole oils. Both oils are essentially 100% distillable under

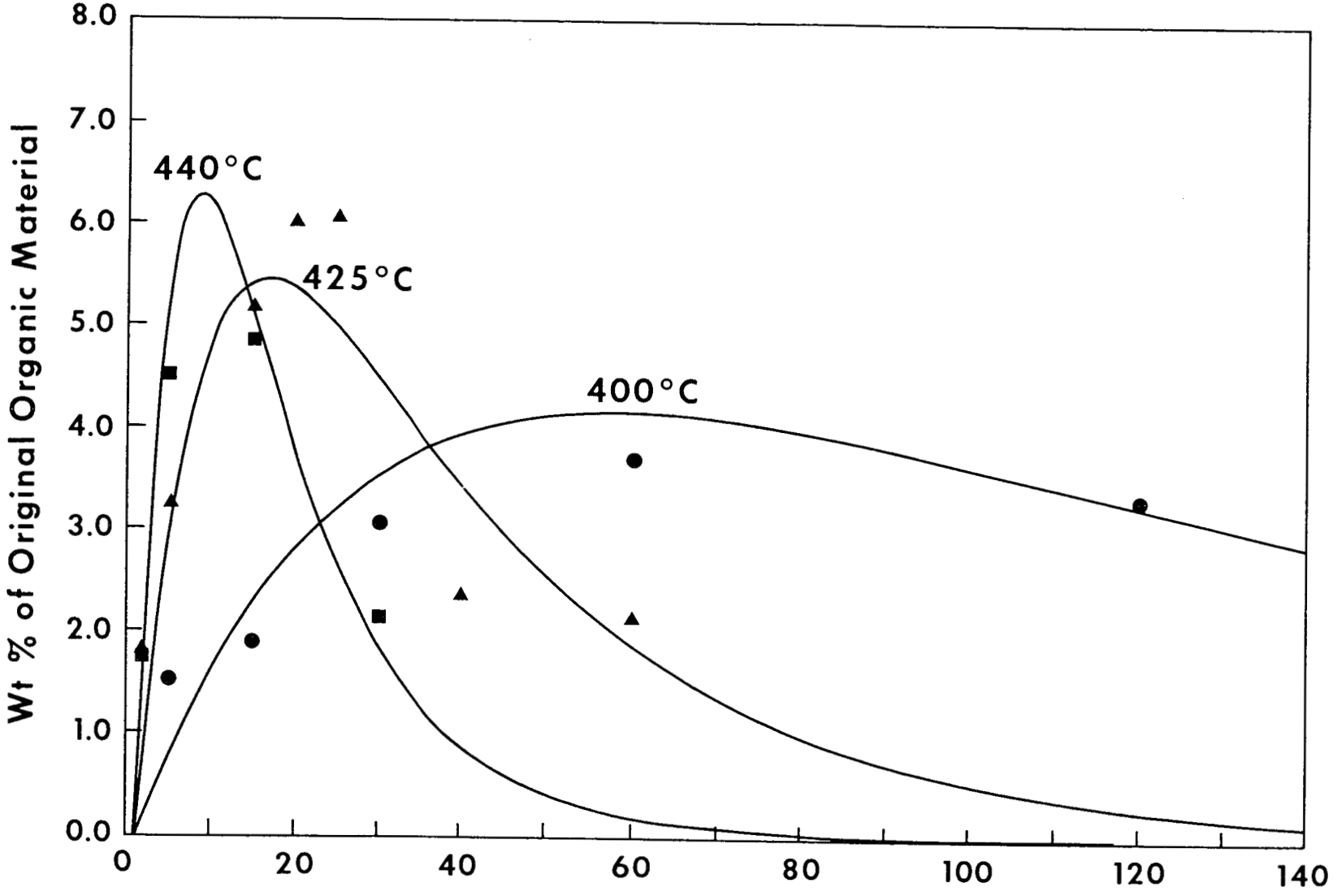

Figure 1-2. Fit of Hydrocarbon Fraction in Western Oil Shale Bitumen vs. Time

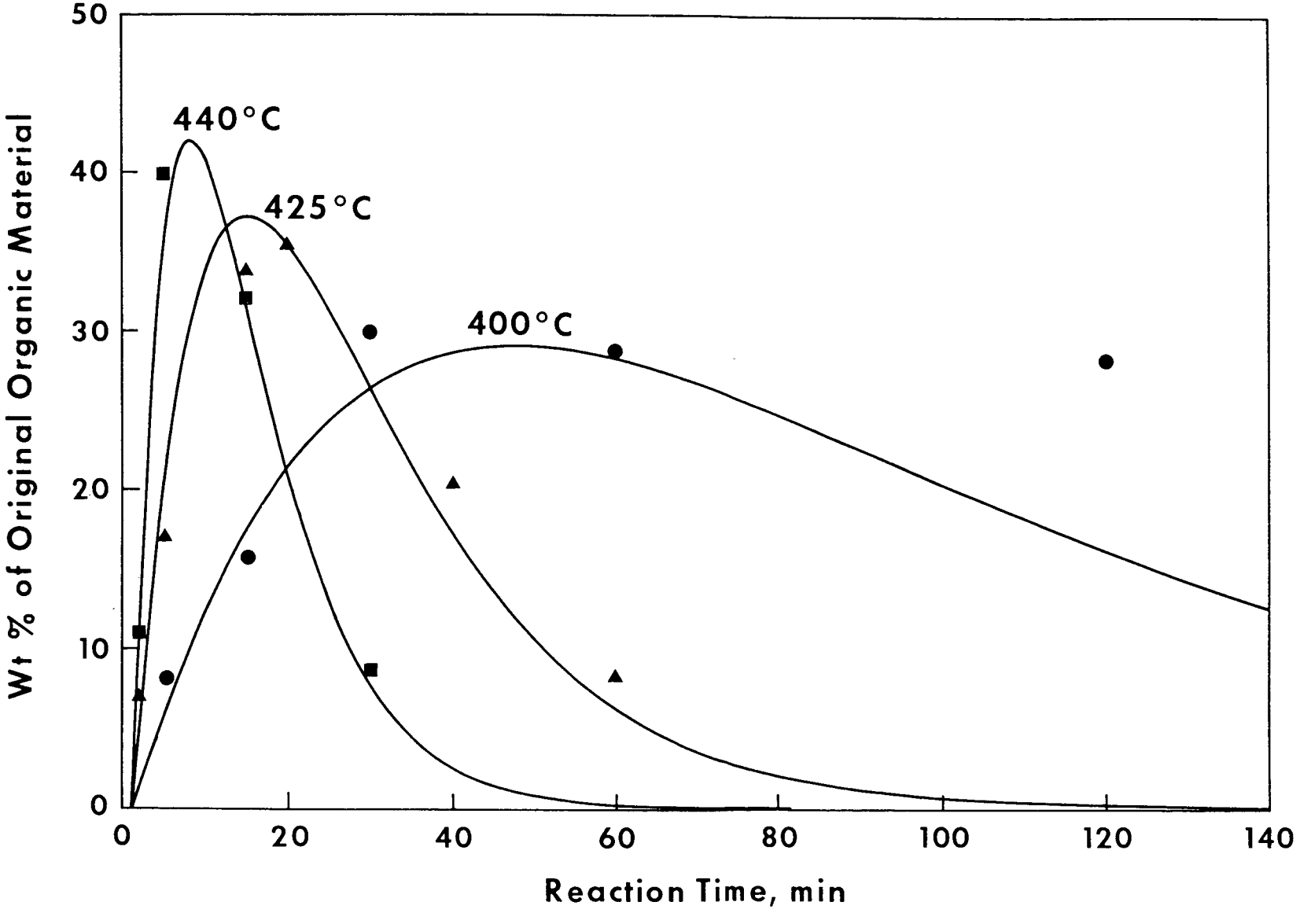

Figure 1-3. Fit of Polar Fraction in Western Oil Shale Bitumen vs. Time

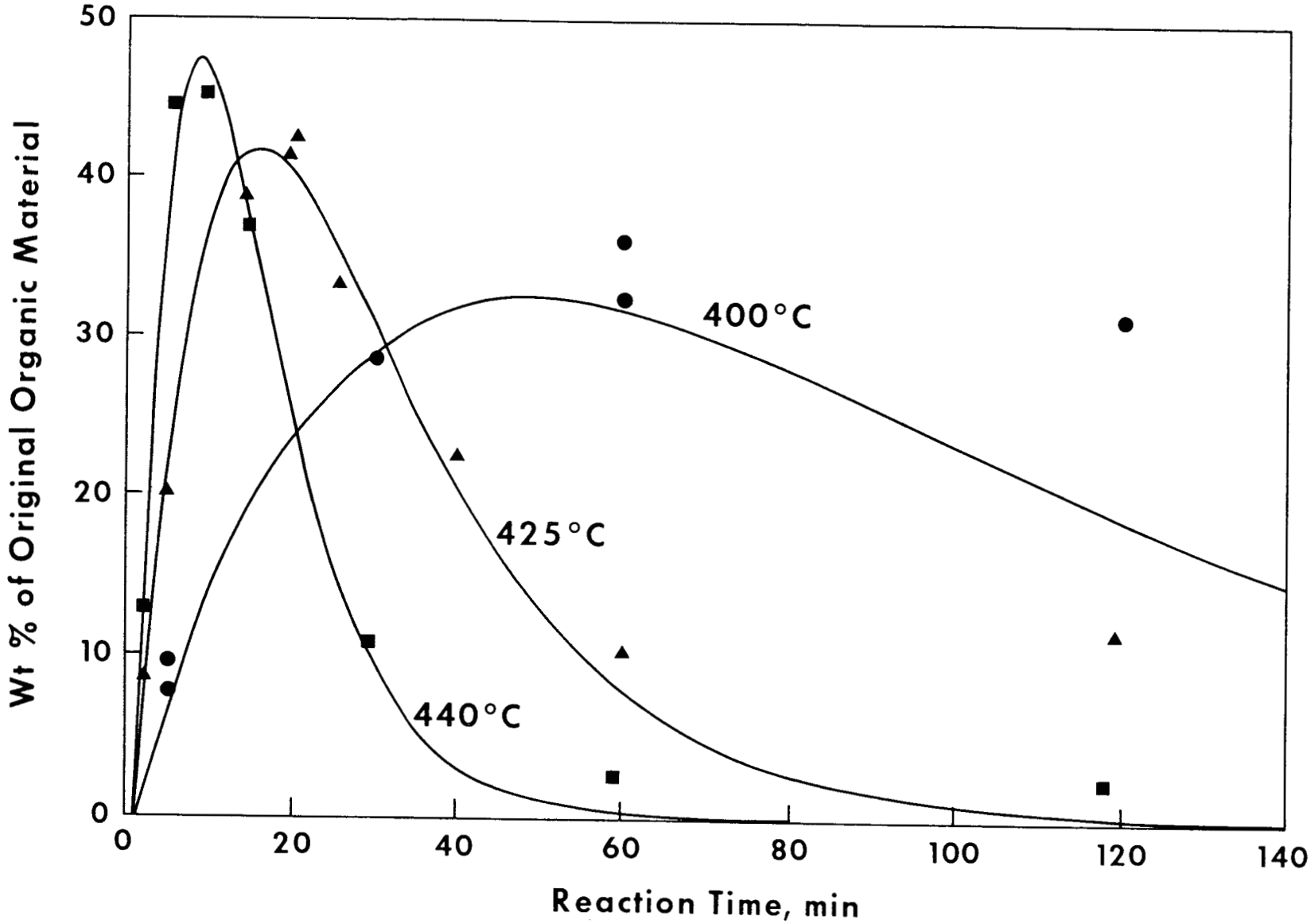

Figure 1-4. Western Oil Shale Bitumen Curves Generated from the Fits of the Polar and Hydrocarbon Fractions

FIMS conditions. Both number and weight average molecular weights were calculated for each oil. The number and weight average molecular weights were calculated to be 330 AMU and 436 AMU, respectively, for the eastern reference shale oil, and 486 AMU and 647 AMU, respectively, for the western reference oil.

The thermal conductivity of each whole oil was determined using a constant heat flux standardized to glycerine, which has a thermal conductivity of 0.20 Watts/meter-°K. The average values for eastern shale oil were 0.28 Watts/meter-°K at 25°C (77°F), 0.29 Watts/meter-°K at 50°C (122°F), and 0.32 Watts/meter-°K at 75°C (167°F). For western shale oil the values were 0.26 Watts/meter-°K at 25°C (77°F) and 0.29 Watts/meter-°K at 50°C (122°F). More detailed information and tabulations of the data are presented in a report (Miknis and Robertson 1987) on the characterization of the reference oil shales and their products.

Measurements have been made to investigate of the total enthalpy required to heat oil shale from ambient temperature, 25°C (77°F), to a selected retorting temperature of 500°C (932°F). Retorting was performed in a nitrogen atmosphere.

Recovery of energy or organic material from oil shale is inhibited as a result of the strong bond between the organic material in the shale and the shale matrix. By definition, the material readily removed by common organic solvents is the bitumen fraction and the remaining material, which is more strongly held, is the kerogen fraction. The bitumen fraction usually constitutes between 1% to 8% of the organic matrix while the remaining 90+% organic material is tightly bound kerogen. The organic elemental composition of kerogen and that of bitumen differ very little.

The enthalpy of retorting is a function of kerogen bonding, bitumen bonding, the specific heat of the inorganic phase, the specific heat of the organic phase (kerogen and bitumen), the energy to remove bound water, the energy of reaction of the organic phase, and the decomposition energy of the several minerals. A detailed discussion of heat of retorting was given recently by Camp (1987).

The results of the measurements in this study gave specific heats of spent shales of approximately 0.24 cal/g°C, as expected, while the heats of retorting of western and eastern shales were approximately 0.43 cal/g°C and 0.36 cal/g°C, respectively.

Several attempts were made to determine the energy requirement to release bound water in shale. The experiments were conducted with a differential scanning calorimeter-thermal gravimetric analyzer (DSC-TGA) instrument. The most promising experiments were several sets in which two riffled shale samples were used for each experiment. Each experiment involved heating one shale sample to a subpyrolysis temperature and then cooling it back to room temperature. Then differential DSC-TGA data were acquired using both the heated and unheated samples. This was done to determine water loss by difference. In all cases, the release of bound water occurred over a wide temperature range and was so small that it could not be measured with any reasonable degree of confidence.

1.2 Oil Shale Retorting Studies

1.2.1 Criteria Development

For in situ retorts, oil yields are usually calculated based on the the oil in place within the rubble column. Any contributions from the surrounding pillars are often ignored because no methods exist to estimate how much oil shale is retorted in the pillars or to determine what percentage of oil and gas is recovered from pillars. The contribution from the pillars thus makes the calculated yield higher than what is actually obtained from just the rubble column.

Two pillar retorting tests were conducted to determine the effect of the oil shale pillars on the vertical modified in situ (VMIS) retorting process. The specific objective of these tests was to compare oil and gas production with and without oil shale pillars.

The base experiment was conducted without pillars. Two specially modified spool pieces with a 1x1-foot inside cross-sectional area were loaded with 2-inch by 4-inch irregularly shaped Green River Formation oil shale rubble. Fine oil shale rubble (0.07 to 0.125-inch diameter) was placed along the retort walls to reduce gas flow channeling.

For the pillar test, the retort was loaded with approximately the same mass of shale rubble from the same sample as the base experiment. Two spool pieces with a 2x2-foot inside cross-sectional area were used. Six-inch-thick pillar walls were first constructed from oil shale bricks. The bricks were cemented together with a 50-50 mixture of class G cement and powdered oil shale. A 1-foot square column of the 2-inch by 4-inch shale, with fine rubble placed along the walls, was then loaded inside the pillar chimney, as in the base experiment. The oil shale grades used in these tests were 29.7 and 23.2 gpt for the shale rubble and the pillars, respectively.

The oil shale was retorted with air preheated to 427°C (800°F). The oil shale rubble was ignited at the top of the retort and retorting proceeded downward. Produced gas and liquids were removed from the bottom collector and routed to the gas cleanup system. A summary of the experimental conditions for the base experiment and the pillar test is presented in Table 1-11.

Table 1-11. Pillar Testing Experimental Conditions

	Base Test	Pillar Test
Oil shale rubble grade, gpt	29.7	29.7
Pillar grade, gpt	--	23.2
Raw shale rubble weight, lbs	374.0	340.8
Raw shale pillar weight, lbs	--	1550.0
Shale bed height, ft	4.0	4.0
Shale bed cross section, ft^2	1.0	1.0
Pillar wall thickness, ft	--	0.5
Void volume, %	32.0	39.0

The two tests were conducted under similar conditions but the results differed significantly (Table 1-12). In the base experiment, the oil shale rubble experienced retorting followed by rapid heating to temperatures of 1,038°C (1,900°F) as the combustion front moved downward, burning off the char left after retorting. As the combustion front moved downward, the shale rapidly cooled to temperatures close to the inlet air temperature. The pillar test experienced similar temperature responses for the first 20 hours. After about 20 hours the shale bed temperatures continued to peak at around 1,038°C (1,900°F) but the rapid decline in temperature stopped occurring. The combustion front was no longer burning the char left after retorting but started to burn the vapors and liquids produced from the pillars. The combustion front advancement slowed and, unlike what happened in the base experiment, the distance between the retorting zone and the combustion zone increased with time.

Table 1-12. Pillar Testing Experimental Results

	Base Case	Pillar Test
Oil yield, % of Fischer assay[a]	79.2	109.5
Average steady state air injection rate, scfm	2.1	2.0
Total air injection, lbs	266.0	463.0
Total dry gas produced, lbs	321.0	540.0
Rubble bed carbon produced, %	93.6	80.2
Pillar carbon produced, %	--	28.6
Postburn gas production, scf[b]	19.0	78.0
Postburn gas average heating value, Btu/scf[b]	3.0	538.0
Pillar wall temperature penetration rate, inch/hr[c]	--	0.2
Oxygen utilization	96.1	90.4

[a] Oil yield based on shale rubble only
[b] Nitrogen-free basis
[c] Based on 500°F (260°C) isotherm

The degree of retorting can be seen in Figure 1-5, which is the spent shale profile of the pillar test after the test was completed. In the base test, the spent shale was almost completely retorted. It was gray in color because the char was burned off. In the pillar test, less than one-half of the char was burned off when retorting of the rubble was completed. Almost none of the char had burned off of the pillar walls. However, the black region indicates that extensive retorting had occurred and the residual carbon content of the spent shale in both the rubble and pillars was greater than that after a typical Fischer assay. Outside the black area was a brown unretorted zone. If the retorting time had been longer, combustion of the char on the rubble would have occurred when pyrolysis products were no longer coming from the pillars immediately adjacent to the combustion front.

The pillar test continued to produce a significant amount of high-heating-value gas after retorting was completed (Tables 1-12 and 1-13). About four times as much postburn gas was produced from the pillar test as in the base experiment, which produced only a small amount of gas, mainly carbon dioxide. The production of high-heating-value gas after completion of retorting has been observed in field tests.

Table 1-13. Postburn Gas Analysis Comparison (Nitrogen-Free Basis)

	Base Test	Pillar Test
H_2	--	46.9
CO	1.0	7.7
CO_2	99.0	21.5
CH_4	--	13.9
C_2H_4	--	2.2
C_2H_6	--	3.1
C_3H_8	--	1.3
C_3H_6	--	1.5
$N\text{-}C_4$	--	1.8

The base experiment had an oil yield of 79.2% of Fischer assay, while the pillar test had a significantly greater oil yield, 109.5% based on the oil content of the shale rubble. The large oil yield from the pillar test demonstrates that the oil and gas recovered from the pillars should be considered in the design of in situ retorts. While it is unrealistic to expect an oil yield greater than 100% of Fischer assay in a field experiment, a pilot test could be expected to have a higher oil yield than a commercial retort because of the greater contributions from the pillars.

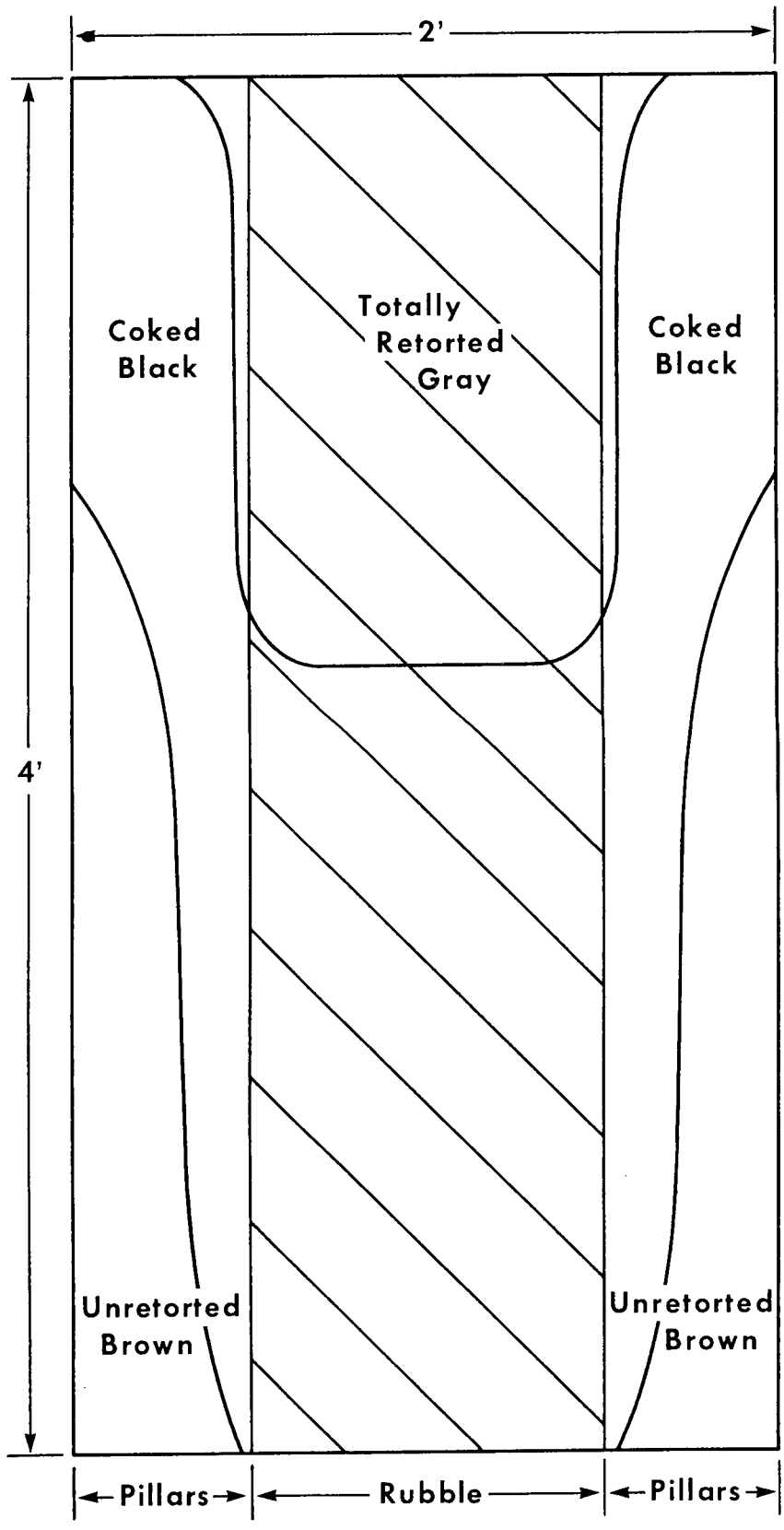

Figure 1-5. Pillar Test Spent Shale Profile

An organic carbon balance was done around the pillars to determine what became of the carbon produced from the pillars (Table 1-14). Inorganic carbon was assumed to be produced as carbon dioxide and was subtracted from the total carbon values. Fischer assay data were available for the raw and spent shale and the amount of carbon removed from the pillars was determined by difference. Estimating whether the pillar organic carbon was produced as oil or gas was done by assuming that the rubble in both the base experiment and the pillar test produced similar amounts of oil and gas for each pound of raw shale rubble that was retorted. The additional organic carbon produced as oil and gas was assumed to have come from the pillars. In this procedure the produced organic carbon was estimated within 3 pounds of the value determined by Fischer assay. It should be noted that this technique cannot distinguish between oil produced from the pillars and additional oil produced from the rubble that might have otherwise been consumed as fuel. Based on this procedure, it appears that two-thirds of the organic carbon removed from the pillars was produced as gas. The remaining organic carbon was either produced directly as oil or was combusted and replaced oil generated at the retort front that otherwise would have been consumed.

Table 1-14. Summary of Pillar Organic Carbon Balance

	Organic Carbon, lbs
Raw shale	148.2
Retorted shale	114.2
Production based on Fischer assay (difference)	33.9
Produced as oil	10.2
Produced as gas	21.1
Production based on base test recoveries	31.3

From the organic carbon balances, the organic carbon produced per pound of affected raw shale was calculated (0.0277 lb organic carbon/lb affected raw shale). The amount of additional oil production that can be attributed to the pillars could be estimated for a field test having a grade of oil shale similar to the grades used in these experiments by using the produced organic carbon factor, the split between gas and oil production, and the average affected wall thickness.

A hypothetical example of the oil yield from adjacent pillars shows that pillars make a significant contribution. The following parameters were assumed as a fairly typical set of field conditions. The retort was assumed to be 164 ft square by 250 ft high. The oil shale grade was assumed to be 25 gpt and the oil shale density assumed to be 135 lb/ft^3. The void volume was assumed to be 20%. The oil yield, including

pillar contribution for 6 ft of pillar wall, was assumed to be 70% of Fischer assay. The calculated oil in place in the rubble bed was 216,190 barrels. The oil produced was calculated to be 151,300 barrels, of which 29,500 barrels were contributed from the pillars. The yield from the rubble bed without pillar effects was then calculated to be 56% of Fischer assay. The retort dimensions and void volume are similar to those used by Occidental in three full-scale retorts. The oil shale grade and density used in the example is similar to the grades used in the laboratory and is similar to the richest oil shale tested in the Rio Blanco field tests. Oil yields of approximately 70% of Fischer assay are typically reported for both Occidental and Rio Blanco VMIS retorting tests. The average affected wall thickness chosen for the example was the same as the value reported for one of the Occidental field tests. Given these conditions and using the factors measured in the pillar tests, the actual oil yield from rubble was 56% of Fischer assay rather than 70%.

The preliminary pillar tests conducted in this study indicate that the contributions of oil and gas from the pillars adjacent to the oil shale retort could be more significant than originally believed. When designing and operating a VMIS pilot-size retort, it is important to be aware of these effects and correct the oil yield and retorting rate accordingly.

1.2.2 Process Studies

Three retorting tests have been conducted in the 10-ton retort to study the use of external fuel to improve oil yields from in situ oil shale retorts having nonuniform permeability. The tests were run using shale beds loaded to duplicate base conditions, test S78, where no external fuel was used.

The first test, S81, was conducted by injecting propane into the retorting air at the retort inlet (Table 1-15). Propane flow was limited to 90% of the lower flammable limit to avoid ignition of the propane-air mixture in the space above the shale bed. Temperatures behind the primary combustion front were high enough to slow the advance rate of the front and spread the retorting zone into part of the low permeable annulus section. Retorting was completed in 80.3 hours.

The second test, S82, was conducted by injecting 130 pounds of fine coal particles into air flowing into the retort before the retort was ignited (Table 1-16). The coal was injected before igniting the retort to avoid the possibility of ignition of the coal dust mixture in the space above the shale bed. The heating value of the coal was equivalent to only 45% of the heating value of propane burned in an earlier test, S80, where the propane was injected through a sparger at the top of the oil shale rubble (Merriam et al. 1986). It was estimated that the pressure drop from the presence of the coal particles would contribute enough resistance to gas flow to permit the use of less fuel. After the coal was loaded, the retort was opened and a layer of coal dust, visually estimated to be less than 10 pounds, was observed on top of the shale bed. A filter in the outlet pipe from the shale bed contained less than 0.1 pounds of coal dust, indicating that nearly all of the coal was contained in the oil shale bed.

Table 1-15. Summary of Test S81 Conditions

Annulus	
Nominal shale size	2x0 inch (5x0 cm)
Mean surface particle diameter	0.474 inches (1.20 cm)
Void fraction	0.392
Core	
Diameter of core	22.75 inches (57.8 cm)
Nominal shale size	4x2 B[a] inches (10x5 cm)
Mean surface particle diameter	1.39 inches (3.53 cm)
Void fraction	0.506
Permeability ratio	0.035
Annual cross section, fraction of retort	0.829
Flows	
Air, scf/ft^2-min.	0.88
Sm^3/m^2-min.	0.268
Propane, scf/ft^2-min.	0.017
Sm^3/m^2-min.	0.00518

[a] B is used to distinguish this 4x2 shale from another 4x2 shale having a different particle-size distribution.

Table 1-16. Summary of Test S82 Conditions

Annulus	
Nominal shale size	2x0 in. (5x0 cm)
Mean surface particle diameter	0.474 in. (1.20 cm)
Void fraction	0.377
Core	
Diameter of core	22.75 in. (57.8 cm)
Nominal shale size	4x2 B[a] in. (10x5 cm)
Mean surface particle diameter	1.39 in. (3.53 cm)
Void fraction	0.516
Permeability ratio	0.027
Annulus cross section, fraction of retort	0.829
Flow	
Air, scf/ft^2- min.	0.88
Sm^3/m^2- min.	0.268

[a] B is used to distinguish this 4x2 shale from another 4x2 shale having a different particle-size distribution.

After the coal was injected, the top layer of shale was loaded and the shale bed was ignited. Rapid retorting occurred in 54.3 hours with a sweep efficiency of only 53%, indicating the test did not have the increased oil yield that was anticipated. When the spent shale was going to be discharged, the production piping was found to contain a large amount of oil-saturated coal dust, indicating that some of the coal dust had been blown through the shale bed and had not been combusted.

The third test, S83, was conducted by injecting coal fines into the top of the high permeability zone during retorting (Table 1-17). Preliminary analysis indicates this test was the most successful of the tests using external fuel to create a secondary combustion front to improve oil yields. The test ran for 126 hours, which was the longest of the series. The preliminary oil yield was estimated to be 45% of Fischer assay, the highest yield of the series. A summary of the 10-ton test results and net energy ratios are presented in Tables 1-18 and 1-19.

Table 1-17. Summary of Test S83 Conditions

Annulus	
Nominal shale size	2x0 in. (5x0 cm)
Mean surface particle diameter	0.474 in. (1.20 cm)
Void fraction	0.381
Core	
Diameter of core	22.75 in. (57.8 cm)
Nominal shale size	4x2 B[a] in. (10x5 cm)
Mean surface particle diameter	1.39 in. (3.53 cm)
Void fraction	0.497
Permeability ratio	0.035
Annulus cross section, fraction of retort	0.829
Flows	
Air, scf/ft^2 - min	0.88
Sm^3/m^2 - min	0.268
Coal, lbs/hr	2.19
kg/hr	0.99

[a] B is used to distinguish this 4x2 shale from another 4x2 shale having a different particle-size distribution.

Table 1-18. Results of Tests on the Use of External Fuel

Parameter	Test				
	S78	S80	S81	S82	S83
Permeability ratio	0.019	0.027	0.035	0.027	0.035
External fuel	None	Propane	Propane	Coal	Coal
Fuel injection point	--	Core	Inlet	Inlet	Core
Retorting time, hours	41.0	99.5	80.3	54.3	126.0
Sweep efficiency, %	50	80	72	53	72
Yield, % of Fischer assay	16.5	32.2	24.9	19.5	45

Table 1-19. Heating Values and Net Energy Ratios for Test Series

Heating Value[a] and Energy Ratio	Test			
	S80	S81	S82	S83
Fuel	3.1	1.9	1.4	2.9
Incremental oil production	4.4	2.4	0.9	8.1
Incremental gas production	3.8	4.2	0.6	1.9
Total incremental production	8.2	6.6	1.5	10.0
Net energy ratio	2.6	3.5	1.1	3.4

[a] All values are million Btu's gross heating value.

The first in situ radio-frequency (RF) retorting test was conducted using a monopole configuration in a 612-pound block of oil shale. The block was encased in an array of electrical heaters to preheat the shale block so heat loss would be reduced during retorting. After preheating the outside of the block, RF heating was initiated with a frequency of 915 MHz at a capacity of 1,000 watts. Temperatures of 260 to 371°C (500 to 700°F) were observed in the block, with the highest temperatures closest to the monopole.

At 80 hours into the test the electrical heaters around the shale block failed and temperatures began to fall. Heat losses from the block exceeded the amount of heat supplied by the 1,000 watts from the RF system. Once it became apparent that the block could not be retorted using the 915 MHz generator, it was disconnected and a 2,450 MHz

generator delivering 1,500 watts was installed. The higher-frequency energy concentrated heating in a small part of the block around the monopole. At 102 hours into the test, temperatures in the shale varied from 271 to 666°C (520 to 1,230°F). Unfortunately, at that time a bolt of lightning caused the RF generator to shut down. When the generator was restarted, dielectric breakdown was observed and the power was reduced to 250 watts. This caused temperatures near the monopole to begin decreasing, so the test was terminated.

Inspection of the shale block revealed the block had been fractured and the monopole had melted off about 2 inches below the surface. The inside of the reactor was coated with a film of oil and 1.5 pounds of dry oil was collected from the recovery system.

The first phase of the second in situ RF test was conducted using the 915 MHz generator at 1,000 watts of forward power to fracture a 24x19x18-inch block of shale at 93 to 149°C (200 to 300°F). Then the second phase of the test was completed, the retorting of shale rubble adjacent to the block to simulate the effects of fractured pillar retorting. Results of the RF tests are being evaluated.

1.3 Environmental Base Studies for Oil Shale

1.3.1 Solid Waste Studies

Three combusted Paraho-retorted western reference oil shales, one indirectly retorted and two directly, were subjected to detailed physical, chemical, and mineralogical characterizations. Standard methods were used to determine total elemental content (including nitrogen, hydrogen, total carbon, inorganic carbon, and organic carbon), calcium carbonate equivalent, specific surface area, cation exchange capacity, clay mineralogy, exchangeable cations, and soluble cations and anions.

With the exception of carbon content, the elemental composition of the spent oil shales was similar. The indirectly retorted oil shale had significantly higher concentrations of total, organic, and inorganic carbon than the directly retorted and combusted oil shales. The alkalinity of the spent oil shale solids, expressed on a percentage of calcium carbonate equivalent basis, ranged from approximately 31% in one of the directly retorted samples to 42% in the remaining spent oil shale samples. The properties of the spent oil shale solids that influence the mobility of elements in a leaching environment (i.e., specific surface area and cation exchange capacity) were greatly influenced by the retorting process. The combusted oil shale had the greatest specific surface area and cation exchange capacity, followed by the indirectly and directly retorted oil shale samples, respectively. Exchange cation content varied with spent oil shale type in a manner similar to that observed for cation exchange capacity. The sum of the exchangeable cations (a measure of the cation exchange capacity) was significantly higher than the measured cation exchange capacities. Spent oil shale saturation extracts were highly saline, sodic, and alkaline. The indirectly retorted and combusted oil shale extracts were observed to have higher alkalinity, salinity, and sodicity than the two

directly retorted oil shale extracts. However, the directly retorted oil shale extracts were elevated in calcium and sulfate concentrations.

Spent oil shale mineralogy was determined by x-ray diffraction following the nondestructive preconcentration of mineral phases into density separates. The indirect characterization of trace and minor mineralogical and solid-phase residencies was performed through an analysis of the partitioning of elements into the density separates. Further, a selective sequential dissolution analysis was performed to partition trace and minor elements first into carbonate and exchangeable elements, then organic and manganese oxide, then iron oxide, and finally into residual combusted oil shale fractions.

The major mineralogy of the spent oil shales was consistent with predictions based upon process temperature. Float-sink density fractionation was effective in preconcentrating mineral phases into distinct density separates. Linear density gradient fractionation of the float-sink separates in general did not result in the identification of any additional minor mineral phases. However, polymorphs of the major mineral phases were detected.

Elemental partitioning of elements into the float-sink density separates provided indirect evidence of minor and trace element mineralogical residencies. Strontium and barium were associated with calcium and magnesium minerals, such as carbonates. Manganese and vanadium were associated with magnesium minerals, such as oxides, carbonates, and silicates. A majority of the trace elements were associated with the iron-bearing minerals--magnetite, hematite, and pyrrhotite. Chromium, cobalt, copper, molybdenum, and nickel distributions in the spent oil shale float-sink density separates matched that of iron. Elements also associated with iron, but observed to have additional solid-phase mineral associations, included vanadium (magnesium minerals), lithium (feldspars), lead (feldspars, carbonates), and zinc (carbonates). Selective dissolution of mineral phases from the combusted oil shale indicated the following trace and minor element mineralogical residencies:

strontium:	carbonates
barium:	carbonates, organic, silicates, and aluminosilicates
manganese:	carbonates, iron sulfides
vanadium:	iron sulfides and oxides
chromium, cobalt, molybdenum, and nickel:	iron sulfides and oxides
copper:	iron sulfides and oxides, carbonates
zinc:	iron sulfides, carbonates
lead:	iron sulfides, carbonates, iron oxides.

The influence of spent oil shale solids on leachate chemistry was examined in a batch equilibrium solubility study. Soluble elemental concentrations, pH, and redox potentials were used as input to a geochemical model to predict the speciation of strontium, barium, fluoride, and molybdenum in the spent oil shale leachates. Geochemical

model predictions were also used to indirectly identify solid phases controlling solution concentrations of strontium, barium, fluoride, molybdenum, and arsenate.

The concentrations of elements, pH, and redox potential of aqueous extracts was influenced by spent oil shale type. Leachates were dominated by sodium, potassium, sulfate, reduced sulfur species, and alkaline conditions. Silver, arsenic, beryllium, cadmium, cobalt, chromium, copper, magnesium, manganese, nickel, lead, antimony, selenium, and zinc were below detectable concentrations in the spent oil shale leachates. The speciation of strontium and barium in the leachates was dependent on spent oil shale type. However, fluoride and molybdate speciation was not influenced by spent oil shale type. All spent oil shale leachates were saturated with respect to strontianite, suggesting the presence of this mineral in the spent oil shales. Further, strontium phosphate was predicted in directly retorted oil shale. Extracts were supersaturated with respect to barite and undersaturated with respect to witherite. Calcium fluoride (fluorite) was predicted in all but the indirectly retorted oil shale. Powellite was predicted to control molybdenum concentrations in directly retorted oil shale samples. However, solutions from the remaining spent oil shale samples were undersaturated with respect to powellite. Evidence for magnesium and barium arsenates in spent oil shales was also presented.

The processes controlling the spent oil shale leachate concentrations of arsenic were examined. The equilibrium solubility product constant for barium arsenate was determined at three different ionic strengths, with equilibrium approached from both undersaturation and supersaturation initial conditions. The adsorption-desorption behavior of arsenate, as well as selenite, was examined with a batch adsorption isotherm technique. The adsorption isotherm data were quantitatively characterized by the Freundlich, Langmuir, and partitioning equations.

The equilibrium solubility product constant (pKsp) of $Ba_3(AsO_4)_2(c)$ was determined to be 21.62. This value is significantly different from the currently accepted value of 50.87. Data from a previous barium arsenate solubility study (Chukhlantsev 1956) were reexamined to yield a pKsp value of 24.64 for $BaHAsO_4 \cdot H_2O(c)$.

Adsorption isotherms indicated that the combusted oil shale had the highest affinity for arsenate and selenite when total metal concentrations in the equilibrium solutions were examined. Using activities to calculate adsorption isotherm parameters helped determine the affinity of combusted oil shale for arsenate. However, one of the directly retorted oil shales had the greater affinity for selenite on an activity basis. The shape of the adsorption isotherms suggested arsenic concentrations to be controlled by adsorption processes. However, saturation index value calculations predicted directly retorted oil shale adsorption solutions to be saturated with respect to calcium and barium arsenates. Selenite concentrations were controlled by adsorption processes, irrespective of spent oil shale type. Dilution of the adsorption isotherm equilibrium systems (desorption study) resulted in an increase in arsenate and selenite adsorption. Weathering reactions,

brought about by hydration and recarbonation during the adsorption and desorption experiments, probably resulted in new mineral surfaces being created for arsenate and selenite adsorption.

The results of this study bring to light a number of spent oil shale properties important in waste management. Trace elements were predicted to reside predominantly in iron sulfide phases. Thus, oxidation of the reduced sulfur would solubilize trace elements. Equilibrium solubility results suggested mineral phases for strontium, barium, fluoride, molybdenum, and arsenate. These data suggest the relevance of geochemical modeling in predicting long-term spent oil shale leachate chemistry. Processes controlling the aqueous concentrations of arsenate were defined. Adsorption isotherm data, as well as saturation index values, suggested adsorption controls on arsenite and selenite. However, because of inaccuracies in arsenate thermodynamic parameters (noted specifically for barium arsenate), precipitation versus adsorption controls on arsenate leachate concentrations are still questionable.

The arsenate and selenite desorption isotherm data, along with data from previous spent oil shale studies, bring into question the relevance of basic chemical, physical, and mineralogical information obtained on spent oil shale unaffected by environmental influences. Hydration and recarbonation of retorted oil shale has been found to influence the mineralogical residencies of trace and major elements significantly. Desorption isotherm results further illustrate the dynamic nature of spent oil shales in the presence of water.

Geochemical models appear to be applicable to the prediction of long-term behavior of elements in spent oil shale disposal environments. This approach is particularly applicable because a majority of the trace and minor elements in spent oil shales reside in mineral phases. The dissolution of these phases and the precipitation of more stable mineral phases likely to occur during hydration, recarbonation, and oxidation may be predicted using geochemical models. However, for this approach to be applicable, model predictions will need to be compared with direct experimental observations.

Several experiments on the adsorption of model organic compounds onto mineral substrates were completed. The organic compounds, chosen to be representative of the compounds found in oil shale leachates, included benzoic acid, benzoate ion, and pyridinium compounds. Dimethyl methylphosphonate (DMMP) was also included for reference, because its behavior is well known. The mineral substrates included montmorillonite clay and hematite, both found to be constituents in the oil shale mineral complex. Fourier transform infrared (FTIR) spectra of the organo-mineral complexes were analyzed to determine the sorption mechanism. The spectra were compared against known literature values.

To determine the strength of these interactions, aqueous high-performance liquid chromatographic mineral columns were produced. The organic compounds were passed through the column and the retention values and behavior of the organic compounds were evaluated. This experimental system has proven to be difficult to work with. The only

unambiguous results were found with DMMP and pyridine. FTIR spectra of the column substrate were recorded to determine if an interaction was taking place in this dynamic system as well as in the nondynamic FTIR analytical system.

Several geochemical codes are available in the literature to model chemical processes such as oxidation-reduction, precipitation-dissolution, formation of solution complexes, adsorption, and ion exchange. However, these models differ as to the types of environments to which they are to be applied. Following the careful preliminary code assessment, EQ3/6, GEOCHEM, MINTEQ, PHREEQE, SOLMNEQ, and WATEQFC geochemical models were selected for further evaluation. An evaluation of these codes suggested that the above models lacked thermodynamic data for minerals and solution complexes, which are important for oil shale solid waste. Further study indicated that selection of any one of the above models would require development of a more reliable thermodynamic data base. So far, critical evaluation of thermodynamic data has been completed for strontium, fluorine, molybdenum, and selenium.

The chemical species of an element in many cases greatly influences both environmental transport and impact. Modeling of either process can be successful only if accurate data on chemical species are available for the input. General approaches have been reviewed to determine chemical species for ionic materials and a feasible approach has been outlined to the analytical speciation of chromium (III) and (VI), and iron (II) and (III) in aqueous solution. The results have been related to existing models through redox electrode potential measurements. An ion chromatographic technique has been selected for the speciation based on separation of anionic species. Detection limits projected into the low parts per billion range have been obtained.

All species were detectable photometrically after derivatization, but only the chromium (VI) anion was readily detectable by nonsuppressed conductivity detection. The separation mechanism in the system used with conductivity detection appeared to involve hydrophobic interaction because the chromic-pyridinedicarboxylic acid complex anion was eluted from the resin-based anion exchange column long after the chromate anion. A second system, using only nonmetallic components, included a column fabricated with both anion and cation exchange sites and separated the chromium and iron complex species based largely on their anionic properties.

The applicability of the ion chromatographic methodology to iron speciation in solutions near neutral or of moderate acidity or alkalinity, as might be encountered in many environments, is much the same for chromium (III) and iron (III). Detection of chromium (III) in natural waters in equilibrium with mineral phases may be possible with sensitivity enhancements as described. However, detection of iron (III) under such circumstances would probably not be possible.

The results of the present work suggest a technique for the quantitative characterization of certain elemental species in an aqueous phase. The significance of the results with respect to geochemical modeling will depend upon the application of the methodology in a variety of geochemical environments.

Although not all direct equilibrium measurements are within reach, it is expected indirect methodologies may be devised in many cases. Observed or predicted sensitivities (below 0.1 micromolar) should be useful in further probing the relationship of measured redox potential to the electron activity and in characterization of potentially hazardous waste materials. In addition to chromium and iron, species of importance to the understanding of oil shale leachate composition and contaminant transport include those of sulfur, selenium, arsenic, vanadium, silicon, aluminum, calcium, and magnesium.

A remote sensing effort has begun to develop a state-of-the-art instrument designed to perform in situ groundwater analysis of organic pollutants with one or more methods of enhanced Raman spectroscopy. In conjunction with this effort, a working optical fiber bundle has been designed and built. This has been coupled to a preliminary Raman spectrometer. Using this instrument and a long-path Raman cell (LPRC), also known as a McCreery cell, phenol can be detected at low parts-per-million levels. A state-of-the-art instrument consisting of gated electronic detection, a computer-controlled tuneable pulsed Nd:YAG-dye laser system, and standardized LPRC is being assembled. This instrument will have the capability of determining the most effective method of remote in situ optical fiber-based environmental analysis. Methods to be investigated include Raman scattering at wavelengths away from fluorescence bands, resonance Raman spectroscopy for the determination of organic mixture components without prior separation, surface-enhanced Raman spectroscopy, and surface-enhanced resonance Raman spectroscopy. Uses for this technology include in situ groundwater analysis for organic pollutants, topological tracking of contaminant plumes, including contaminant degradation, and direct in situ microbial transformation of organic contaminants. The system may also be used for analysis of gases at short range.

1.3.2 Retort Abandonment Studies

An analysis was made of baseline groundwater quality data for Rio Blanco lease tract C-a in Colorado. Because the data are limited, all conclusions must be qualified. In general, the baseline quality of the water was poor relative to Colorado water quality standards. Furthermore, some of the parameters varied considerably from one region of the site to another. A report with a more extensive description of the analysis is being prepared.

Earlier chromatographic research on organic constituents in groundwater near tract C-a indicated that the more hydrophilic organic species tend to disappear with time after retorting, whereas the more organophilic species tend to persist at retort 1. A comparison of groundwater samples from the site confirm this phenomenon. The profiles of waters taken from the retort during 1985 and 1986 show decreases in overall concentrations of organophilics, although the composition of the organophilics indicates little change.

Waters that showed no organophilic species were screened for hydrophilic species through electron capture detection with gas chromatography after labeling. No hydrophilic species were detected in the freeze-dried concentrates from these waters.

Toxicological studies were continued on groundwater samples collected from the site. The primary objectives of the research were to detect the migration of contaminants away from retort 1 and to evaluate the effectiveness of two major pumpdowns of the retort. A map indicating the location of the sampling wells relative to the retort is shown in Figure 1-6. Toxicity tests and chemical analyses were performed on samples collected in October 1986, four months after the second pumpdown.

Chemical analyses of the October 1986 samples indicated that the quality of water at all levels within the retort was generally consistent (Table 1-20). Outside the retort higher levels were consistently observed for total carbon, mineral carbon, alkalinity, magnesium, and bicarbonate; inside the retort higher levels were consistently observed for fluoride, potassium, sulfate, and boron.

The quality of groundwater within the retort improved after each pumpdown operation. The average pH, conductivity, total dissolved solids, and chloride concentrations inside the retort in October 1986 were very similar to the average values outside the retort. However, calcium, sodium, potassium, and sulfate concentrations were higher inside the retort, whereas alkalinity, hardness, magnesium, and bicarbonate were lower inside the retort.

The Microtox™ assay was sensitive to the organic constituents in groundwater collected from the bottom of the retort, but it was not sensitive to the very low concentrations of organic constituents at other levels of the retort or in groundwater outside the retort (Table 1-21).

Groundwater collected outside the retort in October 1986 was more acutely toxic to Ceriodaphnia than groundwater collected inside the retort. Indeed, the groundwater outside the retort was more toxic to Ceriodaphnia in October 1986 than it had been in 1985 or in May 1986.

Inasmuch as the results of the chemical analyses could not be correlated with the results of the Ceriodaphnia toxicity tests, the Ceriodaphnia acute and chronic toxicity tests performed during this study were not effective for detecting the migration of contaminants away from retort 1 or for evaluating the effectiveness of the major pumpdown of retort 1.

Microorganisms present in the native environment near the retort were isolated and identified. Microorganisms identified in the soil were Micrococcus, Flavobacterium, Chromobacterium, Acinetobacter, Corynebacterium, and four colonies of fungi. Many of these isolates were able to survive in the presence or absence of oxygen, and they degraded 2,3,5-trimethylphenol and 2,3,6-trimethylphenol at concentrations of 100 parts per billion of each compound. During a 68-hour retention time, essentially 100% of the organic constituents were removed by passing water through a soil column containing the microorganisms. Tests on a sterilized control soil column, used to determine removal by absorption, were inconclusive because the control column became contaminated with microorganisms.

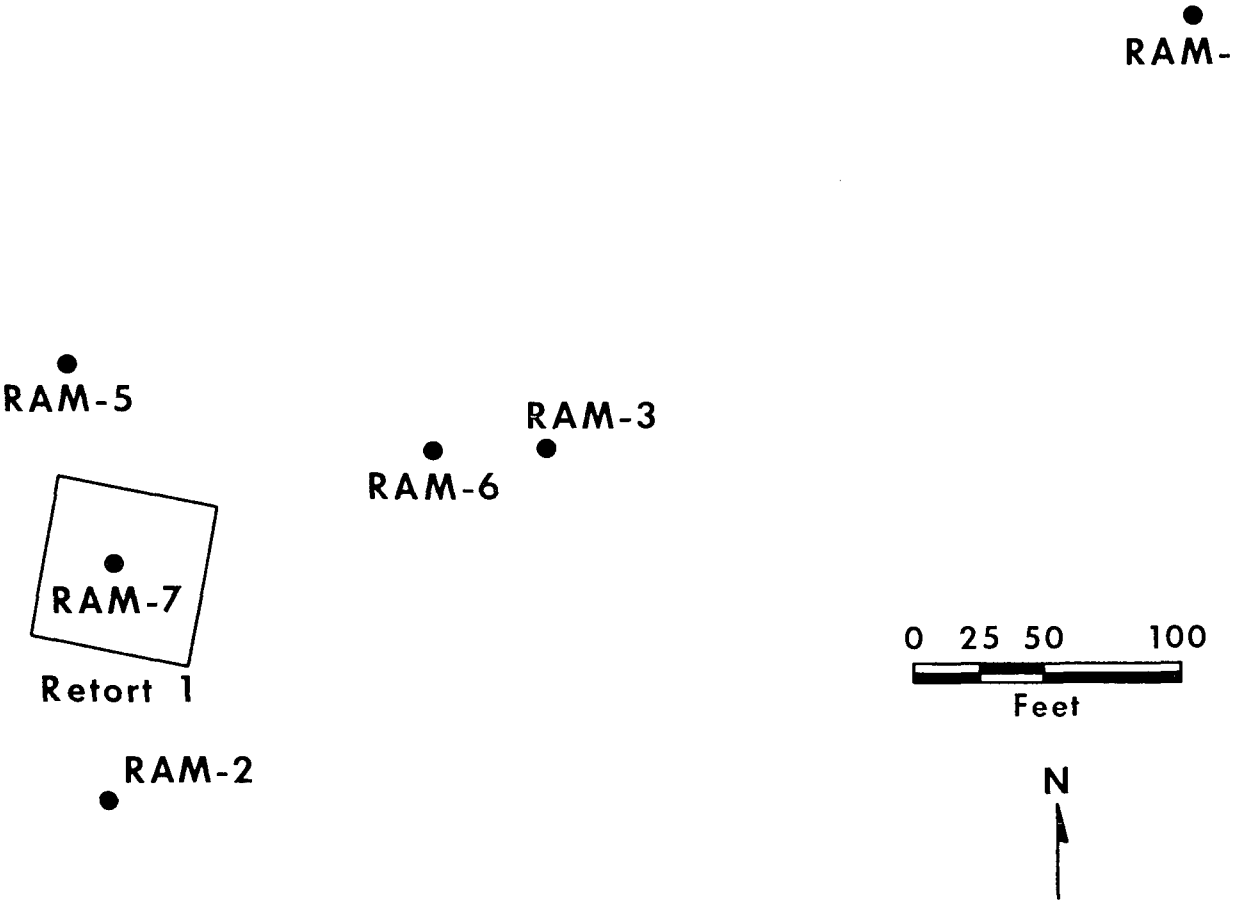

Figure 1-6. Location of Monitoring Wells on Lease Tract C-a

Table 1-20. Results of Physicochemical Analyses of Samples Collected After the Second Pumpdown of Retort 1 in 1986

Parameter, mg/L unless indicated	RAM-4A	RAM-4B	RAM-6A	RAM-6B	RAM-7A	RAM-7B	RAM-7C	RAM-7G
pH	7.0	7.6	7.0	7.4	6.4	7.2	7.9	6.8
Conductivity, umhos/cm at 25°C	1,693[a]	2,009[a]	1,691[a]	2,082[a]	2,110[b]	1,880[b]	1,870[b]	1,850[b]
Total dissolved solids	1,200	1,600	1,200	1,600	1,900	1,500	1,600	1,500
Total suspended solids	510	100	40	40	510	50	40	30
Total carbon	100	100	100	120	13	10	10	10
Mineral carbon	99	104	98	113	15	10	10	10
Dissolved organic carbon	10	10	10	10	10	10	10	10
Alkalinity (as $CaCO_3$)	416	455	436	510	59	36	36	36
Hardness (as $CaCO_3$)	770	970	770	1,000	810	500	580	480
Ammonia (NH_3-N)	0.2	0.42	0.2	0.39	0.73	0.54	0.44	0.84
Fluoride	0.5	0.7	0.6	0.8	2.9	2.8	3.0	4.2
Sulfide	1	1	1	1	1	1	1	1
Major cations								
Calcium	142	159	118	91	241	169	190	148
Magnesium	104	129	106	163	37	22	27	30
Potassium	5	5	5	5	93	125	110	140
Sodium	155	149	114	169	164	167	151	156
Major anions								
Bicarbonate	510[c]	553[c]	513[c]	610[c]	61[b]	23[b]	21[b]	38[b]
Carbonate	<1[c]	<1[c]	<1[c]	<1[c]	<1[b]	5[b]	5[b]	1[b]
Hydroxide	<0.5[c]	<0.5[c]	<0.5[c]	<0.5[c]	<0.5[b]	<0.5[b]	<0.5[b]	<0.5[b]
Sulfate	560[c]	770[c]	510[c]	790[c]	1,230[b]	996[b]	1,010[b]	78[b]
Chloride	19[c]	13[c]	17[c]	14[c]	13[b]	13[b]	13[b]	5[b]
Metals								
Aluminum	1.6	0.4	0.2	0.1	0.9	0.2	0.2	0.1
Arsenic	0.3	0.3	0.2	0.1	0.1	0.1	0.1	0.1
Boron	0.13	0.17	0.13	0.18	0.65	0.68	0.69	0.75
Manganese	0.22	0.27	0.08	0.5	0.52	0.08	0.09	0.14
Strontium	5.72	7.92	6.66	11.3	5.67	4.40	4.72	3.98
Zinc	2.44	4.47	3.52	3.02	1.29	2.17	4.14	5.75

Table 1-20. Results of Physicochemical Analyses of Samples Collected After the Second Pumpdown of Retort 1 in 1986 (continued)

Parameter, mg/L unless indicated	RAM-4A	RAM-4B	RAM-6A	RAM-6B	RAM-7A	RAM-7B	RAM-7C	RAM-7G
Organic compounds[d]								
Benzene, µg/L	--[e]	--	--	ND[f]	ND	6.1	9.6	36
Toluene, µg/L	--	--	--	ND	ND	ND	ND	12
Total, other compounds, µg/L	--	--	--	ND	ND	ND	ND	512

[a] Mean value for samples collected from June 14 to December 31, 1986 (RBOSC 1987)

[b] Analysis was performed on a sample collected in October 1986 (RBOSC 1987).

[c] Analysis was performed on a sample collected in September 1986 (Slawson personal communication).

[d] Determined by gas chromatography/mass spectrometry (RBOSC 1987)

[e] Analysis was not performed.

[f] Not detected

Table 1-21. Results of Microtox™ Assays of Tract C-a Waters[a]

Test Water	Collection Date	Microtox™ EC50 Value (%) 5-minute	15-minute	30-minute
RAM-4A	May 1985	>100	>100	>100
	May 1986	>100	>100	>100
	October 1986	>100	>100	>100
RAM-4B	May 1985	>100	>100	>100
	May 1986	>100	>100	>100
	October 1986	>100	>100	>100
RAM-6A	May 1985	>100	>100	>100
	May 1986	>100	>100	>100
	October 1986	>100	>100	73.1
RAM-6B	May 1985	>100	>100	>100
	May 1986	>100	>100	>100
	October 1986	>100	>100	79.5
RAM-7A	May 1985[b]	<4.5	<4.5	<4.5
	May 1986[c]	<4.5	<4.5	<4.5
	October 1986	>100	>100	>100
RAM-7B	May 1985[d]	<4.5	<4.5	<4.5
	May 1986	>100	>100	>100
	October 1986	>100	>100	>100
RAM-7C	May 1985	>100	>100	>100
	May 1986	>100	>100	>100
	October 1986	>100	>100	>100
RAM-7G	May 1985	16.0	13.1	10.8
	May 1986	26.3	19.7	15.2
	October 1986	38.0	39.4	35.3

[a] All values were calculated by averaging the results of duplicate assays.

[b] The pH of the undiluted water was 12.1. After the pH of the water was adjusted to 7.5 by the addition of 1N hydrochloric acid, the EC50 values for all exposure periods were >100%.

[c] The pH of the undiluted water was 12.4. After the pH of the water was adjusted to 7.4 by the addition of 1N hydrochloric acid, the EC50 values for all exposure periods were >100%.

[d] The pH of the undiluted water was 11.1. After exposure to air for less than 24 hours, the pH of the water dropped to 9.1. The EC50 values determined after the pH of the water dropped to 9.1 were >100% for all exposure periods.

Four oil shale process wastewaters have been generated as the result of recent oil shale retorting tests at WRI. These have been analyzed for their organic and inorganic constituents. Treatment processes were selected with the objective of reuse of the water. The treatments investigated included steam stripping, electrocoagulation, filtration, ozonation, and wet-air oxidation.

REFERENCES

Annual Book of ASTM Standards, American Society for Testing and Materials: Philadelphia, 1984.

API Technical Data Book: Petroleum Refining, American Petroleum Institute: New York, 1978.

Braun, R. R., and A. J. Rothmann. "Oil Shale Pyrolysis: Kinetics and Mechanisms of Oil Production," Fuel, 1975, 54, 129-131.

Brule, M. R., C. T. Liu, L. L. Lee, and K. E. Starling. "Multiparameter Corresponding-states Correlation of Coal Fluid Thermodynamic Properties," Am. Inst. Chem. Eng. J., 1982, 28, 616-625.

Camp, D. W. "Oil Shale Heat Capacity Relations and Heats of Pyrolysis and Dehydration," 20th Oil Shale Symposium Proceedings, Colorado School of Mines, Golden, CO, 1987.

Chukhlantsev, V. G. "Solubility Products of Arsenates," J. Inorg. Chem., USSR, 1956, 1, 1975-1982.

Conn, P. J., H. J. Rollison, and F. P. Miknis. "Comparison of Isothermal Kerogen Decomposition Results Using Reactors with Different Heat-Up Rates," Laramie, WY, October 1984, DOE/FE/60177-1791.

Durand, B., and G. Nicaise. "Procedures for Kerogen Isolation," in Kerogen; B. Durand, Ed.; Editions Technip: Paris, 1980; Ch. 2.

Hubbard, A. B., and W. E. Robinson. "A Thermal Decomposition Study of Colorado Oil Shale," Laramie, WY, 1950, USBM RI-4744.

Johnson, L. S. "Selected Elemental Distributions as Determined by Reference Retorting of Oil Shale," Laramie, WY, July 1986, DOE/FE/60177-2292.

Kessler, M. G., and B. I. Lee. "Improved Predictions of Enthalpies of Fractions," Hydrocarbon Process, 1976, 53, 153-158.

Leventhal, J. S., and R. C. Kepferle. "Geochemistry and Geology of Strategic Metals and Uranium in Devonian Shales of the Eastern Interior United States," Symposium on Synthetic Fuels from Oil Shale II Proceedings, Institute of Gas Technology, Nashville, TN, 1981, 73-96.

Mason, G. M., L. K. Spackman, and H. W. Leimer, "Mineralogic Characterization of a Chattanooga Shale Core from Central Tennessee," 1984 Eastern Oil Shale Symposium Proceedings, Lexington, KY, 1984.

Merriam, N. W., C. Y. Cha, and B. C. Sudduth. "Yield Loss from Oil Shale Retorts with Zones of Contrasting Permeability and Use of External Fuel to Improve Yield," Laramie, WY, August 1986, DOE/FE/60177-2313.

Merriam, N. W., C. Y. Cha, and S. Sullivan. "Production of Spent Shales by Simulation of Surface Oil Shale Retorting Processes," August 1987, DOE report in review.

Miknis, F. P., P. J. Conn, T. F. Turner, and G. L. Berdan. "Isothermal Decomposition of Colorado Oil Shale," Laramie, WY, May 1985a, DOE/FE/60177-2288.

Miknis, F. P., P. J. Conn, and T. F. Turner. "Isothermal Decomposition of New Albany Shale from Kentucky," Laramie, WY, August 1985b, DOE/FE/60177-2213.

Miknis, F. P., S. Sullivan, and G. Mason. "Characterization of Interim Reference Shales," Laramie, WY, March 1986, DOE/FE/60177-2221.

Miknis, F. P., and R. E. Robertson. "Characterization of DOE Reference Oil Shales: Mahogany Zone, Parachute Creek Member, Green River Formation Oil Shale, and Clegg Creek Member, New Albany Shale," Laramie, WY, September 1987, DOE report in press.

Netzel, D. A., and F. P. Miknis. "An NMR Study of Eastern and Western Shale Oils Produced by Pyrolysis and Hydropyrolysis," Fuel, 1982, 61, 1101-1109.

Orr, W. H. "Kerogen/Asphaltene/Sulfur Relationships in Sulfur-Rich Monterey Oils," Org. Geochem, 1986, 10, 499-516.

Raizi, M. R., and T. E. Daubert. "Simplifying Property Predictions," Hydrocarbon Process, 1980, 59, 115-116.

Reid, R. C., J. M. Prausnitz, and T. K. Sherwood. Properties of Gases and Liquids, 3rd ed., McGraw-Hill: New York, 1977.

Ringen, S., J. Lanum, and F. P. Miknis. "Calculating Heating Values from Elemental Compositions at Fossil Fuels," Fuel, 1979, 58, 69.

Robertson, R. E. "Application of Petroleum Demulsification Technology to Shale Oil Emulsions," Liquid Fuels Technology, 1983, 1 (4), 325-333.

Siskin, M., G. Brons, and J. F. Payack. "Disruption of Kerogen-Mineral Interactions in Oil Shales," Energy and Fuels, 1987, 1, 248-252.

Spiewek, I., T. M. Gilliam, and M. D. Silverman. "Development of Process for Recovery of Minerals from Eastern Shale," Symposium on Synthetic Fuels from Oil Shale II Proceedings, Institute of Gas Technology, Nashville, TN, 1981.

Twu, C. H. "An Internally Consistent Correlation for Predicting the Critical Properties and Molecular Weights of Petroleum and Coal Tar Liquids," Fluid Phase Equilibrium, 1984, 16, 137-150.

PUBLICATIONS AND PRESENTATIONS

Publications

Cha, C. Y., N. W. Merriam, and V. Saxena. "Detailed Experimental Plan for Radio-Frequency Heating," April 1987, unpublished DOE report.

Fahy, L. J., and C. Y. Cha. "Oil Shale Pillar Retorting: Preliminary Test Results," July 1987, unpublished DOE report.

Fahy, L. J., J. D. Schreiber, and B. C. Sudduth. "Oil Shale Compaction Results," 20th Oil Shale Symposium Proceedings, Golden, CO, April 1987.

Poulson, R. E., and H. M. Borg. "Separation and Detection of Sulfur-Containing Anions Using Single-Column Ion Chromatography," J. Chromatogr. Sci., 1987, 25, 409-414.

Sudduth, B. C., N. W. Merriam, and C. Y. Cha. "In Situ Retorting of Nonuniform Oil Shale Rubble," 20th Oil Shale Symposium Proceedings, Golden, CO, April 1987.

Turner, T. F., F. P. Miknis, G. L. Berdan, and P. J. Conn. "A Comparison of the Thermal Decomposition of Colorado and Kentucky Oil Shale," Amer. Chem. Soc. Div. of Petrol. Chem. Preprints, 1987, 32(1), 149-156.

Papers in Preparation

Blanche, M. S., S. V. Compton, and J. M. Bowen. "Investigation of Sorption Interactions Between Organic and Mineral Phases of Processed Oil Shale," November 1987, DOE report in review.

Blanche, M. S., and J. M. Bowen. "Effects of Sample Preparation Methods, PAS and Drift on FTIR Spectra of an Organo-Clay Complex," to be submitted to Analytical Chemistry.

Bowen, J. M., C. R. Powers, A. E. Ritcliffe, M. G. Rockley, and A. W. Hownslow. "FTIR and Raman Spectra of Dimethyl Methylphosphonate Adsorbed on Montmorillonite," submitted to Environmental Science and Technology.

Cha, C. Y., and F. D. Guffey. "Development of a Recycle Oil Pyrolysis and Extraction Process," to be submitted to the 1987 Eastern Oil Shale Symposium, Lexington, KY, November 18-20, 1987.

Essington, M. E. "Trace Element Mineral Transformations Associated with Hydration and Recarbonation of Retorted Oil Shale," submitted to Environ. Geol. Water Science.

Essington, M. E. "Modeling Fluoride Chemistry in Hydrated and Recarbonated Spent Western Oil Shales," submitted to the Eastern Oil Shale Symposium, Lexington, KY, November 18-20, 1987.

Essington, M. E. "The Solubility of Barium Arsenate," to be submitted to Soil Sci. Soc. Am. Journal.

Essington, M. E. "Fluoride Chemistry in Hydrated and Recarbonated Spent Western Oil Shales," to be submitted to Journal of Environmental Quality.

Essington, M. E. "The Equilibrium Solubility Relationships of Arsenate in Spent Western Oil Shales," to be submitted to Environ. Sci. Technology.

Essington, M. E. "The Mineralogical Residencies of Trace Elements in Combusted Western Oil Shale," to be submitted to Journal of Environmental Quality.

Essington, M. E., and K. J. Reddy. "Molybdenum Behavior in Spent Oil Shales," to be submitted to Journal of Environmental Quality.

Essington, M. E., L. K. Spackman, and J. D. Harbour. "The Influence of Recarbonation and Hydration of the Mineralogy of Retorted Oil Shale," to be submitted Journal of Environmental Quality.

Essington, M. E., L. K. Spackman, and J. D. Harbour. "The Mineralogy of Density-Fractionated Spent Western Oil Shales," to be submitted to Environ. Sci. Technology.

Essington, M. E., L. K. Spackman, and J. D. Harbour. "Trace Element Partitioning in Spent Western Oil Shale Density Separates," to be submitted to Journal of Environmental Quality.

Essington, M. E., L. K. Spackman, J. D. Harbour, and K. D. Hartman. "Physical-Chemical Characteristics of Retorted and Combusted Western Reference Oil Shale," November 1987, DOE report in review.

Fahy, L. J., J. D. Schreiber, and B. C. Sudduth. "Measurements of Oil Shale Compaction," accepted for publication in In Situ.

Miknis, F. P., and R. E. Robertson. "Characterization of DOE Reference Oil Shales: Mahogany Zone, Parachute Creek Member, Green River Formation Oil Shale, and Clegg Creek Member, New Albany Shale," September 1987, DOE report in press.

Miknis, F. P., T. F. Turner, G. L. Berdan, and P. J. Conn. "Formation of Soluble Products from Thermal Decomposition of Colorado and Kentucky Oil Shale," Energy and Fuels, 1987, in press.

Miknis, F. P., T. F. Turner, and L. W. Ennen. "Isothermal Decomposition of New Albany Oil Shale," to be submitted to the 1987 Eastern Oil Shale Symposium, Lexington, KY, November 18-20, 1987.

Nguyen, S. T., L. J. Noe, and J. M. Bowen. "The Use of Raman Spectroscopic Methods for the In Situ Monitoring of Groundwater Contamination," to be submitted to Environmental Science and Technology.

Nguyen, S. T., L. J. Noe, P. J. Colberg, M. Diependaal, C. R. Powers, and J. M. Bowen. "The Use of Raman Spectroscopy to Follow the Microbial Degradation of Phenols," to be submitted to Applied and Environmental Microbiology.

Poulson, R. E., and H. M. Borg. "Inorganic Studies in the Vicinity of a Post-Operational In Situ Oil Shale Retort," to be submitted to In Situ.

Poulson, R. E., C. R. Powers, and M. E. Essington. "Validation of Inorganic Chemical Speciation for Geochemical Models," November 1987, DOE report in review.

Reddy, K. J., M. E. Essington, J. I. Drever, and P. J. Sullivan. "Chemical Equilibrium Relationships of Strontium in Retorted Oil Shales," to be submitted to Journal of Environmental Quality.

Spackman, L. K., K. D. Hartman, and M. E. Essington. "The Adsorption and Desorption Behavior of Selenite in Spent Western Oil Shales," to be submitted to Environ. Geol. Water Science.

Spackman, L. K., K. D. Hartman, and M. E. Essington. "The Adsorption and Desorption Behavior of Arsenate in Spent Western Oil Shales," to be submitted to Environ. Geol. Water Science.

Patents

Bowen, J. M., P. J. Sullivan, M. S. Blanche, M. E. Essington, and L. J. Noe. "Optical Fiber Raman Spectroscopy Used for Remote In Situ Environmental Analysis," submitted to the U.S. Patent Office on September 23, 1987.

Sullivan, P. J., J. M. Bowen, R. R. Renk, D. C. Lane, and E. L. Clennon. "Decontamination of Liquid Waste Streams Using Singlet Oxygen Generated by Light," to be submitted to the U.S. Patent Office.

Presentations

Fahy, L. J. "Oil Shale Compaction Results," presented at the 20th Oil Shale Symposium, Golden, CO, April 1987.

Sudduth, B. C. "In Situ Retorting of Nonuniform Oil Shale Rubble," presented at the 20th Oil Shale Symposium, Golden, CO, April 1987.

Turner, T. F., F. P. Miknis, G. L. Berdan, and P. J. Conn. "A Comparison of the Thermal Decomposition of Colorado and Kentucky Oil Shale," American Chemical Society National Meeting, Symposium on Advances in Oil Shale Chemistry, Denver, CO, April 5-10, 1987.

WESTERN RESEARCH INSTITUTE

ANNUAL TECHNICAL PROGRESS REPORT

APRIL 1986 - MARCH 1987

TAR SAND

2.0 TAR SAND

TABLE OF CONTENTS

2.0 TAR SAND

2.1 Resource Evaluation

2.1.1 Reference Resources for In Situ Processes

Included with 2.1.2.

2.1.2 Reference Resources for Surface Processes

Based on developed criteria for recovery process selection (WRI 1986) three tar sand deposits were selected as sources of samples for research on in situ (2.1.1) and surface (2.1.2) extraction processes. The selection criteria used included the measured resource present in the deposit, the bitumen saturation, other reservoir properties, and selected chemical properties of the bitumen. In addition, the presence of outcrops and evidence of recent surface activity were considered for logistical reasons. An initial screening identified deposits in California, Kentucky, New Mexico, Texas, the tri-state area (Kansas, Missouri, and Oklahoma), Utah, and Wyoming. Twenty deposits were included in the initial screening; for logistical reasons this number was reduced to nine. From these the Asphalt Ridge and Sunnyside deposits in Utah and the Arroyo Grande deposit in California were selected. Approximately 6 tons of tar sand was obtained from the Asphalt Ridge deposit and 7 tons from the Sunnyside deposit. Final arrangements have been made with Shell Western for acquisition of tar sand from the Arroyo Grande deposit.

2.2 Resource Chemical and Physical Properties

2.2.1 Reference Resources for In Situ Processes

Prior to the initiation of in situ process development research the pertinent chemical and physical properties of the Asphalt Ridge reference resource were determined. These properties are shown in Table 2-1. Standard WRI or ASTM procedures were used for the acquisition of the data. The bitumen was obtained by solvent extraction of the tar sand with toluene followed by pyridine. The recovered bitumen samples were combined and the solvents were removed by rotary evaporation. Two methods were used to determine viscosity. One involved the use of a mechanical spectrometer and the other a Brookfield viscometer (ASTM D-4402-84). The differences in the data at the same temperature are due to the different measurement techniques. The values shown in the table are comparable to other data obtained on samples from this deposit.

The mass balance Fisher assay data are shown in Tables 2-2, 2-3, and 2-4. The amounts shown are the averages of the results of two analyses, except for the elemental composition of spent sand and feed. Noncryogenic grinding of these samples during one of the analyses resulted in nonhomogenous samples and, consequently, poor elemental balances. However, cryogenic grinding of these samples during the other analyses resulted in homogeneous samples and improved elemental balances. Only the latter data are included in Table 2-4. A fairly good elemental balance is shown for the four elements measured (carbon,

Table 2-1. Properties of Asphalt Ridge Bitumen

Property		
Carbon, wt %	85.8	
Hydrogen, wt %	11.5	
Nitrogen, wt %	1.1	
Sulfur, wt %	0.4	
Oxygen (by difference), wt %	1.2	
H/C ratio	1.61	
Molecular weight	690	
Specific gravity,		
16°C	0.999	
38°C	0.948	
60°C	0.855	
Specific heat,		
48.5°C	0.41	
79.0°C	0.50	
98.0°C	0.52	
Viscosity, cp		
38°C	2,200,000	ND[a]
60°C	96,000	59,000[b]
71°C	ND	7,050[b]
Distillation data, wt %		
Amb.-204°C	0.5	
204-260°C	0.8	
260-316°C	3.0	
316-371°C	5.5	
371-427°C	7.0	
427-482°C	12.1	
482-538°C	10.2	
>538°C	60.9	

[a] Not determined
[b] Viscosity determined by ASTM D-4402-84

Table 2-2. Product Distribution Determined from Mass Balance Fisher Assay Analysis of Asphalt Ridge Tar Sand

Product Component	Weight %
Oil	11.48
Water	0.25
Gas	0.57
Spent sand	87.55
Total	99.85

Table 2-3. Gas Composition Determined by Mass Balance Fischer Assay Analysis of Asphalt Ridge Tar Sand

Gas Component	Mole % of Product Gas	Weight % of Product Gas
Hydrogen	22.67	2.22
Carbon monoxide	2.60	3.53
Carbon dioxide	3.70	7.88
Hydrogen sulfide	5.06	8.36
Carbonyl sulfide	0.11	0.29
Methane	41.16	31.89
Ethylene	2.66	3.62
Ethane	9.32	13.52
Propylene	3.91	7.93
Propane	5.52	11.73
Isobutane	0.47	1.32
n-Butylene	1.71	4.61
n-Butane	1.11	3.10
Total	100.00	100.00

Table 2-4. Elemental Composition of Asphalt Ridge Tar Sand and its Fisher Assay Products

Sample	Carbon	Hydrogen	Nitrogen	Sulfur	Ash	Total
Oil, g	9.97	1.40	0.08	0.06	0	11.48
Water, g	0	0.03	0	0	0	0.25
Gas, g	0.37	0.11	0	0.04	0	0.57
Spent sand, g	1.66	0.04	0.04	0.37	85.67	87.55
Total, g	12.00	1.58	0.12	0.47	85.67	99.85
Feed, g	11.60	1.40	0.05	0.40	85.20	100.00
Recovery, %	103.44	112.86	240.00	117.50	100.55	--

hydrogen, nitrogen, and sulfur). No mineral carbon was detected in the two samples from the Asphalt Ridge deposit.

A study is being conducted to develop a better understanding of the interaction between bitumen and the mineral matrix. An improved bitumen extraction efficiency may result from this study. This interaction is being investigated by measuring several bonding energies and then calculating the bonding energy between bitumen and the mineral matrix (sand).

Three types of energies were measured in order to calculate this bonding energy: (1) the heat of dissolution of bitumen on tar sand, (2)

the heat of dissolution of bitumen, and (3) the heat of wetting of extracted tar sand. Dichloromethane was used as the solvent for all measurements. A microcalorimeter maintained at 25°C (77°F) was used to measure all interaction energies. The energy absorbed or released during the interaction was detected by a thermopile and the resulting signal was amplified and recorded. Electrical calibration allowed energy flow in mcal/g (gram of sample) to be calculated.

Using these data and Hess's law, the bonding energy between bitumen and the mineral matrix was calculated. The necessary equations are shown below.

1. T.S. + 2 Sol. → S.-Sol. + B.-Sol. $\Delta H_1 = 0.92$ cal/g

2. B. + Sol. → B.-Sol. $\Delta H_2 = +1.03$ cal/g

3. S. + Sol. → S.-Sol. $\Delta H_3 = -0.12$ cal/g

4. T.S. → S. + B. $\Delta H_4 = 0.01$ cal/g

5. $\Delta H_4 = \Delta H_1 - \Delta H_2 - \Delta H_3$

T.S.	represents tar sand (bitumen on sand).
Sol.	represents the solvent (i.e., dichloromethane).
S.	represents extracted tar sand.
B.	represents bitumen.

The bonding energy between the bitumen and the inorganic matrix (sand) is nearly zero (0.01 cal/g). This is perhaps one reason the bitumen on tar sand is easily removed with solvent.

Bonding between two materials is dependent upon the number of bonding sites occupied and the average strength per bonding site. Values are usually expressed in units of energy per unit area. Determination of the number of bonding sites occupied would be difficult for a heterogenous material such as tar sand because of its large range of particle sizes. The bonding strength per site could be evaluated from the thermodynamic measurement of the energy of bonding and the total number of sites occupied. Since the latter is not known for our system, bonding between the bitumen and mineral matrix can only be determined qualitatively.

One immediate observation is apparent. The energy required to dissolve the recovered bitumen does not differ greatly from the energy required to dissolve bitumen on the mineral. This could be due to the bitumen-mineral bond being weak or the bonding of most of the bitumen in tar sand to itself (i.e., few adsorption sites are occupied). That is, the tar sand is essentially globules of bitumen distributed throughout the mineral matrix.

Regardless of whether the adsorption sites are few in number or weak, the thermodynamic measurements indicate the bond between the

bitumen and the sand is weak. Therefore, in a dissolution recovery process of bitumen from tar sand, the energy consumed in the extraction process is principally used to dissolve the bitumen.

Future work in this area should consider the following points. Selection of solvents for tar sand bitumen recovery should be based on their ability to dissolve tar sand bitumen easily and the energy needed to remove the solvent from the bitumen.

Solvent-bitumen separation can usually be performed by distillation but the energy consumption is high. Phase separation techniques such as used in Beaver-Herter process require little energy and offer promise for tar sand bitumen recovery. Techniques of this type are possible because of the low interaction energy between the bitumen and inorganic matrix.

Solvents such as maltenes, which naturally occur in bitumens, might offer possibilities for bitumen recovery. The maltenes would dissolve the tar sand bitumen. Then heating might be necessary to separate the sand and maltene/bitumen phases. A portion of the maltenes would be recycled for bitumen dissolution. The remainder would be treated further as refinery feedstock. Asphaltenes would be removed with pentane.

2.2.2 Reference Resources for Surface Processes

Before process development of bench-scale, hot oil extraction began in a screw reactor, the pertinent chemical and physical properties of the reference resources were determined. Tar sands from two deposits were investigated using the hot oil-extraction process. The properties of the first deposit, Asphalt Ridge, are shown in Tables 2-1, 2-2, 2-3, and 2-4. The chemical and physical properties of the second deposit, Sunnyside, are shown in Table 2-5. Standard WRI or ASTM procedures were used for the acquisition of the data. The bitumen was obtained by solvent extraction of the tar sand with toluene and pyridine. The recovered bitumen samples were combined and the solvents removed by rotary evaporation. Two methods were used to determine viscosity. One involved the use of a mechanical spectrometer and the other a Brookfield viscometer (ASTM D-4402-84). The differences in the data at the same temperature are due to the different measurement techniques. The data shown in the table are comparable to other data obtained on samples from this deposit.

The mass balance Fisher assay data are shown in Tables 2-6, 2-7, and 2-8. The amounts presented are the averages of the results of two analyses, except for the elemental composition of the spent sand and feed (see 2.2.1). A fairly good elemental balance was obtained for the four elements measured. In addition, mineral carbon was measured in the samples from the Sunnyside deposit.

Table 2-5. Properties of Sunnyside Bitumen

Property		
Carbon, wt %	86.3	
Hydrogen, wt %	11.7	
Nitrogen, wt %	0.87	
Sulfur, wt %	0.46	
Oxygen (by difference), wt %	0.67	
H/C ratio	1.62	
Molecular weight	680	
Specific gravity,		
16°C	0.997	
Specific heat,		
44.0°C	0.56	
51.5°C	0.55	
69.5°C	0.57	
Viscosity, cp		
38°C	160,000,000	ND[a]
60°C	14,000,000	82,000[b]
91°C	160,000	21,450[b]
Distillation data, wt %		
Amb.-204°C	0	
204-260°C	0.5	
260-316°C	2.1	
316-371°C	4.2	
371-427°C	6.5	
427-482°C	9.7	
482-538°C	8.2	
>538°C	68.8	

[a] Not determined
[b] Viscosity determined by ASTM D-4402-84

Table 2-6. Product Distribution Determined by Mass Balance Fisher Assay Analysis of Sunnyside Tar Sand

Product Component	Weight %
Oil	7.60
Water	0.34
Gas	0.55
Spent sand	91.51
Total	100.00

Table 2-7. Gas Composition Determined by Mass Balance Fisher Assay Analysis of Sunnyside Tar Sand

Gas	Mole % of Gas	Weight % of Gas
Hydrogen	33.23	3.47
Carbon monoxide	2.94	4.19
Carbon dioxide	10.13	23.00
Hydrogen sulfide	1.33	2.12
Carbonyl sulfide	0	0
Methane	30.68	24.83
Ethylene	2.50	3.54
Ethane	7.87	11.93
Propylene	3.60	7.64
Propane	4.28	9.49
Isobutane	0.74	1.08
n-Butylene	1.78	5.00
n-Butane	1.28	3.71
Total	100.00	100.00

Table 2-8. Elemental Composition of Sunnyside Tar Sand and its Fisher Assay Products

Sample	Mineral Carbon	Carbon	Hydrogen	Nitrogen	Sulfur	Ash	Total
Oil, g	0	6.56	0.91	0.05	0.03	0	7.60
Water, g	0	0	0.04	0	0	0	0.34
Gas, g	0	0.34	0.10	0	0.01	0	0.55
Spent sand, g	0.46	2.01	0.05	0.04	0.49	86.24	91.51
Total, g	0.46	8.91	1.10	0.09	0.53	86.24	100.00
Feed, g	0.40	9.90	1.10	0.05	0.72	87.00	100.00
Recovery, %	115.00	90.00	100.00	180.00	73.61	99.13	--

2.3 Recovery Processes

2.3.1 Physical Simulations of In Situ Processes

Three one-dimensional simulations of the in situ forward combustion process were conducted to evaluate its effectiveness for recovering oil from the Sunnyside (Utah) tar sand deposit. The injectants used in these tests were steam-oxygen, air-oxygen, or air. A summary of the experimental conditions and results for the three Sunnyside combustion tests is presented in Table 2-9.

Table 2-9. Experimental Conditions and Results for Sunnyside Combustion Tests

Condition	FC63	FC64	FC65
Permeability, darcy	1.2	1.0	1.3
Porosity, %	41	39	40
Oil saturation, % PV	51	55	54
Injection flux, scfh/ft^2			
Steam	33	--	--
Oxygen	8.5	1.4	--
Air	--	64.3	79.2
Steam-oxygen ratio	3.9:1	--	--
Nitrogen-oxygen ratio	--	3.4:1	3.7:1
Cumulative injectant			
Steam, PV	0.55	--	--
Oxygen, scf	11.53	0.93	--
Air, scf	--	58.15	76.87
Maximum injection pressure, psig	1000	1000	1000
Peak combustion temperature, °C	888	910	960
Oil yield, wt % initial bitumen	30.6	22.5	46.2
Time to plug from start of oxidant injection, hrs	5.7	5.0	4.0

The first simulation (FC63) with steam-oxygen experienced severe plugging of the reactor tube within 6 hours after oxygen injection was established. To resolve the plugging problem, the injection end of the reactor tube was vented several times through the production system to relieve the high pressure. With each venting, water (steam), light liquid hydrocarbons and hydrogen-rich gas were produced. Only limited flow through the tube was noted when injection was resumed.

To evaluate the plugging problem, the second simulation (FC64) was operated as an enriched-air, dry-combustion simulation. Enriched air was selected over steam-oxygen to minimize any effect that steam or its condensation may have had on the plugging problem. Within 5 hours of establishing oxygen injection, the same plugging problem was experienced.

In an attempt to determine the reason for the plugging problem, a sample of the residual oil ahead of the pyrolysis zone was extracted and

analyzed. It was determined that the oil saturation had increased from the original 11.6 wt % to 14.6 wt % and the viscosity at 91°C (194°F) was 207,000 cp, a 150-fold increase over the original bitumen viscosity of 1300 cp at the same temperature. This significant change in viscosity was believed to be caused by one or more of the following mechanisms: (1) polymerization of the bitumen, (2) formation of oxidation products, or (3) the devolatilization of the bitumen.

The third simulation (FC65) was conducted as a dry forward combustion test with air as the only injectant and no preheating of the tube. Within 4 hours of the start of the test, the injection pressure began to mirror that of the previous two simulations. However, increasing the temperature with the guard heaters in the zone immediately ahead of the combustion and pyrolysis zones to 232-260°C (450-500°F) reduced the plugging problem to a point where the test could be conducted at a constant injection rate and pressure. This test produced 46% of the bitumen as a highly upgraded oil (Table 2-10) by establishing and maintaining a sharp combustion front throughout the reactor tube. However, even though the yield and product oil quality were good, the extrapolation of this type of process to a field test is not practical at this time.

Table 2-10. Properties of Original Bitumen and Produced Oils (Sunnyside)

Property	Original Bitumen	FC63[a]	FC64[a]	FC65[a]
Elemental composition, wt %				
Carbon	86.3	86.1	87.0	86.3
Hydrogen	11.7	12.8	12.1	12.3
Nitrogen	0.9	0.2	0.5	0.9
Sulfur	0.5	0.5	0.4	0.4
Oxygen (by difference)	0.6	0.4	TR	0.1
H/C ratio	1.63	1.78	1.67	1.71
Molecular weight	680	265	250	305
Gravity, °API	10.4	25.5	22.6	21.6
Distillation data, wt %				
0-316°C	2.9	--	40.7	37.3
316-538°C	28.8	--	59.3	62.7
>538°C	68.3	--	0	0
Viscosity, cp				
16°C	--	26.2	--	--
38°C	1,600,000	--	11.7	36.9
60°C	140,000	--	6.1	15.4
91°C	1,300	--	3.5	7.0

[a] Produced oil properties are for the composite produced oil and includes all produced light hydrocarbons from venting procedures.

2.3.2 Screw Reactor Process Development Unit

Western Research Institute (WRI) is developing a new pyrolysis process called ROPE© (recycle oil pyrolysis and extraction) for recovering products that require a minimum of upgrading to produce a finished, marketable fuel. The process consists of two pyrolysis steps: (1) retorting tar sand at a lower temperature (≪ 430°C [806°F]) with product oil recycling and (2) completing the pyrolysis of residue at a higher temperature (≫ 430°C) in the absence of product oil recycle. WRI has constructed both a 2-inch-diameter process development (PDU) and a 6-inch-diameter bench-scale unit to conduct experiments required for the development of the ROPE© process.

Ten experiments were conducted in the 2-inch PDU using Utah tar sand from the Asphalt Ridge and Sunnyside tar sand deposits. Asphalt Ridge tar sand is semiconsolidated and averages 13.5 wt % bitumen. Sunnyside tar sand is consolidated and averages 11 wt % bitumen. Sunnyside bitumen is more highly aromatic than bitumen from Asphalt Ridge. Both resource materials can be obtained by surface mining.

Eight tests were conducted using the Asphalt Ridge tar sand to determine the effects of pyrolysis temperature and residence time on the oil yield and product distribution and to produce samples for the evaluation of product oil characteristics. A 48-hour test was conducted to measure the operating time required to reach a steady state with respect to the composition of product gas and the elemental compositions of light product oil and heavy recycle oil. A 30-hour test was conducted using the Sunnyside tar sand to obtain preliminary data. The product oil samples were analyzed to determine the distribution of hydrocarbon types and to relate this distribution to that found in different fuel types.

A summary of test conditions and oil yields is presented in Table 2-11. Five temperatures, 370°, 385°, 400°, 415°, and 430°C (698°, 725°, 752°, 779°, and 860°F), and three residence times, 30, 40, and 50 minutes, were used to determine the effects of pyrolysis temperature and residence time on the oil yield and characteristics of product oil from the Asphalt Ridge tar sand.

Oil yields for the Asphalt Ridge tar sand tests were in the range of 80 to 89% of total organics. The oil yield increased with increasing pyrolysis temperature, to a maximum at 400°C (752°F), and then decreased with further increase in the pyrolysis temperature (Table 2-11). When the pyrolysis temperature increased to 430°C (860°F), the oil yield decreased significantly. The oil yield slightly increased as the residence time increased from 30 to 50 minutes. Since the increase in the oil yield was negligible when the residence time increased from 40 to 50 minutes, the optimum pyrolysis temperature and residence time of solids were 400°C (752°F) and 40 minutes, respectively.

The product distribution as a weight percentage of total organics is shown in Figure 2-1 and also in Table 2-12 as a function of pyrolysis temperature. The distribution of organics produced from the Fischer assay analysis is also given in Table 2-12 for comparison. The product

Table 2-11. Summary of Test Conditions and Oil Yields (Asphalt Ridge Tar Sand)

SPR Test No.	47	45	44	46	55	56	57	58	59[a]	64[b]
Horizontal SPR[c]										
Third zone temp., °C	370	385	400	415	415	415	430	430	415	393
Residence time, min	50	50	50	50	40	30	40	30	40	40
Oil yield										
Gallons/ton	29.6	32.0	34.3	33.0	30.4	31.2	32.7	30.0	30.1	22.7
wt % of total organics	86.6	88.9	89.4	86.1	85.7	85.0	80.8	80.0	82.1	76.7
% Fischer assay (volume)	106	115	123	118	109	112	117	107	108	119

[a] Extended steady-state experiment

[b] Sunnyside tar sand test

[c] First and second zone temperatures were 260° and 370°C

gas yield increased as the pyrolysis temperature increased. The residence time did not significantly affect the gas yield (Table 2-12). The coke yield was closely related to the oil yield. A comparison of test data with the Fischer assay product distribution indicates that the gas yields were about the same at the 370°C (698°F) pyrolysis temperature but coke yield from the Fischer assay was much greater than the yield from the ROPE© process tests (Table 2-12). As a result, the ROPE© process produced greater oil yields even if the gas yield was higher than the Fischer assay.

The oil yield from the 48-hour test (SPR-59) was lower than that from the 12-hour test (SPR-55) at the same condition. This was caused mainly by plugging problems in the transition between the horizontal screw pyrolysis reactor (HSPR) and the inclined screw pyrolysis reactor (ISPR) that occurred after 24 hours. As a result, the coke and gas yields from SPR-59 were greater and the oil yield was lower than SPR-55. The 2-inch-diameter PDU has been modified to reduce plugging problems.

When a 370°C (698°F) pyrolysis temperature was used, more than 90% of produced oil was a heavy oil, as shown in Figure 2-2. On the other hand, more than 90% of produced oil was a light oil distillate at the retorting temperature of 400°C (752°F). Since the light oil was the desired oil product and the maximum oil yield was obtained at 400°C (752°F), the optimum retorting temperature and residence time of solids were 400°C (752°F) and 40 minutes, respectively.

Evaluation of the composition of the distillable products from the 48-hour experiment indicated that steady state may have been achieved. The product gas achieved a steady composition after 4 hours of operation. The potential use of the distillable products was evaluated for the products obtained from processing of Asphalt Ridge and Sunnyside tar sands. The IBP-177°C (350°F) distillate fraction from both resources

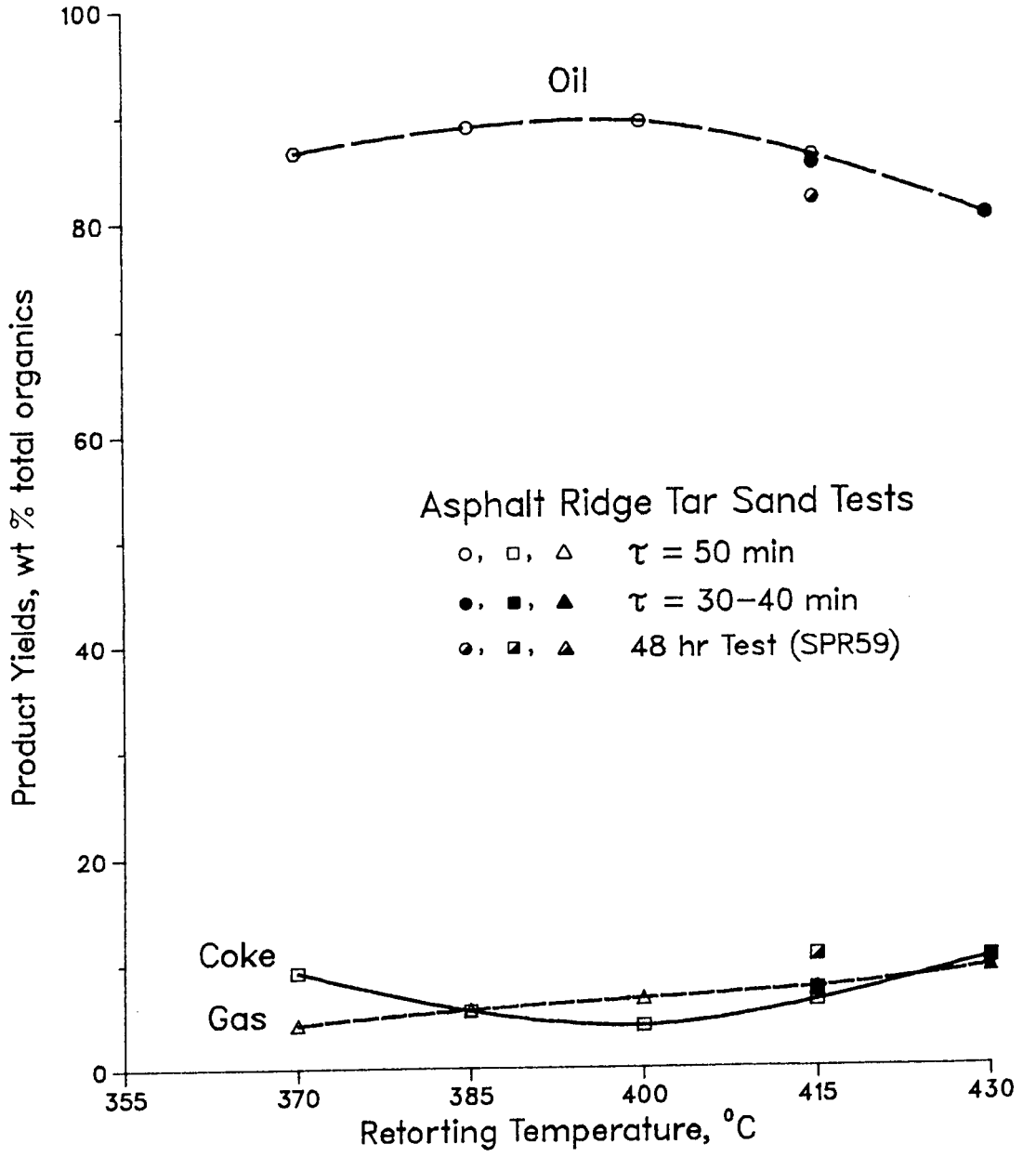

Figure 2-1. Effect of Retorting Temperature and Residence Time on the Product Yields

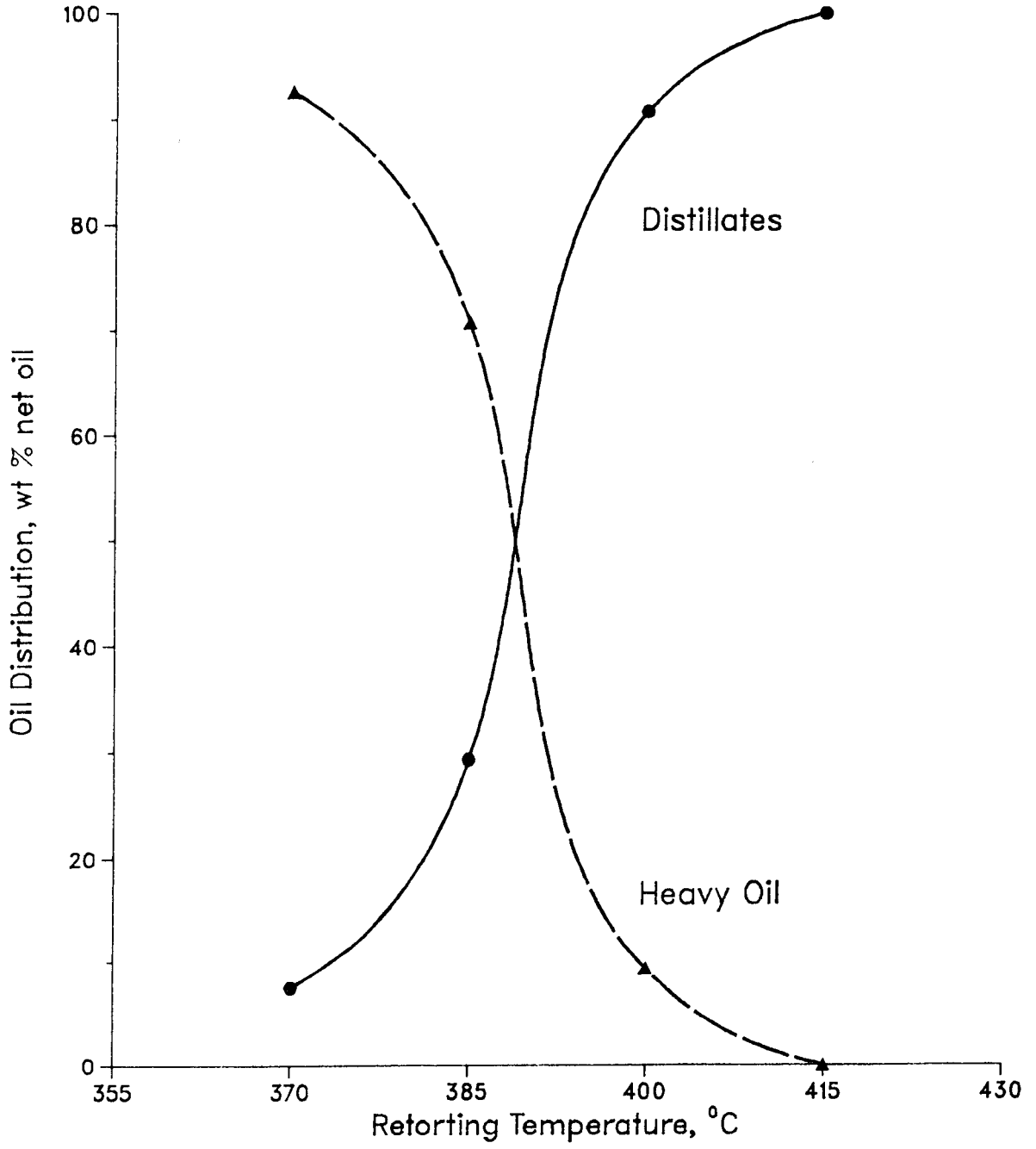

Figure 2-2. Effect of Retorting Temperature on Product Oil Distribution for Asphalt Ridge Tar Sand Tests

Table 2-12. Distribution of Organic Products (wt % of Total Organics)

Test No.	Oil	Gas	Coke
Asphalt Ridge			
SPR-47	86.6	4.2	9.2
45	88.9	5.6	5.5
44	89.4	6.6	4.0
46	86.1	7.6	6.3
55	85.7	6.8	7.5
56	85.0	7.6	7.4
57	80.8	10.0	9.2
58	80.0	8.8	11.2
59	82.1	7.2	10.7
MBFA[a]	76.9	4.3	18.8
Sunnyside			
SPR-64	76.7	11.1	12.2
MBFA[a]	68.2	4.9	26.9

[a] Material balance Fischer assay

appeared to have potential as blending streams for production of gasoline. The 177-371°C (350-700°F) distillate fraction from processing of Asphalt Ridge tar sand has economic value for the production of diesel fuels because of the high concentrations of alkanes and alkenes. The 177-371°C (350-700°F) distillate fraction from processing of Sunnyside tar sand has potential, with proper refinery processing, to produce both high-density and advanced endothermic aviation turbine fuels.

The results presented to date demonstrate the feasibility of the ROPE© concept. Future research to develop the process will require longer experiments in a 6-inch bench-scale unit that will allow steady-state conditions to be achieved and more reliable product yield evaluations to be performed.

2.3.3 Oxygen-Steam Ratios for Wet Forward Combustion

Three one-dimensional (FC60-FC62) and one three-dimensional (BR16) simulations of forward combustion with steam-oxygen injection were conducted using Asphalt Ridge (Utah) tar sand. Experimental conditions and results for these experiments are summarized in Table 2-13.

The one-dimensional simulations were initiated by using the guard heaters to raise the temperature of the packed sand to 121-149°C (250-300°F). When this temperature range was attained, saturated steam was

Table 2-13. Experimental Conditions and Results for Four Asphalt Ridge Steam-Oxygen Combustion Tests

Conditions	Results			
	FC60	FC61	FC62	BR16
Permeability, darcy	1.2	1.1	1.6	--
Porosity, %	40	38	40	36
Oil Saturation, % PV	62	66	61	73
Injected flux, scfh/ft^2				
Steam	34	37	48	--
Oxygen	10.8	8.6	8.0	--
Steam-oxygen ratio	3.1/1	4.3/1	6.0/1	3.0/1
Steam preheat, PV	0.087	0.133	0.140	0
Cumulative co-injection				
Steam, PV	0.29	0.40	0.53	0.38
Oxygen, scf	7.46	7.02	5.40	2.54
Maximum injection pressure, psig	630	450	400	670
Peak combustion temperature, °C	649-816	732-871[a]	704	538-927
Combustion front velocity, ft/day	4.3	3.5	5.4	5.0-20.0
Oxygen demand, lb O_2/ft^3 sand	5.1	4.3	3.0	15.9
Fuel consumed				
wt % initial bitumen	9.3	8.9	7.6	17.5
lb/ft^3 sand	1.8	1.6	1.2	9.1
Oil Yield				
wt % initial bitumen	80.3	80.1	90.1	41.3[b]
% OOIP	82.7	82.2	93.0	42.4[b]
wt % Fischer assay	102.9	102.7	115.5	53.7[b]

[a] Maximum temperatures observed were 927-982°C because of controller overriding.

[b] Based on sweep area

injected at the specified rate to maintain a communication path through the tube. Once communication was confirmed, the top guard heater was raised to 343-371°C (650-700°F) and oxygen injection was established. At these conditions the bitumen ignited and the oxygen in the product gas rapidly decreased to zero. Injection pressures were generally less

than 120 psig with no backpressure on the reactor. The experiments were terminated when combustion temperatures exceeded 260°C (500°F) at the bottom of the tar sand, or when the oxygen content in the product gas exceeded 3 vol %, or when oil production was negligible.

For the three-dimensional simulation, a block had to be reconstructed from crushed tar sand material. To produce the block, 24 increments of the material were packed into a 2x2x1-ft frame while a bulk density equal to that of the one-dimensional simulations was maintained. The block was then completed with a production and injection well at opposite corners to simulate a quarter of a five-spot pattern. Eighteen monitor wells were also included.

To initiate the simulation, the guard heaters were activated to raise the temperature of the block to 93 to 121°C (200 to 250°F). When the desired temperatures were achieved, the ignition heater was activated at the same time air injection was established at a flux of 80 to 120 scfh/ft^2 at a distance of 3 inches from the wellbore. Air injection continued until temperatures of 316-427°C (600-800°F) were achieved in the first ring of temperature wells, approximately 4 inches from the injection well. Oxygen was then added to the injectant stream as the air rate was decreased such that the oxygen content in the injection stream was 35% by volume. With the indication of a vigorous combustion front, complete oxygen utilization and 538°C+ (1000°F+) temperatures, the injectant stream was changed from air-oxygen to steam-oxygen at a ratio of 3.0/1. This ratio was then used throughout the remainder of the test.

Results from the one-dimensional simulations show a reduction in the fuel consumption and oxygen demand as the steam/oxygen ratio increases. In conjunction with the reduction in fuel consumption was an increase in the combustion front velocity and oil yield with an increase in the steam/oxygen ratio. These trends were the result of improved displacement efficiency of the steam zone that precedes the pyrolysis and combustion zones in the forward combustion process. The size of the steam front also increased as the steam/oxygen ratio increased.

The effect of combustion front fingering was demonstrated by the three-dimensional simulation. The volumetric sweep efficiency of the simulation was 26.1% for the combusted zone with an additional 6.0% for the pyrolysis zone. This total sweep efficiency of 32.1% is well below the theoretical sweep efficiency of 50% for an unconfined five-spot pattern. The lower sweep efficiency was caused by the rapid growth of a channel between the injection and production wells, which limited the areal extent of the affected zone.

The oil yield for the three-dimensional test was 41.3 wt % of the original bitumen whereas it was an average of 83.5 wt % for the one-dimensional simulations (Table 2-13). The low oil yield indicates that a large portion of the pyrolysis-produced oils were either consumed by oxidation or were further pyrolyzed during the test.

Product oil quality from all simulations was significantly improved compared with the original bitumen (Table 2-14). The product oils had significantly lower molecular weights, viscosities, and percentages of components boiling above 538°C (1000°F).

Table 2-14. Properties of Original Asphalt Ridge Bitumen and Oils Produced from Four Tests

Properties	Bitumen	FC60	FC61	FC62	BR16
Elemental composition, wt %					
Carbon	85.8	86.1	86.0	86.5	86.4
Hydrogen	11.5	11.9	12.0	11.9	11.3
Nitrogen	1.1	1.4	1.4	1.0	0.7
Sulfur	0.4	0.6	0.6	0.6	1.3
Oxygen (by difference)	1.2	TR	TR	TR	0.3
H/C ratio	1.61	1.66	1.67	1.65	1.57
Molecular weight	670-710	460	510	450	320
Gravity, °API	10.4	14.5	14.1	15.0	14.1
15.6/15.6°C	0.997	0.969	0.972	0.966	0.972
Distillation data, wt %					
0-316°C	5.2	14.0	13.7	13.9	36.0
316-538°C	34.7	38.4	40.2	37.9	51.0
>538°C	60.1	47.6	46.1	48.2	13.0
Viscosity, cp					
16°C	--	166,000	--	--	--
38°C	--	10,700	21,800	7,270	108
60°C	59,000	940	2,200	1,040	--
91°C	--	--	270	--	--

2.3.4 Kinetics and Stoichiometry of Bitumen Pyrolysis

Kinetics and stoichiometry data on Asphalt Ridge tar sand pyrolysis were collected for incorporation into WRI's tar sand processing model. The current work is an extension of previous work in which preliminary isothermal and nonisothermal kinetics and stoichiometries were derived. It was evident from the earlier work that the accurate measurement of kinetic parameters using isothermal methods is difficult for this tar sand without pretreatment of some kind. The problem is caused by a bimodal weight loss distribution in the differential thermogravimetric analysis data. The low-temperature peak represents a distillation of material while the high-temperature peak represents weight loss caused by thermal degradation of a portion of the tar sand bitumen. During isothermal pyrolysis the distillation masks the pyrolysis of the bitumen, hindering the measurement of kinetic parameters for the

pyrolysis. The overlap of the two weight loss regions in the nonisothermal data limits the utility of nonisothermal techniques for determining pyrolysis kinetics.

Two pretreatment techniques have been evaluated for removing the material corresponding to the low temperature weight loss peak in the nonisothermal data. In the first method, tar sand bitumen was extracted and then vacuum distilled to remove the lighter material in the bitumen. The amount of material distilling at a given effective temperature, however, did not correspond well with the thermogravimetric data. This method was abandoned.

Because of the difficulties encountered in the distillation of the bitumen, a series of experiments was performed in which whole tar sand was heated to preselected isothermal temperatures and allowed to soak for 90 minutes. The residual material was cooled and analyzed using a standard nonisothermal thermogravimetric analysis at a nominal heating rate of 10°C/min (50°F/min) with a helium sweep gas. The sample weight loss in three temperature regions of the nonisothermal data is plotted as a function of pretreatment temperature in Figure 2-3. The three temperature regions correspond to the low temperature peak (0-350°C [32-662°F]), the pyrolysis peak (350-500°C [669-932°F]), and the region above the pyrolysis temperature where some additional weight loss occurred in tests of tar sand not subjected to pretreatment (500-800°C [932-1472°F]). The data clearly show that removal of the low-temperature, distillation peak is possible. However, at 300°C (572°F), where that peak no longer exists, a substantial amount of the pyrolysis peak has also been removed. Surprisingly, there is a net increase in material released above 500°C (932°F). This represents high-molecular-weight, polar, or coke-like species formed during the lower-temperature pretreatment. This is especially interesting because it indicates that reactions are occurring below the temperature considered necessary for the onset of pyrolysis.

The 300°C (572°F) pretreatment was selected as the best compromise for preparing samples for isothermal analyses. A limited number of two-stage isothermal experiments have been completed. In these tests a nominal 30-gram sample of raw tar sand has been heated in a U-tube reactor and sand-bath system to 300°C (572°F) and has been allowed to soak for 30 minutes. The reactor has been removed, cooled and weighed, and any liquid product has been removed for later analyses. The sand bath has then been heated to the desired experiment temperature and a standard isothermal run has been performed for a preselected reaction duration. No product-analysis data are available at this time.

2.3.5 Yield and Properties of Pre-Pyrolysis Products

The light oils produced in the isothermal pretreatment of the Asphalt Ridge tar sand are being saved for later analysis.

2.3.6 Residual Carbon Combustion

Small portions of the spent tar sand are being saved for later thermogravimetric analyses with air sweep to determine combustion kinetics.

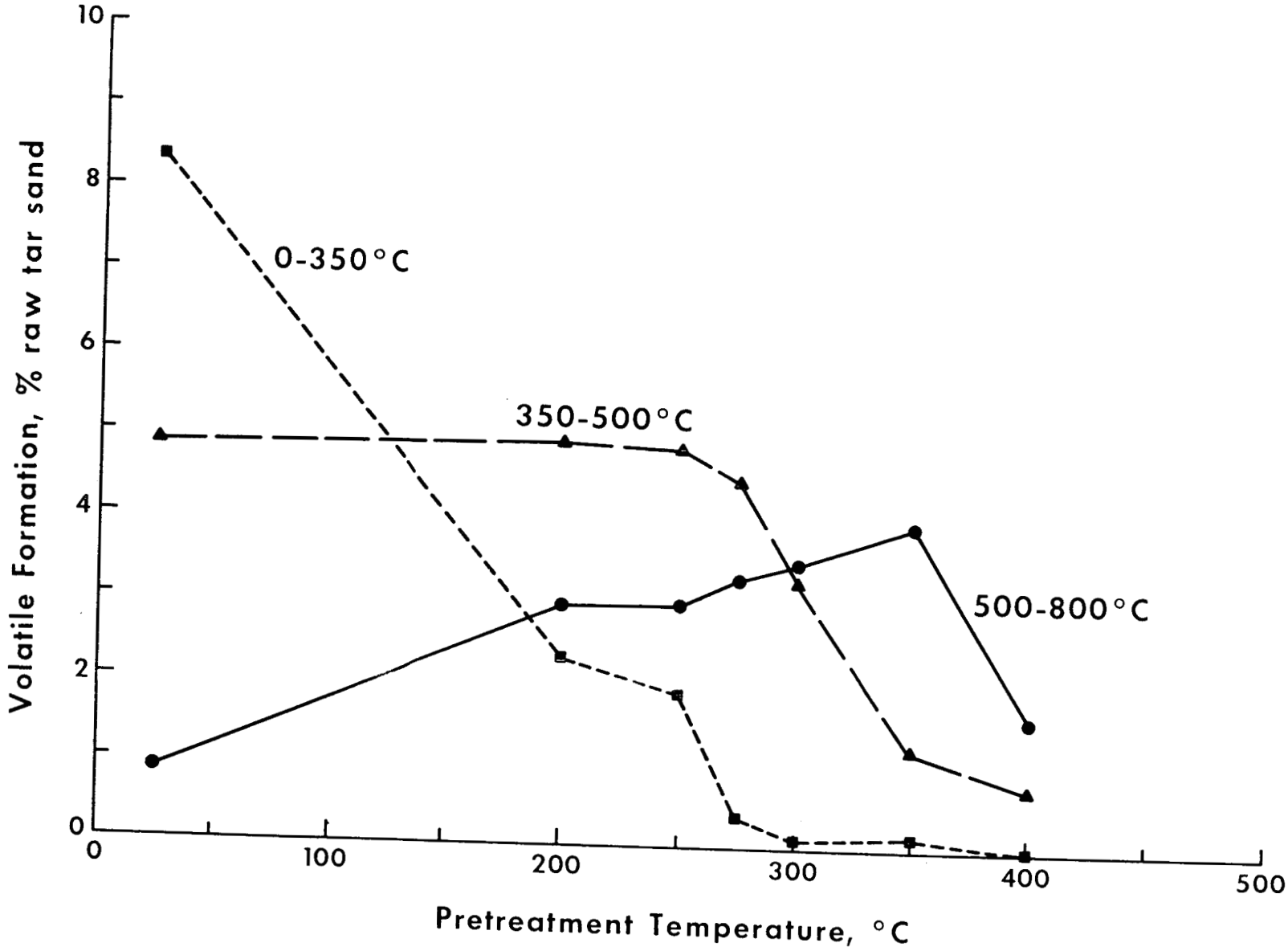

Figure 2-3. Changes in Thermogravimetric Analysis

2.4 Mathematical Modeling

2.4.1 Single Dimensional

Several modifications were made to the one-dimensional tar sand simulator. Some preliminary simulations were made to check the performance of the model.

The one-dimensional model was modified to account for gravity drainage of the mobile phases through a tar sand bed. Another enhancement to the model addresses the occupation of void volume by coke which is deposited during pyrolysis. In addition, a heat loss-heat source algorithm was added to the model to better simulate the tube and block reactor. A steady-state transport assumption is used in the algorithm.

A series of preliminary simulations of test FC59, a steam-O_2 combustion of Asphalt Ridge tar sand in the tube reactor, was completed to validate the model with the enhancements. Relative permeability relationships were adjusted so that measured and simulated reactor pressure drops agreed. Predicted and measured temperature peaks agreed within 656°C (150°F), while oil yield and front velocities agreed within 7%.

Preliminary simulations were made using the most recent pyrolysis kinetics and physical property data for Asphalt Ridge bitumen. The experiments simulated were tube reactor experiments 60, 61, and 62. Coke combustion kinetics were not available, so estimated values were used.

For these simulations, the model was run in the nonadiabatic mode to account for heat input from the zone wall heaters during the preheat phase and after the passage of the combustion front. Except in the tube exit zone, the results from the simulations showed good agreement with experimental combustion peak temperatures and front velocities. Bitumen pyrolysis stoichiometry appeared to vary slightly among the three tests. However, in each case the coke deposition was significantly less than that measured by Fischer assay and slightly greater than that determined from pyrolysis kinetic data. Oil yields from the simulations were within 8% of experimental values. However, pressure profiles were as much as 400 psia lower than experimental values.

Additional simulations of Asphalt Ridge test 60 were done to investigate the pressure response discrepancies. It was hypothesized that during this test the oil and bitumen underwent a chemical change that increased the viscosity of the oil phase. The hypothesis was based on qualitative oil data from the pyrolysis kinetics study and characterization data from oil produced during the high-pressure portion of the tube tests. These data indicated a 3-fold increase in bitumen molecular weight during pyrolysis and a 25-fold increase in viscosity in the high pressure-produced oil.

Incorporation of the oil viscosity and molecular weight effects resulted in an improved pressure profile with a peak pressure identical

to the 650 psia value observed in test 60. Oil production and temperature profiles were virtually unchanged.

Final simulations will be done with the Asphalt Ridge and Sunnyside experimental conditions.

2.4.2 Multi-Dimensional

A two-dimensional version of the tar sand reservoir simulator has been developed in order to evaluate the performance of the block reactor combustion experiments and to lay the groundwork for potential field size modeling. The two-dimensional model contains all of the features of its one-dimensional predecessor including heat loss and gravity effects and has the additional ability to evaluate areal sweep efficiency.

Instead of a radial orientation, the model geometry incorporates a two-dimensional rectangular grid oriented in the width and length dimensions of the block or reservoir. All variables are constant with respect to the direction perpendicular to the areal grid. This geometry was deemed most appropriate after considering the block reactor's geometry and the ease of numerically representing wall and edge effects.

A preliminary two-dimensional simulation of the wet combustion of Asphalt Ridge tar sand has been performed in order to debug and evaluate the numerical performance of the model. Results from the preliminary simulation showed qualitative agreement with experimental results and adequate numerical stability and performance.

A timing study of the model was done to estimate the computational costs required for running the two-dimensional model. The results of this study in terms of central processing unit (CPU) seconds per numerical iteration are presented in Table 2-15. Actual times will vary with the processing conditions specified for a given simulation. However, a relative comparison of the CPU time per iteration is a good indicator of the increased overhead required for running the model. For simulating the block reactor a 5x5 grid should be adequate.

Table 2-15. Time Study Results for a Two-Dimensional Model[a]

Model	Grid	CPU Sec[b] / Iteration
1-D	6x1	4.1
2-D	3x3	9.6
2-D	4x4	34.8
2-D	5x5	71.3

[a] 500-1000 iterations per simulation
[b] Prime computer

A detailed evaluation of the model and verification by comparisons with the Asphalt Ridge block reactor combustion test results is planned after all the pyrolysis and coke combustion kinetics and stoichiometry for the Asphalt Ridge resource are finalized.

2.5 Product Evaluation

2.5.1 Physical and Chemical Properties

The effect of the steam-oxygen ratio on the production of oil from Asphalt Ridge tar sand was investigated in tests FC60, 61, and 62. The chemical and physical properties of the cumulative oils produced during these tests are discussed in section 2.3.1. In general, the properties of the oil were not affected significantly by variations in the steam-oxygen ratio. The ratios were 3.1/1 (FC60), 4.3/1 (FC61), and 6.0/1 (FC62). In this section the properties of the individual oil samples will be discussed and the residual composition of the spent cores. The chemical and physical properties of the oils collected during tests FC60, 61, and 62 are shown in Tables 2-16, 2-17, and 2-18.

The four oils analyzed were obtained from knockouts one and two. Knockout one, because it is located immediately below the tube reactor, operates at a temperature of about 38°C (100°F). Knockout two is chilled to about 0°C (32°F). Three oil samples for each test were obtained from knockout one and one oil sample for each test from knockout two. The three oil samples from knockout one were the result of oil produced during the three different operational stages used during the conduct of the wet forward combustion tests. The first stage involved the injection of steam to confirm the presence of a communication path in the preheated tube. Before steam injection the tar sand was preheated to 121-149°C (250-300°F). The first oil sample, produced during this stage, was improved in quality relative to the original bitumen (see Table 2-1). The chemical and physical differences were due to an increase in the amount of distillate in the produced oil that distills in the temperature range 204-316°C (400-600°F). The steam injection temperature was about 204°C (400°F). The distillate component was the result of steam distillation while the majority of this oil was produced by the mechanisms of thermal expansion and viscosity reduction. The next stage of the test began with the injection of oxygen with the steam. This resulted in the production of an oil bank, which constitutes the second oil sample. The additional oil that was collected after the oil bank constitutes the third sample. These two samples from knockout one and the oil from knockout two constitute the oil produced by combustion. Very little oil was collected in knockout two during the steam injection phase of the test. The properties of the oil produced during the wet forward combustion phase were improved in quality relative to the bitumen (see Table 2-1).

After the tests were completed, the spent core was removed from the tube reactor. As shown in Tables 2-19, 2-20, and 2-21 very little bitumen (2.4% or less) remained on the mineral matter. Small amounts of coke (2.8 to 4.4 wt %) also present on the mineral matter were concentrated near the bottom of the tar sand core. Little residual organic material was present because the tests were conducted until the

Table 2-16. Properties of Oil Produced During the Wet Forward Combustion of Asphalt Ridge Tar Sand, Test FC60

Property	Knockout One			Knockout Two
	Steam Phase	Oil Bank	Additional Oil	
Carbon, wt %	86.3	85.9	86.2	82.0
Hydrogen, wt %	12.2	11.7	11.8	12.7
Nitrogen, wt %	1.3	1.6	1.5	<0.1
Sulfur, wt %	0.60	0.63	0.59	0.67
Oxygen (by diff), wt %	--	0.17	--	4.53
H/C ratio	1.71	1.62	1.63	1.85
Molecular weight	410	520	500	210
Specific gravity, 16°C	0.958	0.969	0.975	0.850
Viscosity, cp				
16°C	26,600	1,110,000	522,000	4
38°C	2,490	--	24,100	--
60°C	23	--	2,540	--
91°C	--	--	--	--
Distillation Data, % recovered				
Amb.-149°C	0.2	0	0.1	9.4
149-204°C	2.2	0.2	0.2	22.1
204-260°C	11.7	5.0	2.7	29.9
260-316°C	11.8	9.0	7.0	23.6
316-371°C	8.0	8.4	10.0	13.0
371-427°C	5.9	7.5	9.7	1.5
427-482°C	8.6	10.9	11.4	0.5
482-538°C	7.7	9.5	9.2	0
>538°C	43.9	49.5	49.7	0

Table 2-17. Properties of Oil Produced During the Wet Forward Combustion of Asphalt Ridge Tar Sand, Test FC61

Property	Knockout One			Knockout Two
	Steam Phase	Oil Bank	Additional Oil	
Carbon, wt %	86.1	86.5	86.5	85.8
Hydrogen, wt %	12.0	11.7	12.1	12.7
Nitrogen, wt %	1.6	1.1	1.5	0.31
Sulfur, wt %	0.62	0.56	0.58	1.1
Oxygen (by diff), wt %	--	0.14	--	0.09
H/C ratio	1.66	1.61	1.67	1.76
Molecular weight	--	645	550	260
Specific gravity, 16°C	0.970	0.986	0.975	0.904
Viscosity, cp				
16°C	--	--	--	--
38°C	14,100	714,000	44,600	10
60°C	1,660	33,000	3,900	5
91°C	229	1,780	400	4
Distillation data, % recovered				
Amb.-149°C	0.1	0	0.1	0
149-204°C	2.4	0.5	0.3	4.4
204-260°C	9.2	2.3	3.9	18.2
260-316°C	8.6	3.9	7.3	27.4
316-371°C	7.2	5.8	9.4	25.6
371-427°C	6.6	7.4	9.1	13.4
427-482°C	10.0	12.3	12.0	7.7
482-538°C	9.5	11.9	10.5	3.3
>538°C	46.4	55.9	47.4	0

Table 2-18. Properties of Oil Produced During the Wet Forward Combustion of Asphalt Ridge Tar Sand, Test FC62

Property	Knockout One: Steam Phase	Knockout One: Oil Bank	Knockout One: Additional Oil	Knockout Two
Carbon, wt %	86.9	87.3	87.1	--
Hydrogen, wt %	12.1	11.8	11.9	--
Nitrogen, wt %	0.86	1.0	1.1	--
Sulfur, wt %	0.60	0.57	0.55	--
Oxygen (by diff), wt %	--	--	--	--
H/C ratio	1.66	1.61	1.63	--
Molecular weight	450	590	470	--
Specific gravity, 16°C	0.963	0.985	0.968	--
Viscosity, cp				
16°C	75,000	--	156,000	--
38°C	5,500	222,000	8,910	3
60°C	825	15,700	1,190	2
91°C	--	1,060	--	2
Distillation data, % recovered				
Amb.-149°C	0.1	0.1	0.3	18.3
149-204°C	2.9	0.1	0.2	25.9
204-260°C	9.4	2.0	3.3	20.2
260-316°C	9.1	4.2	7.6	16.2
316-371°C	7.6	5.0	10.6	13.0
371-427°C	7.0	6.7	11.2	4.4
427-482°C	9.5	11.4	11.2	2.0
482-538°C	9.0	10.5	8.5	0
>538°C	45.4	60.0	47.1	0

Table 2-19. Residual Composition of Spent Core from Test FC60

Inches from Top of Tube	Water, wt %	Toluene Soluble, wt %	Pyridine Soluble, wt %	Coke, wt %
0-16	0.04	0	0	0
16-24	0.02	0	0	0.02
24-30.5	0.01	0	0	0.25
30.5-32	0.03	2.20	0.18	2.54
Bottom sand	0.01	2.28	0.04	0.35

Table 2-20. Residual Composition of Spent Core from FC61

Inches from Top of Tube	Water, wt %	Toluene Soluble, wt %	Pyridine Soluble, wt %	Coke, wt %
0-13.5	0.02	0	0	0
13.5-24	0.02	0	0	0.01
24-27.8	0.01	0	0	0.32
27.8-32	0.03	0	0	4.03
Bottom sand	0	6.17	0.28	0.10

Table 2-21. Residual Composition of Spent Core from FC62

Inches from Top of Tube	Water, wt %	Toluene Soluble, wt %	Pyridine Soluble, wt %	Coke, wt %
0-15	0.03	0	0	0.03
15-30.3	0.03	0	0	0.10
30.3-32	0.04	0	0	3.32
Bottom sand	0.02	0.76	0.03	0.47

bottom of the tar sand experienced temperatures in excess of 260°C (500°F). This temperature is near the pyrolysis temperature for tar sand bitumen.

A series of wet forward combustion tests was also planned for Sunnyside tar sand. However, tube reactor plugging problems were encountered, and the tests were modified. Steam-oxygen was used as the injectant in test FC63 while nitrogen-oxygen was used as the injectant in tests FC64 and 65. Tests FC63 and 64 were considered unsuccessful because pressure buildup in the reactor (>900 psi) could not be relieved and oil production was low. Test FC65 was considered partially successful because the increase in pressure was resolved by heating the tar sand in front of the pyrolysis and combustion zones to 232-260°C (450-500°F). However, this technique would be difficult to apply during a similar in situ field project. Because of the difficulties encountered during the operation of this series of tests a detailed discussion of the properties and mechanisms of production of the oils is inappropriate. However, the properties are shown in Tables 2-22, 2-23, and 2-24 and when compared to those of the bitumen (see Table 2-5) are improved in quality. This improvement is due to the thermal cracking of the bitumen during the pyrolysis/combustion phase of the tests.

A reason for plugging of the tube reactor can, in part, be inferred from the data contained in Tables 2-25 and 2-26. The amount of bitumen

Table 2-22. Properties of Oil Produced During the Wet Forward Combustion of Sunnyside Tar Sand, Test FC63

Property	Knockout One		Knockout Two
	Steam Phase	Combustion Phase	
Carbon, wt %	85.9	86.2	85.6
Hydrogen, wt %	13.5	12.5	13.3
Nitrogen, wt %	<0.1	0.3	<0.1
Sulfur, wt %	0.42	0.50	0.60
Oxygen (by diff), wt %	0.08	0.50	0.40
H/C ratio	1.87	1.73	1.85
Molecular weight	240	285	230
Specific gravity, 16°C	0.886	0.921	0.835
Viscosity, cp			
16°C	12	63	3
38°C	7	-	-
60°C	4	-	-
91°C	-	-	-
Distillation data, % recovered			
Amb.-149°C	0	0.5	26.5
149-204°C	4.5	3.8	24.2
204-260°C	47.2	12.5	14.4
260-316°C	33.3	22.9	11.2
316-371°C	9.3	26.2	11.8
371-427°C	2.5	17.7	8.0
427-482°C	1.7	10.3	3.4
482-538°C	1.4	3.8	0.5
>538°C	0.1	2.3	0

Table 2-23. Properties of Oil Produced During the Forward Combustion of Sunnyside Tar Sand, Test FC64

Property	Knockout One	Knockout Two
Carbon, wt %	87.3	86.8
Hydrogen, wt %	11.9	12.4
Nitrogen, wt %	0.27	0.76
Sulfur, wt %	0.45	0.43
Oxygen (by diff), wt %	0.08	-
H/C ratio	1.62	1.70
Molecular weight	250	260
Specific gravity, 16°C	0.926	0.908
Viscosity, cp		
16°C	-	-
38°C	13	10
60°C	7	6
91°C	4	3
Distillation data, % recovered		
Amb.-149°C	0	7.7
149-204°C	3.8	10.7
204-260°C	13.6	10.1
260-316°C	26.5	9.7
316-371°C	29.8	15.0
371-427°C	14.8	21.2
427-482°C	7.7	20.2
482-538°C	3.8	5.4
>538°C	0	0

Table 2-24. Properties of Oil Produced During the Forward Combustion of Sunnyside Tar Sand, Test FC65

Property	Knockout One	Knockout Two
Carbon, wt %	87.1	85.9
Hydrogen, wt %	12.1	12.5
Nitrogen, wt %	0.87	0.97
Sulfur, wt %	0.47	0.40
Oxygen (by diff), wt %	-	0.23
H/C ratio	1.66	1.73
Molecular weight	330	280
Specific gravity, 16°C	0.941	0.899
Viscosity, cp		
16°C	-	-
38°C	106	10
60°C	36	6
91°C	13	3
Distillation data, % recovered		
Amb.-149°C	0	0.5
149-204°C	1.7	12.6
204-260°C	10.1	18.7
260-316°C	18.7	15.3
316-371°C	20.8	23.3
371-427°C	15.6	15.4
427-482°C	10.5	8.6
482-538°C	4.3	5.6
>538°C	18.3	0

Table 2-25. Residual Composition of Spent Core from FC63

Inches from Top of Tube	Water, wt %	Toluene Soluble, wt %	Pyridine Soluble, wt %	Coke, wt %
0-6	0.04	0	0	0.95
6-19.5	0.06	0	0	0
19.5-23.5	0.08	0	0	3.12
23.5-26	0.61	3.66	0.21	2.21
26-30.5	0.47	12.22	0.11	0.51
30.5-32	0.17	13.72	0.09	0.82
Bottom sand	0.02	3.90	0.01	0

Table 2-26. Residual Composition of Spent Core from FC64

Inches from Top of Tube	Water, wt %	Toluene Soluble, wt %	Pyridine Soluble, wt %	Coke, wt %
0-8.5	0.03	0	0	0.04
8.5-17.5	0.02	0	0	0
17.5-21	0.02	0	0	3.10
21-24	0.01	0	0	3.71
24-25	0.04	5.88	0.72	1.37
25-28	0.03	9.56	0.03	0.48
28-32	0	11.23	0.11	1.50
Bottom sand	0.01	0.29	0.01	0.06

near the bottom of the tube was 11.3 to 13.8 wt % in tests FC63 and 64, and the viscosity of a sample of this material was about 207,000 cp at 91°C (195°F). The residual core composition for test FC65 (Table 2-27) is comparable to those observed for tests conducted on Asphalt Ridge tar sand. This is because the test was conducted until the bottom of the tar sand zone was 260°C (500°F). This temperature is near the pyrolysis temperature for tar sand bitumen.

Table 2-27. Residual Composition of Spent Core from FC65

Inches from Top of Tube	Water, wt %	Toluene Soluble, wt %	Pyridine Soluble, wt %	Coke, wt %
0-15	0.04	0	0	0.05
15-30	0.03	0	0	0.17
30-32	0	0	0	2.50
Bottom sand	0.02	0.17	0.20	0.66

2.5.2 End Uses

A composite of the oil produced during the wet forward combustion of Asphalt Ridge tar sand was evaluated for potential end use. The oil was produced during block reactor test #16. The oil was vacuum distilled to produce an ambient-to-412°C (775°F) distillate and a +412°C (+775°F) residue. The distillate was evaluated as a feedstock for aviation turbine fuel and the residue as an asphalt binder. The chemical and physical properties of the original bitumen, the thermally produced oil, and distillate are shown in Tables 2-28 and 2-29. The thermally produced oil was significantly improved in quality relative to the original bitumen. For example, the gravity was increased from 10.1 to 16.0° API, and the viscosity at 60°C (140°F) was decreased from 59,000 to 41 cps.

Table 2-28. Properties of the Asphalt Ridge Bitumen and its Products

Property	Bitumen	Thermally Produced Oil	Amb.-to-412°C Distillate
Carbon, wt %	85.8	86.4	87.0
Hydrogen, wt %	11.5	11.6	11.8
Nitrogen, wt %	1.1	1.1	0.6
Sulfur, wt %	0.4	1.3	0.7
Oxygen (by diff), wt %	1.2	-	-
H/C ratio	1.61	1.60	1.62
Gravity, °API	10.1	16.0	22.8
Molecular weight	690	320	220
Viscosity, cp			
16°C	-	-	15
38°C	-	134	-
60°C	59,000	41	-

Table 2-29. Distillation Data for the Asphalt Ridge Bitumen and its Products

Temperature, °C	Bitumen, % Recovered	Thermally Produced Oil, % Recovered	Amb.-to-412°C Distillate, % Recovered
149-204	0.5	3.4	5.0
204-260	0.8	12.4	19.2
260-316	3.0	15.3	28.3
316-371	5.5	16.0	29.8
371-427	7.0	13.2	14.7
427-482	12.1	10.9	3.0
482-538	10.2	6.6	0
>538	60.9	22.2	0

In addition, the percentage of residue distilling above 538°C (1000°F) was decreased from 60.9 to 22.2%. The observed alteration in properties was, of course, due to the thermal cracking of the bitumen to lighter products.

The ambient-to-412°C (775°F) distillate was improved in quality relative to the thermally produced oil. The gravity was increased to 22.8° API, the molecular weight was decreased to 220, and the oil was 100% distillable below 538°C (1000°F). The group type analysis of the neutral fraction (87 wt %) from the distillate sample is shown in Table 2-30. The distillate sample was composed of primarily tricyclic alkanes and two- and three-ring aromatics. The presence of these compound

Table 2-30. Results of the GC/MS Group Type Analysis of the Neutral Fraction from the Ambient-to-412°C Distillate Fraction

Example of Hydrocarbon Class	Wt %
Alkanes	1.9
Alkenes	0.0
Monocyclic Alkanes	0.0
Dicyclic Alkanes	0.0
Tricyclic Alkanes	11.0
Tetracyclic Alkanes	0.0
Total Saturates	12.9
Alkylbenzenes	7.0
Indans/Tetralins	19.3
Naphthalenes	41.6
Fluorenes	11.6
Anthracenes/Phenanthrenes	7.6
Total Aromatics	87.1

classes indicates that this distillate has potential to be a hydrogenation feedstock for the production of advanced aviation turbine fuels. These fuels are composed of primarily mono-, di-, and tricyclic alkanes. In addition, a low n-alkane content in the feedstock is desirable in order to insure that the freeze point specification of the finished fuel is met.

The vacuum distillation residue was evaluated as a pavement binder. The viscosity of the residue met the viscosity specification for an AC-10 viscosity-graded asphalt. In addition, the +412°C residue (+775°F residue) met all of the Table 1 requirements of ASTM D-3381 (Table 2-31). Only one specification (viscosity at 135°C [275°F]) was not met for the more restrictive Table 2 requirements of ASTM D-3381.

Performance predictive aging tests were also conducted on the residue. These included the thin-film accelerated aging test (TFAAT) and the water susceptibility test (WST). The aging index determined by TFAAT is quite low (40). Specification-grade asphalts usually have aging indexes in the 100 to 300 range. This may indicate that the residue may not harden properly, resulting in low pavement stability. However, the results of the WST indicate that the residue, when coated on appropriate aggregates (Hol limestone and Texas silica), is as good as or better than some petroleum asphalts. The residue was compared with Boscan and California coastal asphalts.

Table 2-31. ASTM D-3381 Specification Tests on +412°C Residue

Test	Specifications for AC-10	+412°C Residue
Viscosity, 60°C, poise	1000 ± 200[a]	1174
Viscosity, 135°C, centipoise, min	150[b], 250[c]	202
Penetration, 25°C, 100 g, 5 sec, dmm, min	70[b], 80[c]	102
Flash point, Cleveland open cup, °C, min	219[a]	263
Solubility in trichloroethylene, %, min	99.0[a]	99.9
Test on residue from thin-film oven test		
Viscosity, 60°C, poise, max	5000[a]	3124
Ductility, 25°C, 5 cm/min, cm, min	50[b], 75[c]	105+

[a] Value common to ASTM D-3381 Tables 1 and 2.
[b] ASTM D-3381, Table 1.
[c] ASTM D-3381, Table 2.

2.6 Environmental

2.6.1 Characterization of Effluents and Residuals

The effluents from physical simulations of wet forward in situ combustion of Utah Asphalt Ridge and Sunnyside tar sands were characterized. Three wet combustion tests were conducted in the tube reactor and one test in the block reactor.

The raw tar sand samples were chilled in dry ice and ground to approximately 1/4 inch. The 1/4-inch samples were again chilled in dry ice and a representative fraction was then cryogenically ground, using liquid nitrogen in an SPEX shatterbox. This procedure was repeated five times to give five samples each of Asphalt Ridge and Sunnyside tar sand.

Only 5 to 8 standard cubic feet of gas was generated during a tube reactor test. The gas flow varied from 0 to 1 liter per minute. Some of the off-gas was routed to gas chromatographs for measurement of oxygen, nitrogen, carbon dioxide, carbon monoxide, hydrogen, gaseous sulfur species, and various hydrocarbons. A few cubic centimeters of gas were periodically withdrawn for measurement of nitric oxide. The remaining gas was diverted to an impinger assembly for capture of ammonia and trace metals.

Most metals in the raw tar sand, the spent sand, produced oil, produced water, and gaseous effluent were analyzed by inductively

coupled plasma atomic emission spectroscopy (ICP). Mercury was analyzed by cold vapor atomic absorption spectroscopy. Cadmium, arsenic, selenium, and lead were determined by graphite furnace atomic absorption. An evaluation of the resulting data will be forthcoming.

2.6.2 Environmental Significance of Effluents and Residuals

The characterization data for effluents and residuals are being evaluated to determine if any compounds may pose an environmental or health concern. A literature review has been completed to determine the potential fates of these compounds and the dangers associated with these fates.

2.6.3 Partitioning of Chemical Species

Analytical results have been examined to determine the partitioning of selected chemical species into the solid, liquid, and gaseous streams. Elemental closure generally varied between 50 and 100%, but there were exceptions. Aluminum concentrations in the raw tar sand were significantly higher than could be accounted for in the product streams. Chromium concentrations were higher in the spent tar sands than could be accounted for in the raw material. Nearly all of the metals remained in the combusted material, with very little emitted in the produced water, oil, or off-gas. That which was measured in the off-gas occurred primarily as particulates.

2.6.4 Mineralogical Effects of Processing

The presence of clay minerals in tar sand ores can cause problems both in the extraction process and in the environment. The PR Spring tar sand deposit contains approximately 7% clay minerals. Recent research suggests that the presence of organic acids can cause rapid dissolution of aluminosilicate minerals and precipitation of clay minerals under geologic conditions. These mineral reactions, termed clastic diagenesis, could potentially lead either to enhanced bitumen recovery caused by increased permeability and porosity or to formation damage caused by plugging and a resulting loss of permeability.

Laboratory experiments were conducted to assess the mineralogical changes that occur in tar sand as a result of exposure to process water. Unaltered samples of sandstone strata from the PR Spring tar sand deposit were immersed in tar sand process water containing high concentrations of organic acids. Detailed characterizations of samples were performed at predetermined time intervals to observe changes in mineralogy, porosity, and permeability. Samples were characterized using x-ray diffraction, optical microscopy, and scanning electron microscopy.

Preliminary results indicate that contact with the process water increased porosity and permeability within the test samples as a result of selective dissolution of aluminosilicate and carbonate minerals, with a corresponding precipitation of clay minerals. The final samples are still in contact with the process water.

REFERENCES

Western Research Institute. "Factors That Influence the Selection of Tar Sand Resources for In Situ Thermal Recovery," Laramie, WY, June 1986, DOE/FE/60177-2162.

PUBLICATIONS AND PRESENTATIONS

Publications

Biezugbe, G. B. O., and B. G. Place. "Wet Air Oxidation of TS-1S Wastewater," September 1985, DOE/FE/60177-2424.

Cha, C. Y., F. D. Guffey, and K. P. Thomas. "Preliminary Results of Tar Sand Pyrolysis with Product Oil Recycling," September 1986, DOE/FE/60177-2370.

Ensley, E. K., and M. A. Scott. "Bonding Energies of Bitumen to Tar Sand Mineral," March 1986, DOE/FE/60177-2307.

Guffey, F. D., and R. E. Cummings. "Preliminary Evaluation of Chemical Indicators for the Analysis of Production Losses from Tar Sand Recovery," March 1986, DOE/FE/60177-2421.

Holmes, S. A. "Isolation and Characterization of Saturates from Tar Sand Bitumens and Thermally Produced Oils," March 1986, DOE/FE/60177-2311.

Holmes, S. A., L. J. Romanowski, Jr., and K. P. Thomas. "Saturate Distributions in Bitumens and in Oils from Tar Sand: Effect of Thermal Processing," In Situ, 1987, 11(2-3).

Johnson, L. A., Jr. "Process Engineering Research Plan for the Five-Year Tar Sand Program, FY 1987-1991," March 1986, unpublished DOE report.

Johnson, L. A., Jr. "The Second Three-Dimensional Physical Simulation of Forward Combustion in Tar Sand Triangle Material," March 1986, DOE/FE/60177-2203.

Johnson, L. A., Jr., and L. J. Romanowski, Jr. "Laboratory Evaluation of Forward Combustion in Sunnyside Tar Sand," September 1987, DOE/MC/11076-2435.

Kocornik, D. J. "Characterization of Two Commercial Tar Sand Process Waters," September 1985, DOE/FE/60177-2223.

Kocornik, D. J. "Proposed Water Treatment Approach for Commercial Tar Sand Wastewaters," September 1986, DOE/FE/60177-2410.

McTernan, W. F., S. L. Hill, and W. E. Blanton. "Physical, Chemical, and Toxicological Characterization of Untreated and Treated Tar Sand Wastewaters," April 1985, DOE/FE/60177-2431.

Marchant, L. C. (editor). "Publications and Presentations: Final Report for the Period April 1983-September 1986, Volume 2," December 1986, DOE/FE/60177-2305.

Mason, G. M., T. E. Owen, R. L. Daley, and R. C. Donovan. "Clay Minerals in a Utah Tar Sand and Their Potential Effects on Processing," June 1986, DOE/FE/60177-2147.

Netzel, D. A. "The Quantitation of Carbon Types Using the DEPT/QUAT NMR Pulse Sequences: Application to Fossil Fuel Derived Oils," Anal. Chem., 1987, 59(14).

Owen, T. E., and D. J. Kocornik. "Tar Sand 5-Year Environmental Research Plan," March 1986, unpublished DOE report.

Petersen, J. C. "The Potential Use of Tar Sand Bitumen as Paving Asphalt," 1987 Interstate Oil Compact Commission Summer Meeting Proceedings, Oklahoma City, OK, June 1987.

Poulson, R. E., and J. A. Clark. "Organic Solute Profile from Two Commercial Tar Sand Processes," February 1986, DOE/FE/60177-2426.

Romanowski, L. J., Jr., and K. P. Thomas. "Steamflooding of Preheated Tar Sand," February 1985, DOE/FE/60177-2326.

Romanowski, L. J., Jr., and K. P. Thomas. "Reverse Combustion in Asphalt Ridge Tar Sand," April 1985, DOE/FE/60177-2365.

Romanowski, L. J., Jr., and K. P. Thomas. "Laboratory Studies of Forward Combustion in the Tar Sand Triangle Resource," March 1986, DOE/FE/60177-2208.

Romanowski, L. J., Jr., and K. P. Thomas. "Steam-Oxygen Combustion in Asphalt Ridge Tar Sand," August 1986, DOE/FE/60177-2437.

Romanowski, L. J., Jr., and K. P. Thomas. "Laboratories Studies of Forward Combustion in the Tar Sand Triangle Resource," In Situ, 1987, 11(2-3).

Smith, V. E., L. C. Marchant, J. R. Covell, and D. C. Sheesley (editors). "Research Investigations in Oil Shale, Tar Sand, Underground Coal Gasification, Advanced Process Technology, and Asphalt Research: Final Report for the Period April 1983-September 1986, Volume 1," December 1986, DOE/FE/60177-2305.

Thomas, K. P. "Chemical and Physical Parameters Necessary for the Interpretation of In Situ, Thermal Recovery of Tar Sand Deposits," June 1986, DOE/FE/60177-2220.

Thomas, K. P. "A Research Plan Identifying Needs in the Area of Physical and Chemical Properties Evaluation for Tar Sand," August 1986, unpublished DOE report.

Thomas, K. P., P. M. Harnsberger, and F. D. Guffey. "An Evaluation of the Potential End Uses of a Utah Tar Sand Bitumen," September 1986, DOE/FE/60177-2423.

Turner, T. F., and L. G. Nickerson. "Pyrolysis of Asphalt Ridge Tar Sand," August 1986, DOE/FE/60177-2315.

Vaughn, P. "A Numerical Model for Thermal Recovery Processes in Tar Sand: Description and Application," April 1986, DOE/FE/60177-2219.

Vaughn, P. "The Numerical Simulation of Four Forward Combustion Tube Experiments Using the Tar Sand Triangle Resource," September 1986, DOE/FE/60177-2327.

Vaughn, P. "Mathematical Modeling for In Situ Thermal Recovery Processes in Tar Sand: Model Description and Verification," In Situ, 1987, 11(2-3).

Westhoff, J. D., and L. C. Marchant (editors). "Proceedings of the 1986 Tar Sand Symposium," July 1986, DOE/METC-87/6073.

Papers in Preparation

Biezugbe, G. B. O., and J. S. Nordin. "Characterization and Environmental Significance of Emissions from Laboratory Process Experiments of Utah Tar Sand," September 1987, DOE report in review.

Cha, C. Y., F. D. Guffey, and L. J. Romanowski, Jr. "Tar Sand Pyrolysis with Product Oil Recycling," July 1987, DOE report in review.

Ensley, E. K., and M. A. Scott. "Bibliography of Bitumen Extraction from Tar Sand: Identification of Novel Concepts," March 1985, DOE report in review.

Johnson, L. A., Jr., and C. Y. Cha. "Design and Shakedown of an Inclined Liquid Fluid-Bed Reactor System," September 1987, DOE report in review.

Johnson, L. A., Jr., and L. J. Romanowski, Jr. "Evaluation of Steam to Oxygen Ratios for Forward Combustion in Asphalt Ridge Tar Sand," July 1987, DOE report in review.

Johnson, L. .A., Jr., and L. J. Romanowski, Jr. "Laboratory Evaluation of Forward Combustion in Sunnyside Tar Sand," September 1987, DOE report in press.

Netzel, D. A., and P. T. Coover. "An NMR Investigation of the Chemical Association and Molecular Dynamics in Asphalt Ridge Tar Sand Ore and Bitumen," September 1987, DOE report in review.

Thomas, K. P., P. M. Harnsberger, and F. D. Guffey. "Potential End Uses of Oil Produced by Wet Forward Combustion of Asphalt Ridge Tar Sand," September 1987, DOE report in review.

Presentations

Holmes, S. A., and F. A. Barbour. "Characterization of Heavy Oil and Residua by TLC with Flame Ionization and Chemiluminescent Nitrogen Detection," presented at Confab '87, Silver Creek, CO, July 28-31, 1987.

Marchant, L. C., et al. "Technical Progress Review for Cooperative Agreements DE-FC21-87MC11076 and DE-FC21-83FE60177: Tar Sand," presented to DOE program managers, Laramie, WY, May 5-6, 1987.

Petersen, J. C. "The Potential Use of Tar Sand Bitumen as Paving Asphalt," presented at the Interstate Oil Compact Commission 1987 Summer Meeting, Coeur D'Alene, ID, June 21-24, 1987.

Thomas, K. P. "An Evaluation of the Potential End Uses of a Utah Tar Sand Bitumen," presented at the 1987 Rocky Mountain Fuel Society Symposium, Salt Lake City, UT, February 26-27, 1987.

Turner, T. F., and L. G. Nickerson. "Pyrolysis of Asphalt Ridge Tar Sand," presented at Confab '87, Silver Creek, CO, July 28-31, 1987.

WESTERN RESEARCH INSTITUTE

ANNUAL TECHNICAL PROGRESS REPORT

OCTOBER 1986 - SEPTEMBER 1987

UNDERGROUND COAL GASIFICATION

3.0 UNDERGROUND COAL GASIFICATION

TABLE OF CONTENTS

3.0 UNDERGROUND COAL GASIFICATION

3.1 Environmental Base Studies for UCG

3.1.1 Environmental Impact Assessment

UCG Groundwater Data Base. As part of the research for the Department of Energy, WRI maintains a water quality data base. The data base was designed by WRI and provides easy data entry, access, and manipulation, as well as permanent, compact, and cost-effective data storage. The data base contains water quality information from the Hanna, Hoe Creek, and Rocky Mountain 1 (RM1) underground coal gasification (UCG) sites. Data are collected, added to the data base, and evaluated on a periodic basis. WRI also develops computer programs that aid in the evaluation of the data quality, the characteristics of the sites, and the impact of UCG.

Objectives of work related to the UCG water quality data base are the following:

- store measured and calculated UCG groundwater data
- test all programs on the new VAX system
- provide permanent, compact data storage
- limit programming and maintenance requirements
- limit costs
- insure accurate and complete data entry
- develop and upgrade programs that aid in the evaluation of data quality, site characteristics, and UCG impact

Data have been entered and edited on the University of Wyoming's CYBER mainframe computer with an entry program developed by WRI. The data base is in a compact format and is permanently stored on magnetic tape to limit costs. Transferal of data and software from the CYBER to the VAX is being done with tapes. Transferal by tape avoids the interfacing of the two computers and saves computer time. Transfer of the data base and related programs to the VAX appears to be smooth.

The data entry and retrieval programs are efficient, user friendly, and accurate. The data entry program now allows easy editing of the data. The retrieval program presents the output according to the needs of the user. Most of the data evaluation programs are up-to-date and easy to use. The overall programming, maintenance, and cost requirements have been low.

The accuracy of the data entry and the quality of the data are analyzed differently depending on the site. If a value in the Hanna and Hoe Creek data is an order of magnitude (or more) different from the historical average value for the well, or the value is unusual for some other reason, the value is compared with the value in the laboratory reports. Checking the data in this manner helps insure accurate data entry. It also helps identify trends and outliers (values that are entered correctly but significantly different from the historical data).

However, since the RM1 data set is small, all RM1 data are checked against the laboratory reports, thereby insuring the accuracy of data entry. Computer programs calculate the cation-anion balance and the coefficient of variation of parameter concentrations in RM1 wells. Coefficient of variation analysis is used to evaluate variability in the RM1 baseline data. Both data evaluation techniques are used to locate outliers and evaluate the data quality.

Trends in the data and general site characteristics are generally evaluated using graphical and statistical techniques. Data are retrieved and portrayed in either a two-dimensional or three-dimensional format. Changes over distance and time are analyzed in this manner and are discussed elsewhere in this report.

The data base presently contains all the available inorganic water quality and water level data. It also contains all the organic water quality data from the Hanna and Hoe Creek sites, and some of the organic data from the RM1 site. Accurate data entry has been verified. The Hanna and Hoe Creek data that were collected and entered during the past year contain outliers. Values for some parameters fluctuate dramatically. No set of parameters or wells was measured consistently. A large drop in conductivity occurred at the Hanna site in November 1986, but since a large drop also occurred at the RM1 site and the sites are sampled by different contractors, the low conductivity values appear to be valid. A slight increase in phenols concentrations occurred in many of the Hoe Creek wells in February 1987.

The type-curve program is still being developed. The program fully supports four methods: Theis, Hantush-Jacob, Papadopulos-Cooper-Bredhoft, and Jacob. The program partially supports the Hantush (1960), Boulton, Stone (based on Neuman-Witherspoon 1972), Neuman-Witherspoon, and Cooley-Case methods.

Environmental Evaluation of Rocky Mountain 1. As a continuing effort to advance UCG technology, a dual-module test is planned for the Fall of 1987 at the Rocky Mountain 1 test site near Hanna, Wyoming. Preliminary location of the Rocky Mountain 1 test site was determined through analysis of site characterization data from the Hanna tests. Desirable site characteristic parameters were compared with data to locate a site that best met the criteria. Among the parameters evaluated were coal, overburden, and unit A thickness; proximity to faults; dip of the coal seam; proximity to outcrop; hydraulic proximity to previous tests; and land ownership constraints. Other parameters evaluated included structural characteristics, cleating and fracturing, and the lithologic nature of unit A. The wells installed as water and monitoring wells were used to evaluate the site. Drill cuttings and geophysical log data were available for these wells also.

Thirty drill, core, and drill/core holes were completed and geophysically logged to characterize the site and the surrounding area (Figure 3-1). Initial exploratory coreholes were located to provide data for both site characteristics and process well installation. Coreholes and monitor wells were drilled in a prioritized order to establish site suitability as early in the field project as possible.

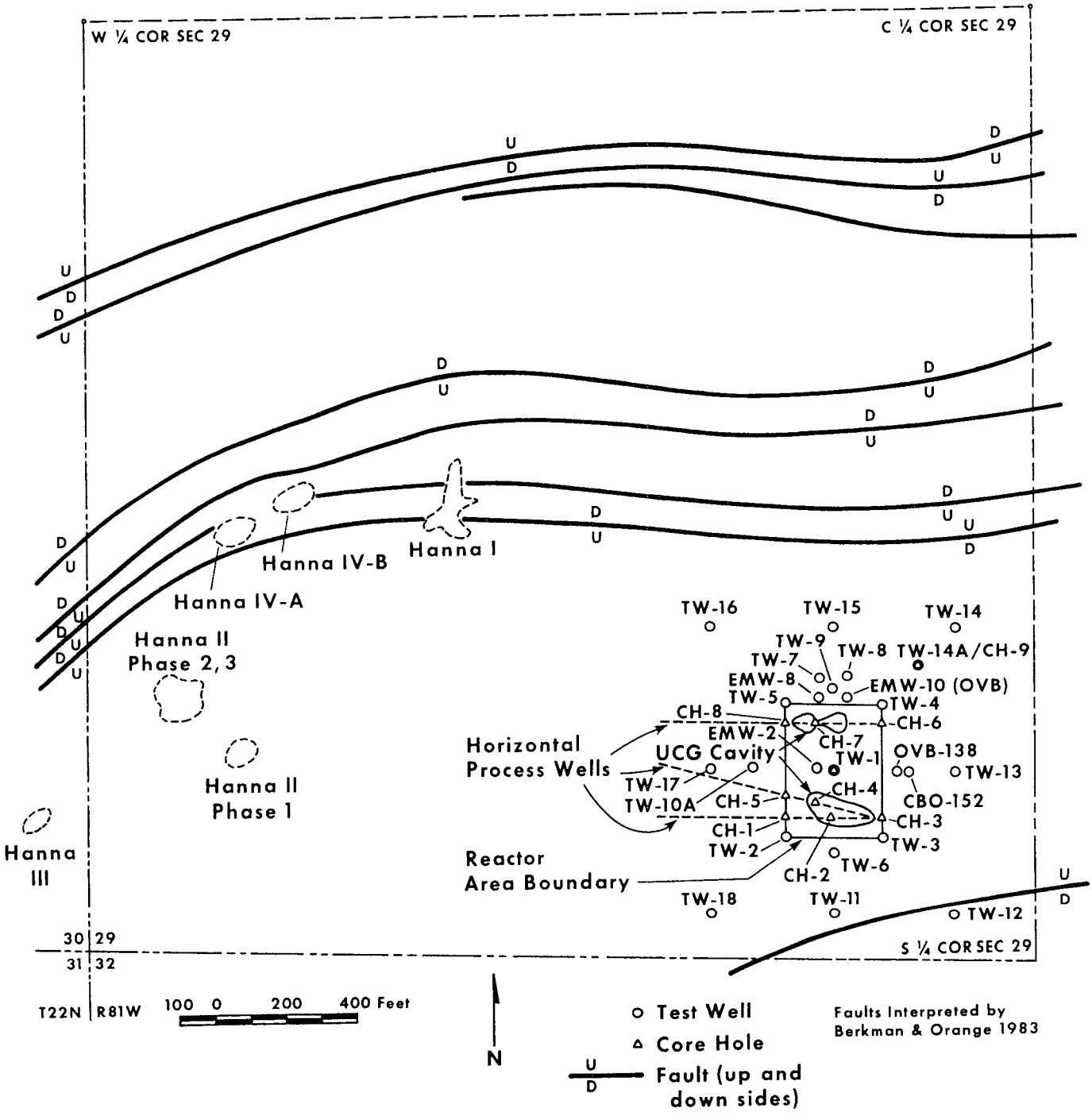

Figure 3-1. Location Map of Hanna UCG Sites and Drill Holes for RM1

After completion of the first four bore holes (TW-1, TW-6, TW-9, and TW-10) both north-south and east-west straight-line cross sections were constructed to verify site suitability. Further coreholes and monitor wells provided data that supported the suitability and data for process well installation.

Data from the field program (Table 3-1) were used to construct geologic characterization maps to identify the structural and stratigraphic nature of the test site. The coal seam dips 7° to the northeast and has no major structural discontinuities within the test area (Figure 3-2). A large-scale fault was discovered as a result of drilling TW-14 (right side, Figure 3-2). This well cut through the fault and indicated a stratigraphic displacement of 30 feet (one coal seam thickness). The fault appeared on the surface as a lineament trending to the northwest towards the Hanna I and Hanna IV test sites. The fault is normal and upthrown on the northeast. It is interpreted to be nearly vertical but does exhibit at least a slight dip to the southwest. The fault will not inhibit the test because it is located 300 feet from the actual burn area.

Examination of the core indicated very little tectonic fracturing and small-scale faulting. The coal did exhibit a well-formed vertical cleat system consisting of two trends nearly perpendicular to each other. The cleats were filled with secondary calcite and pyrite. Additional field studies indicated the trends to be downdip (N35°E) and parallel to strike (N55°W) (Figure 3-3). The coal core was continuous and only exhibited a few crumbly zones.

Stratigraphic analyses indicated the nature of the overburden units to be very similar to those at the Hanna sites with the exception of unit A (Figure 3-4). Unit A at the Hanna test area had much more sandstone than at the Rocky Mountain 1 site. The unit consists dominantly of siltstone with some minor sandstone and is more homogeneous, harder, and less permeable than unit A at the Hanna sites. All of these factors are advantageous to UCG operation and should contribute to less water influx and roof collapse.

The coal has three correlatable shaley zones, one near the top and two near the base (Figure 3-5). The partings are carbonaceous and range from 1 to 2 feet in thickness. A sample of the shaley zone material exhibited a heating value of 3656 Btu/lb and it was concluded that the shaley zones would not inhibit gasification significantly. Proximate analyses indicated an average as-received heating value of 8640 Btu/lb, volatile matter at 32 wt %, fixed carbon at 32 wt %, ash at 27 wt %, and moisture at 9 wt %. Ultimate analyses showed average moisture- and ash-free values of 73.4 wt % carbon, 17.3 wt % oxygen, 6.0 wt % hydrogen, 1.8 wt % nitrogen, and 1.5 wt % sulfur. Porosity and swelling index measurements on one sample were 0.2% and 0%, respectively. The average thickness of the coal above the lowest shaley parting is approximately 28 feet.

Structural, stratigraphic and coal quality analyses all indicated favorable characteristics at the Rocky Mountain 1 site for a UCG test.

Table 3-1. Summary of Unit Tops Drill Holes and Core Holes at Rocky Mountain 1 Site

Well Names	Well Type[a]	Ground Elev., ft	Total Depth (elev.), ft	Core Interval (total), ft	Unit D[b]		Unit C[b]		Units B/A[b]		Unit B[b]		Unit A[b]		Coal[b]	
					Depth	T[c]	Depth	T	Depth	T	Depth	T	Depth	T	Depth (elev.)	T
CH-1	D/C	6993.9	402.0 (6591.9)	333.0-379.8 (49.8)	0-38	38[d]	38-158	120	158-346	188	158-315	157	315-346	31	346-377 (6647.9-6616.9)	31
CH-2/TC-1	C	6995.6	397.0 (6598.6)	23.2-397.0 (373.8)	0-39	39[d]	39-165	126	165-356	191	165-321	156	321-356	35	356-386 (6639.6-6609.6)	30
CH-3	D/C	6991.8	400.0 (6591.8)	323.0-400.0 (77.0)	0-54	54[d]	54-191	137	191-355	164	191-308	117	308-355	47	355-386.5 (6636.8-6605.3)	31.5
CH-4/TC-2	D/C	6995.0	392.0 (6603.3)	350.0-392.0 (42.0)	0-52	52[d]	52-182	130	182-356	174	182-333	151	333-356	23	356-386 (6639.0-6609.0)	30
CH-5	D/C	6995.4	402.0 (6593.4)	342.0-402.0 (60.0)	0-49	49[d]	49-186	137	186-356	170	186-320	134	320-356	36	356-386.5 (6639.1-6608.9)	30.5
CH-6	D/C	6966.0	402.0 (6564.0)	364.0-402.0 (38.00)	0-61	61[d]	61-181	120	181-369	188	181-347	166	347-369	22	369-397.5 (6597.0-6568.5)	28.5
CH-7/VIW-3	C	6971.6	395.0 (6576.6)	23.0-395.0 (372.0)	0-34	34[d]	34-184	150	184-358	174	184-329	145	329-358	29	358-389 (6613.6-6582.6)	31
CH-8	D/C	6972.5	408.0 (6564.5)	342.0-401.8 (59.8)	0-45	45[d]	45-174	129	174-358	184	174-324	150	324-358	34	358-389 (6614.5-6583.5)	31
EMW-2	D	6984.5	352.1 (6632.4)	--	0-49	49[d]	49-184	135	184-[d]	--	184-336	152	336-[d]	--	--	--
EMW-8	D	6962.5	355.0 (6607.5)	--	0-59	59[d]	59-187	128	187-[d]	--	187-[d]	--	--	--	--	--
EMW-10	D	6962.0	185.0 (6777.0)	--	0-61	61[d]	61-[d]	--	--	--	--	--	--	--	--	--
TW-1/SC-1/EMW-1	D/C	6983.1	385.0 (6598.1)	340.0-385.0 (45.0)	0-40	40d	40-182	142	182-357	175	182-336	154	336-357	22	357-e (6626.1-e)	--

Table 3-1. Summary of Unit Tops Drill Holes and Core Holes at Rocky Mountain 1 Site (continued)

Well Names	Well Type[a]	Ground Elev., ft	Total Depth (elev.), ft	Core Interval (total), ft	Unit D[b]		Unit C[b]		Units B/A[b]		Unit B[b]		Unit A[b]		Coal[b]	
					Depth	T[c]	Depth	T	Depth	T	Depth	T	Depth	T	Depth (elev.)	T
TW-2/SC-2	D	6994.5	368.0 (6626.5)	--	0-32	32[d]	32-149	117	149-338	189	149-308	159	308-338	30	338-[e] (6656.5-[e])	--
TW-3/SC-3	D	6996.2	379.0 (6617.2)	--	0-48	48[d]	48-185	137	185-350	165	185-303	118	303-350	47	350-[e] (6646.2-[e])	--
TW-4/SC-4	D	6962.2	402.5 (6559.7)	--	0-63	63[d]	63-179	116	179-372	193	179-350	171	350-372	22	372-[e] (6590.2-[e])	--
TW-5/SC-5	D	6996.7	386.0 (6580.7)	--	0-42	42[d]	42-167	125	167-356	189	167-320	153	320-356	36	356-[e] (6610.7-[e])	--
TW-6/EMW-3	D	7004.0	376.0 (6628.0)	--	0-45	45[d]	45-173	128	173-350	177	173-317	144	317-350	33	350-[e] (6654.0-[e])	--
TW-7/EMW-7	D	6958.9	389.0 (6569.9)	--	0-56	56[d]	56-173	117	173-358	185	173-[d]	--	[d]-358	--	358-[e] (6600.9-[e])	--
TW-8/EMW-6	D	6959.8	446.0 (6513.1)	--	0-62	62[d]	62-188	126	188-361	173	188-[d]	--	[d]-361	--	361-392 (6598.1-6567.1)	31
TW-9/EMW-9	D	6959.8	393.3 (6566.5)	--	0-57	57[d]	57-180	123	180-362	182	180-[d]	--	[d]-362	--	362-[e] (6597.8-[e])	--
TW-10A/EMW-11A	D	6978.7	377.0 (6601.7)	--	0-37	37[d]	37-162	125	162-347	185	162-298	136	298-347	49	347-[e] (6631.7-[e])	--
TW-11	D	7005.5	357.8 (6647.7)	--	0-44	44[d]	44-137	93	137-329	192	137-300	163	300-329	29	329-[e] (6676.5-[e])	--
TW-12	D	7007.0	371.0 (6636.0)	--	0-46	46[d]	46-159	113	159-342	183	159-330	171	330-342	12	342-[e] (6665.0-[e])	--
TW-13	D	6976.5	401.0 (6575.5)	--	0-63	63d	63-193	130	193-374	181	193-337	144	337-374	37	374-e (6602.5-e)	--

Table 3-1. Summary of Unit Tops Drill Holes and Core Holes at Rocky Mountain 1 Site (continued)

Well Names	Well Type[a]	Ground Elev., ft	Total Depth (elev.), ft	Core Interval (total), ft	Unit D[b]		Unit C[b]		Units B/A[b]		Unit B[b]		Unit A[b]		Coal[b]	
					Depth	T[c]	Depth	T	Depth	T	Depth	T	Depth	T	Depth (elev.)	T
TW-14	D	6948.6	404.0 (6544.6)	--	0-105	105[d]	105-195	90	195-372	177	193-303	108	303-372	69	372-[e] (6576.6-[e])	--
TW-14A/CH-9	D/C	6954.0	426.2 (6527.8)	345.6-426.2 (80.6)	0-81	81[d]	81-194	113	194-384	190	194-321	127	321-384	63	384-414 (6570.0-6540.0)	30
TW-15	D	6965.3	420.0 (6545.3)	--	0-83	83[d]	83-198	115	198-391	193	198-347	149	347-391	44	391-[e] (6574.3-[e])	--
TW-16	D	6984.5	416.0 (6568.5)	--	0-72	72[d]	72-181	109	181-384	203	181-325	144	325-384	59	384-[e] (6600.5-[e])	--
TW-17	D	6971.9	357.0 (6614.9)	--	0-17	17[d]	17-131	114	131-327	196	131-276	145	276-327	51	327-[e] (6644.9-[e])	--
TW-18	D	6992.6	323.0 (6669.6)	--	eroded	--	0-93	93[e]	93-291	198	93-256	163	256-291	35	291-[e] (6701.6-[e])	--
CBO-152/EMW-5	D	6980.6	420.0 (6560.6)	--	0-67	67[d]	67-196	129	196-374	178	196-333	137	333-374	41	374-[e] (6606.6-[e])	--

[a] D - drill hole
C - core hole
D/C - combination drill and core hole

[b] Unit intervals determined from well logs and measured in feet

[c] Thickness

[d] Unit eroded at surface

[e] Insufficient drilling or logging for determination

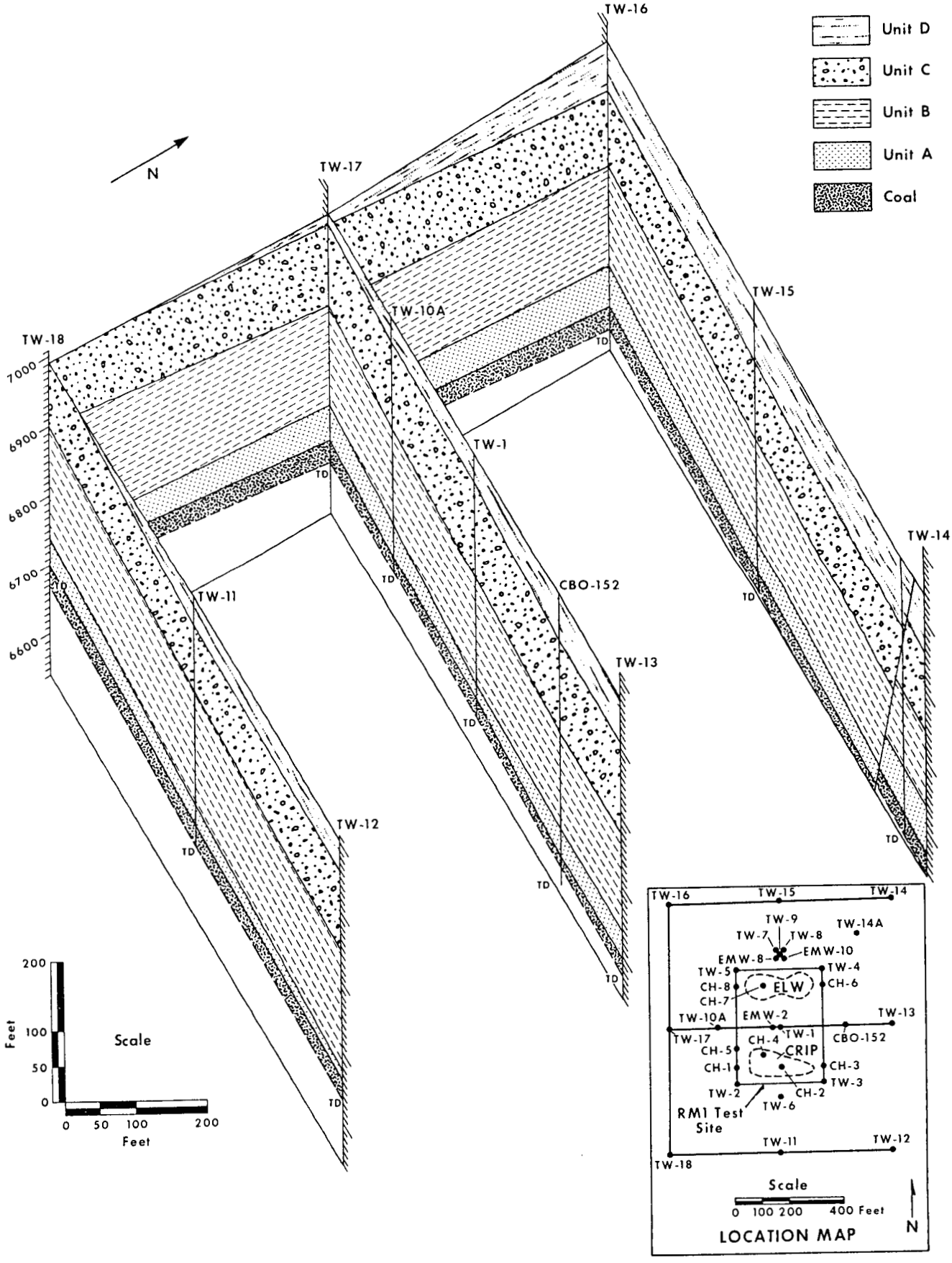

Figure 3-2. Fence Diagram of the RM1 Site

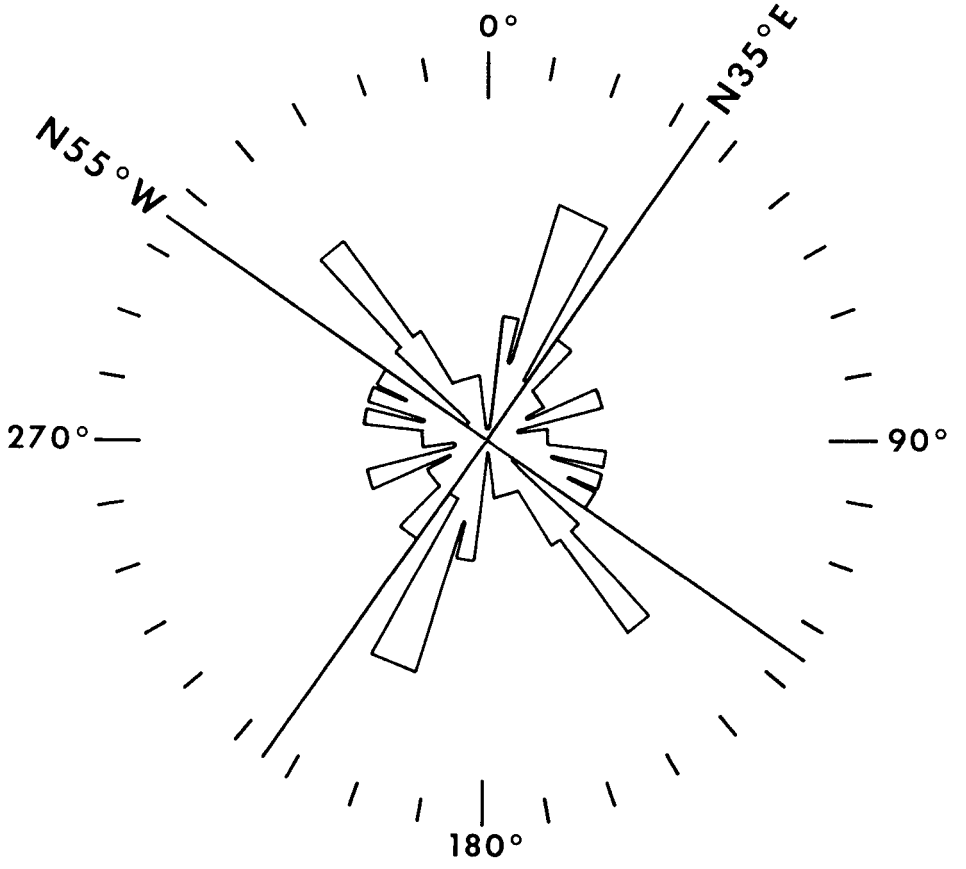

Figure 3-3. Comparison of Cleat Orientations from Existing and Field Study Data for the Hanna Basin (Rose diagram from oriented core and mine data, Pasini et al. 1972; Glass and Roberts 1980)

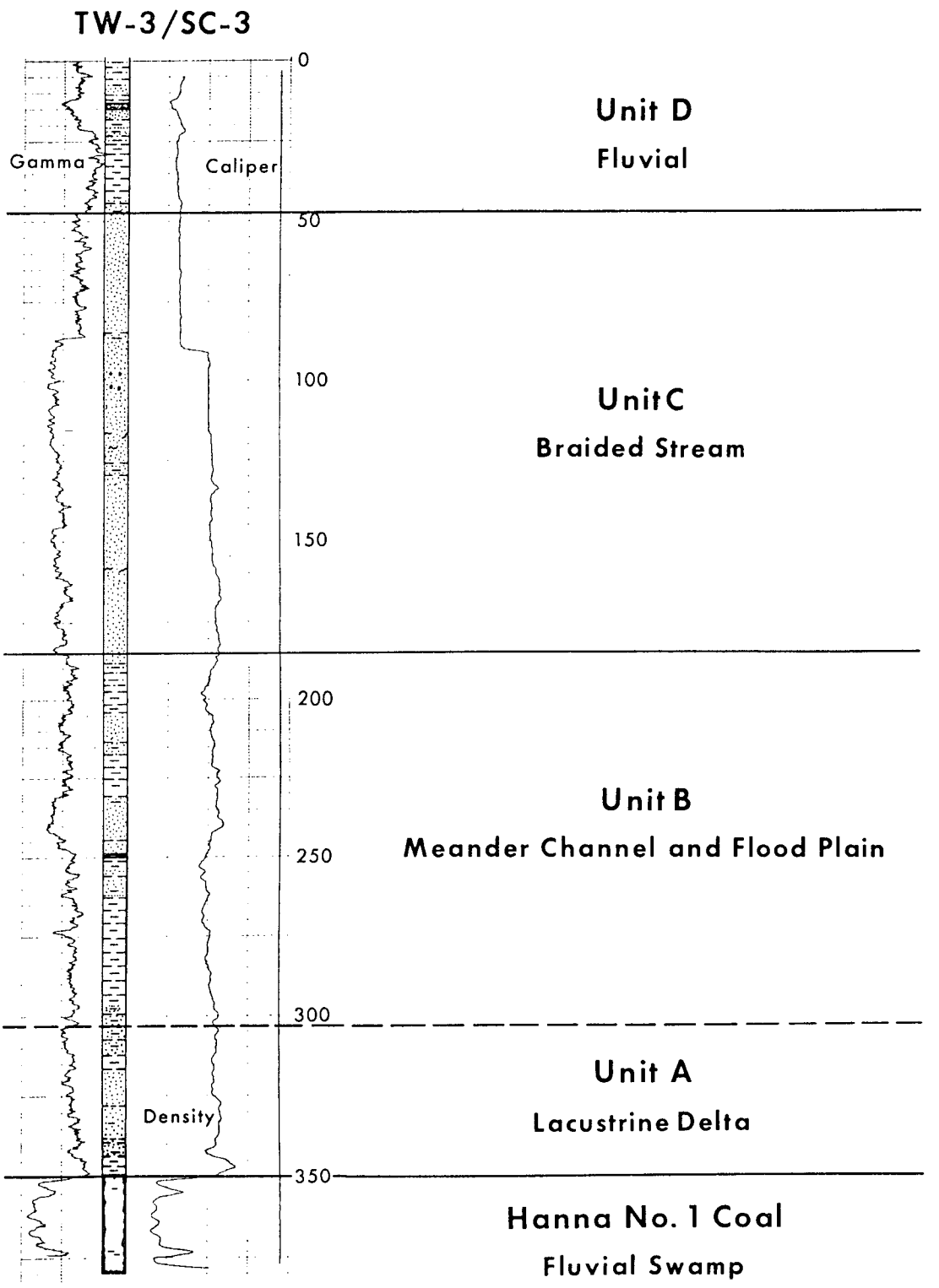

Figure 3-4. Overburden Units at the RM1 Site

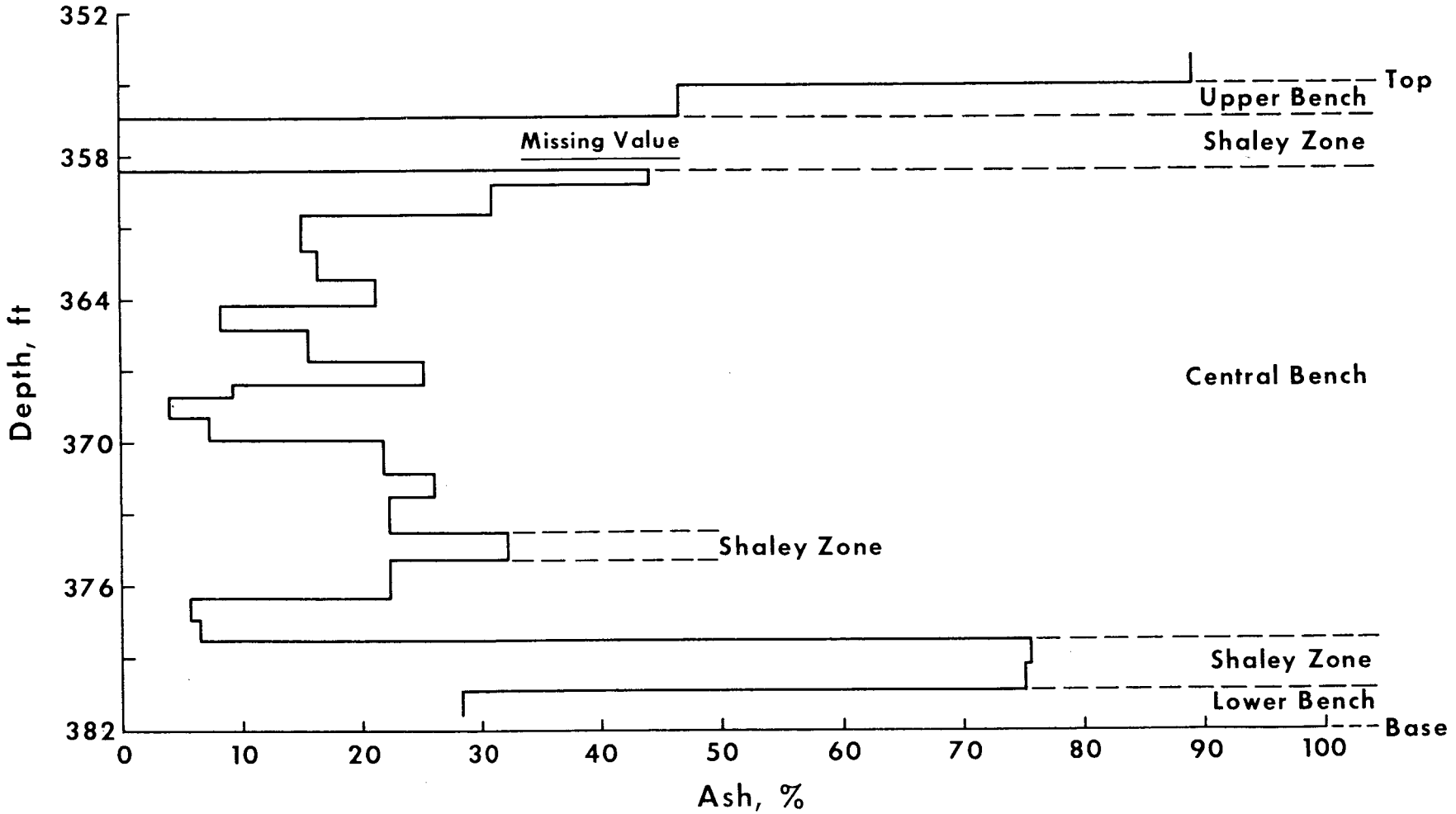

Figure 3-5. Percentage Ash vs. Depth, SC-1

Environmental Results of Tono Excavation. The underground coal gasification cavity resulting from the 1983 controlled retracting injection point (CRIP) experiment, conducted at a site near Centralia, Washington, was excavated by Western Research Institute during the summer of 1986. Samples were taken from the cavity and through the cavity sidewalls to use in laboratory studies designed to identify groundwater impacts resulting from the process. An unaltered section was also sampled to use for comparison and for preparation of heat-affected samples of known temperatures.

A major environmental concern of underground coal gasification is groundwater contamination through leaching of heat-altered material. Laboratory experiments were conducted to identify major leachate constituents and their relationships to the various altered rock types. In addition, information was gained that had implications for groundwater restoration design, including postburn and operating techniques.

Thirty-day batch equilibration tests were used to simulate a leaching environment. Five different sample types were leached in the laboratory with deionized-distilled water kept at a constant temperature of 25°C (77°F). The first three types were prepared by heating unaltered coal at three different temperatures, 300°, 400°, and 500°C (572°, 752°, and 932°F). The 500°C (932°F) sample was heated under oxygen to ash the material, while the other two samples were heated without oxygen to make char. Slag and altered overburden taken from the cavity were used as the fourth and fifth types. The material was leached for 30 days with water samples taken after days 1, 4, 15, and 30 to examine time-dependent equilibrium conditions. The water samples were analyzed by various techniques for parameters with known association with UCG. Analytical accuracies were ± 10%. In addition, the bulk mineralogy of the material was identified by x-ray diffraction analyses.

Mineral matter in the coal, altered coal, ash, and slag sequence (Table 3-2) changed from quartz, feldspars, and clay minerals with minor amounts of calcite, pyrite, and gypsum to quartz and high-temperature minerals. The sequence exhibits a gradual loss of clay minerals, calcite, pyrite, and gypsum, indicating these minerals were decomposed with increasing temperature. Minerals in the overburden indicated changes toward sodium, calcium, and iron-rich minerals with increasing temperature.

Constituents in the leachates from the two char samples were similar within analytical accuracy and precision. High concentrations of calcium, magnesium, sodium, sulfate, and total dissolved solids were observed with smaller amounts of boron, ammonia, and total organic carbon. The leachate from the ash contained similar constituents with the exception of ammonia and total organic carbon. Leachates from the slag and altered overburden contained minor amounts of calcium, magnesium, sodium, sulfate, total dissolved solids, and total organic carbon. No changes within analytical accuracies were noted over time.

Table 3-2. Mineralogic Summary for Material Types Subjected to Leaching

Mineral	Unaltered Coal	Char 300°C	Char 400°C	Ash 500°C	Slag	Unaltered Overburden	Altered Overburden
Quartz (SiO_2)	XXX	XXX	XX		XX	XXX	XXX
Feldspars[a]	XXX	XXX	XX	XX		XX	X
Clay Minerals[b]	XX	XX	X			X	X
Calcite ($CaCO_3$)	X	X					
Pyrite (FeS_2)	X	X					
Gypsum ($CaSO_4 \cdot 2H_2O$)	X	XX	XX				
Mullite ($Al_6Si_3O_{15}$)					XX		
Tridymite (SiO_2)				XXX			XX
HiT° Feldspars[c]				X	XX		XX
Ferrocordierite ($Fe_2Al_4Si_5O_{18} \cdot nH_2O$)			XX				
Alkermanite/Gehlinite $Ca_2MgSi_2O_7$-$Ca_2Al(Al,Si)_2O_7$			X				
Cordierite ($(Mg,Fe)_2Al_4Si_5O_{18} \cdot nH_2O$))							XX

Note:
X = minor
XX = moderate
XXX = abundant

[a] Feldspars identified include albite ($NaAlSi_3O_8$) and orthoclase or microcline ($KAlSi_3O_8$).

[b] Clay minerals identified include illite [$KAl_2(Si_3AlO_{10})(OH)_2$], kaolinite [$Al_2Si_2O_5(OH)_4$], chlorite [$(Mg,Al)_6(Si,Al)_4O_{10}(OH)_8$], and smectite [$Na_x((Al_{2-x}Mg_x)Si_4O_{10}(OH)_2)$].

c High-temperature feldspars include albite, high ($NaAlSi_3O_8$) and anorthite ($CaAl_2Si_2O_8$)

The major constituents (calcium, magnesium, sodium, sulfate, and total dissolved solids) were generated predominantly from char and ash (Table 3-3). The minor constituents (boron, ammonia, and total organic carbon were generated predominantly from the char. Leaching of calcium, magnesium, sodium, sulfate, and total dissolved solids was probably related to the partial alteration of carbonate, clay, and sulfurous mineral structures by moderate temperatures of 300°-500°C (572°-932°F). Since boron, ammonia, and total organic carbon were primarily leached from the char, it was assumed that these constituents remained on the char after partial pyrolysis and were subsequently leached. An order of magnitude difference in concentrations generated from the char and ash compared with those generated from the slag and altered overburden was observed (Table 3-3). The low concentrations of constituents leached from the slag and altered overburden suggest that high-temperature minerals found in these samples were insoluble or impermeable.

Table 3-3. Comparison of Leachate from Various Rock Types (Day 30 Samples), mg/l^{-1}

Parameter	Char 300°C	Char 400°C	Ash 500°C	Slag	Altered Overburden
Calcium	605	680	784	23.0	60.5
Magnesium	146	61.5	1.9	5.7	20.7
Sodium	82.5	62.5	98.1	20.1	39.1
Sulfate	2000	1900	2100	82	830
TDS	3500	3200	3500	210	470
Boron	23.7	24.5	19.2	0.29	<0.25
Ammonia	10.4	2.8	0.4	<0.2	<0.2
TOC	28	29	12	<10	<10

The fact that the majority of leachate from a gasification cavity is derived from char and ash has great significance for operational and restoration procedures. Char and ash comprise a small part of a UCG cavity and are usually located around the cavity perimeter. The perimeter area is, therefore, the major source for potential contamination of groundwater by leaching. Test operation and shutdown procedures should operate below hydrostatic head to allow for maximum influx of groundwater through the sidewalls and into the cavity. Groundwater treatment designs should allow for removal of calcium, magnesium, sodium, sulfate, boron, ammonia, and organic carbons.

Western Non-Swelling Coal Contaminant Control. Previous field tests have demonstrated the technical feasibility and confirmed the commercial potential of underground coal gasification (UCG); however, groundwater contamination may hamper further research. A laboratory simulator has been developed to study postburn UCG coal pyrolysis and groundwater contamination. To date, 30 simulation tests have been completed. The first 24 experiments were funded by the Gas Research Institute (GRI) and the last six tests, discussed here, were funded by DOE.

For the six experiments, cored samples, 3 inches in diameter and 1-foot long, were taken parallel to the bedding plane from blocks of Hanna No. 1 coal. Each sample was placed in the reactor vessel, which allowed for the simulation of a differential element of the cavity sidewall (Figure 3-6, Detail A). Simulations in the reactor included the basic physical components of the differential element: rubble, char, pyrolyzed coal and unaltered coal. The coal char and pyrolyzed zones were created by heating the coal face with hot air. When the reaction temperature was achieved, a combustion zone was allowed to develop at the coal face and then injection was terminated.

Besides duplication of the physical components of the simulation element, the reactor was designed to simulate a variety of postburn conditions that the element might be exposed to in actual field conditions. Controlled cooling of the rubble zone simulated the heat transfer that could occur at field conditions. Water and steam injection into the coal and rubble zones simulated natural water influx.

The last six tests (experiments 25-30) were designed to address the effects of fractures, both naturally occurring in the virgin coal and thermally induced by postburn pyrolysis. Experiments 25 and 26 were designed to evaluate postburn pyrolysis in a cavity sidewall in the presence of a wide steam plateau during the gasification phase. Experiment 27 was designed to simulate an extensive tight natural fracture in the coal seam, while experiment 28 simulated a wide thermally induced fracture. For experiment 29 a coal core was soaked and then frozen to produce a microscopic fracture network to simulate a tight random fracture network. The last test, experiment 30, was conducted on a competent coal core with no visible fractures to simulate a case where the coal was not fractured.

The results of the contamination control research have led to the conclusion that minimization of postburn pyrolysis requires cooling of the rubble-coal char interface. This cooling is best achieved by reducing the cavity pressure to promote natural groundwater intrusion (Table 3-4). The wide fractures (experiment 25) typically present after gasification relieve steam-generated pressure and reduce penetration into the coal. Tighter fractures (experiments 27 and 29) did not produce pressures sufficient to fracture the coal, but sufficient injection pressure increases that caused the steam zone to penetrate deeper into the coal.

Previous work (experiment 23) showed that competent coal cores could spall with gasification-induced fractures on the face. Steam generation occurred in low permeability regions behind the fracture network, causing pressure buildups sufficient to fracture not only the coal, but the castable refractory surrounding it. Consequently, the reduction of postburn pyrolysis and contaminant generation by cavity depressurization is very strongly influenced by the native permeability of the coal seam.

The results of the UCG contaminant control research, conducted to date, indicate that ignition of a coal seam can be accomplished at pressures slightly above hydrostatic. However, the remainder of the

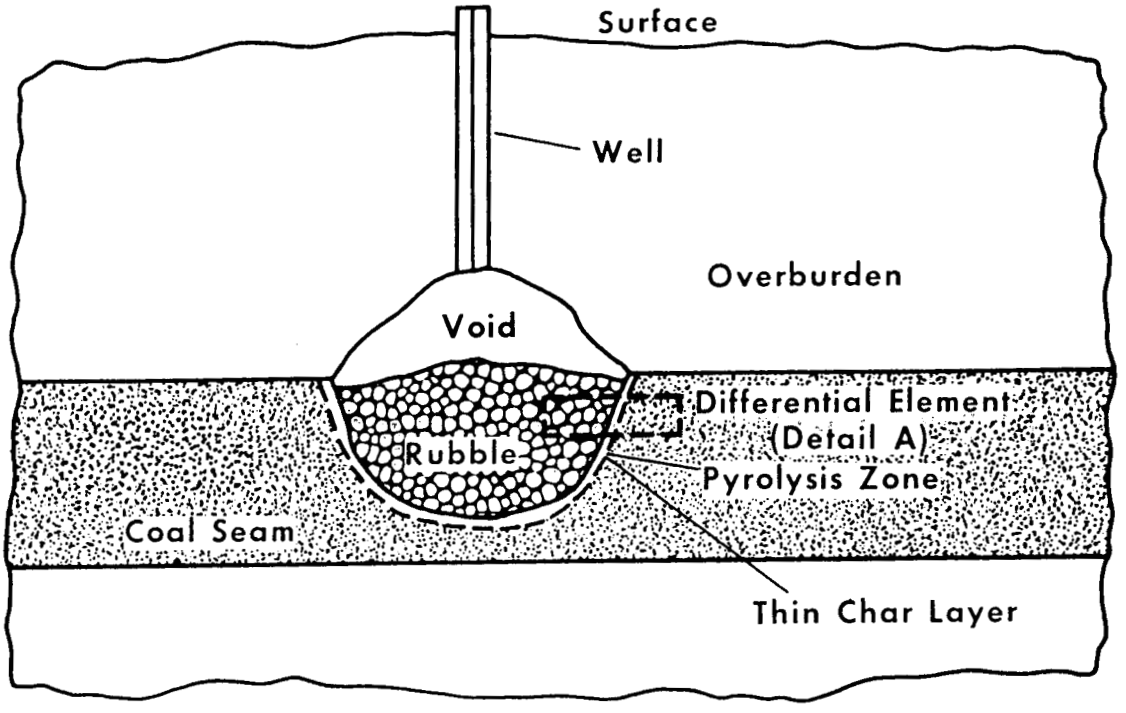

FIELD SITUATION

DETAIL A

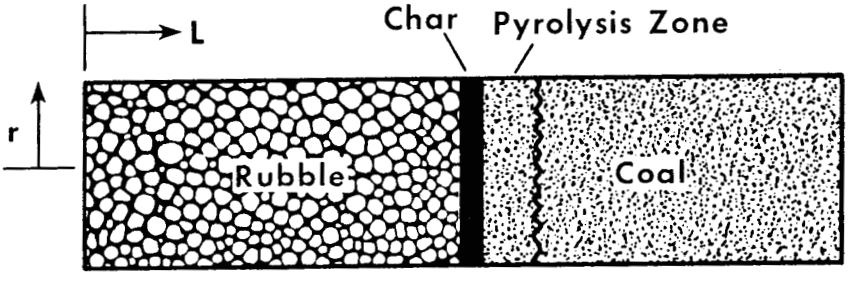

DIFFERENTIAL ELEMENT
FOR SIMULATION

Figure 3-6. Simulation of UCG Postburn Pyrolysis

Table 3-4. Experimental Pressure Drops

Experiment	Flow, g/min	Pressure Drop, psi	Remarks
26	4	<1	Steam injection in preheated core
27 cold	1.0	4	Tight fracture through core
27 hot	1.0	65	
28 cold	0.3	45	1/8" fracture halfway through core
28 hot	0.3	20	
29 cold	0.2	6	Tight random fracture
29 hot	0.15	22	Network
23 cold	2.2	80	Competent coal core
23 hot	2.2	105	Showed multiple fractures after test

gasification phase should be operated below hydrostatic pressure to minimize gas losses. A gradual reduction in cavity pressure from gasification to postburn venting is recommended to prevent coal spalling, which can cause contaminants to be deposited into the cavity and more coal surface area exposed for continued generation of contaminants. If widespread spalling is occurring, as evidenced by an increase in pyrolysis gases, then the cavity pressure should be increased to prevent spalling.

Eastern Bituminous Coal Containment Generation and Control. The removal of residual contaminants from Illinois Herrin #6 coal cavities was the subject of this study. Simulated 6-inch UCG cavities were generated in two 18-inch cubes of Herrin #6 coal. The gasification was effected using a 60% by volume oxygen mixture of steam and oxygen. One of the blocks was cooled and contaminant residues on the coal and char were sampled. The second was leached using a circulating batch technique for 1200 hours. The leach rate was found to be an inverse function of the square root of time. Application of a transient diffusion model for a semi-infinite wall allowed the determination of phenolic species concentrations in the coal pores. This concentration agrees well with known solubilities of phenolic compounds in water. Simulation conditions did not allow bulk flow. It is concluded that removal of contaminants from the cavity sidewall can be hastened by promoting water influx from the coal seam aquifer into the UCG cavity. Under these conditions, it is expected that the bulk flow term in the

transport equation will dominate, greatly reducing the time required for cavity cleanup. Data analysis is currently in progress.

3.1.2 Groundwater Impact Mitigation

Hanna Groundwater Restoration. The research design for the Hanna restoration was developed to test the effectiveness of contaminant removal and the cost of techniques to restore UCG cavities to preburn conditions. Two different contaminant conditions existed at the Hanna UCG site. The Hanna III cavity (Figure 3-7) had concentrations of total dissolved solids (TDS) and sulfate above the limits established by the Wyoming Department of Environmental Quality (WDEQ) and the Hanna I cavity (Figure 3-7) had a total phenols concentration above WDEQ water quality limits.

The techniques chosen for contaminant abatement at the Hanna UCG site were selected for cost effectiveness, ability to meet regulatory requirements, and to permit abandonment of the site within one year.

To accomplish the objectives of the project a two-phase clean-up approach was taken. Phase one was the cleanup of the Hanna cavity III waters. The most effective method to remove the contaminants from the cavity is pumping the waters into an evaporation pond, which will allow land disposal of the solids. However, the hydrology of the area allows for very slow recharge of the cavity. It would take about 10 years to fully refill the cavity, which would require groundwater monitoring on a quarterly basis until the cavity had fully recharged. To avoid this, clean water was pumped into the cavity.

Phase two of the project was the cleanup of the Hanna I cavity waters. The cleanup technique chosen was carbon adsorption. In this technique cavity water is pumped through a carbon adsorption system and the effluent is suitable for surface discharge. The hydrology in this area of the site allows for a much faster recharge rate than for the Hanna III cavity, so long-term groundwater monitoring will not be necessary. Since the result of this cleanup technique is clean water, it was used as the recharge water for the Hanna III cavity.

Phase one began with the construction of an evaporation pond with a synthetic liner and leak detection system. The capacity was large enough for the estimated volume of water contained in the cavity. The cavity was pumped continually at 25 gallons per minute for five days for a total volume of 172,147 gallons. Water level measurements indicated additional water remained in the cavity; therefore, an additional 35,953 gallons were removed for a total of 208,100 gallons. Water level data and daily pumping totals for the site are shown in Table 3-5.

Quality of the cavity water remained constant throughout cavity evacuation (Table 3-6), indicating a homogeneous system with negligible dilution from or influx of additional water. The water level measurements in Table 3-5 support this indication. Recharge of the cavity before injection of water was negligible.

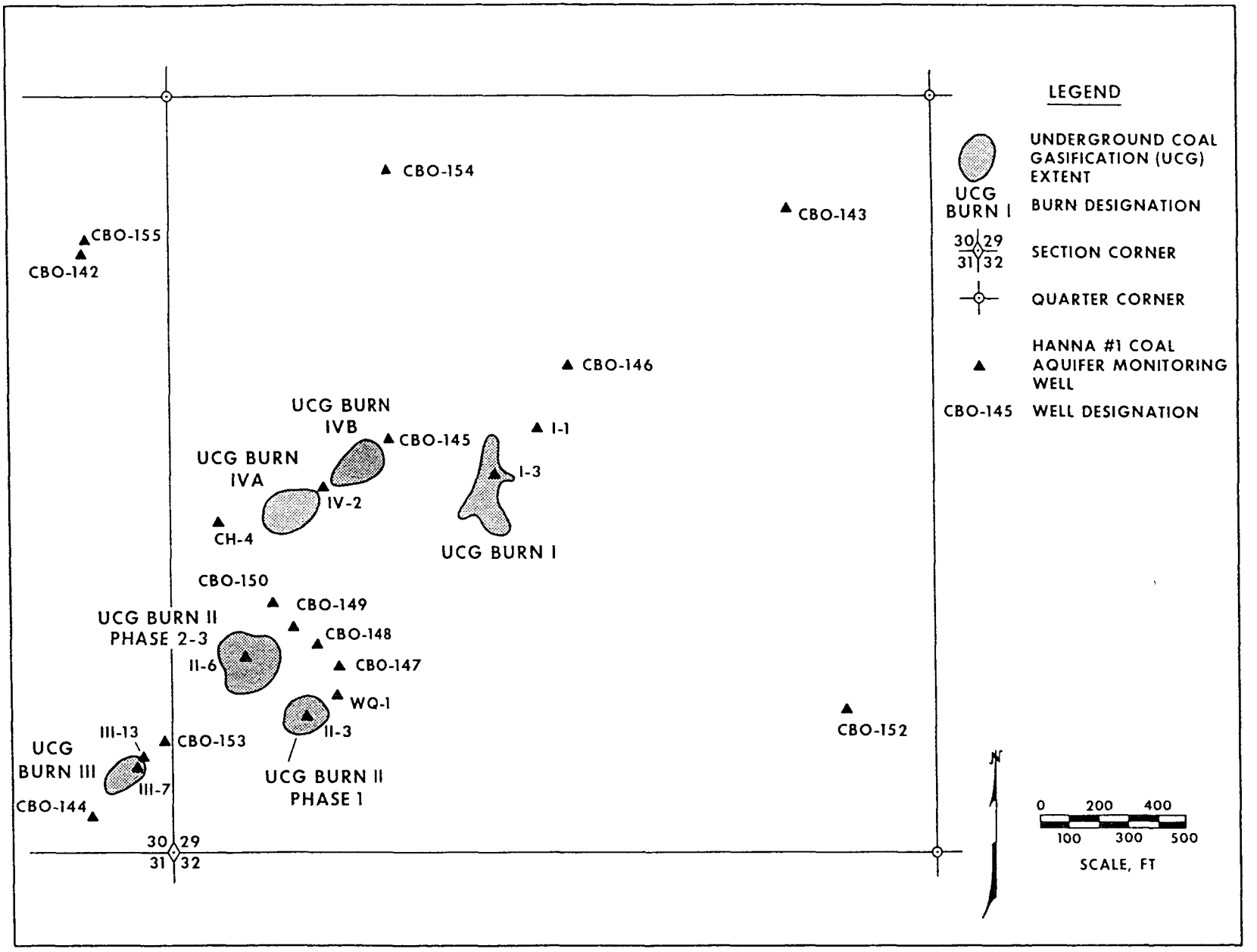

Figure 3-7. Hanna Underground Coal Gasification Site, T22N, R81W, Carbon County, Wyoming

Table 3-5. Water Levels (in feet)

Day	1	2	3	4	5	6	7	
Volume	0 gal	32,510 gal	69,360 gal	102,170 gal	139,810 gal	172,147 gal	208,100 gal	
				Water Levels (in feet)				Total Drop
Well								
III-7	120.5	145.5	153.7	159.7	164.5	169.4		
III-4	118.7	120.2	122.0	123.5	124.7	125.5		
CBO 144	119.0	122.3	124.2	125.7	127.1	127.9	ND	8.9
OVB 139	132.0	132.3	133.0	133.6	134.2	134.6	ND	2.6
CBO 153	125.0	132.8	138.5	142.8	146.9	150.0	ND	25.0
III-13	122.8	131.7	138.6	143.7	148.5	152.8	ND	30.0
II-6	157.6	157.6	157.6	ND	ND	157.6	ND	0.0
CBO 150	153.7	153.7	153.7	ND	153.7	153.7	ND	0.0
CBO 149	151.8	ND	ND	ND	ND	151.6	ND	0.2
CBO 148	147.2	147.1	146.9	ND	146.6	146.5	ND	+0.7
WQ-1	148.3	ND	ND	ND	148.2	148.2	ND	+0.1
II-3	153.7	153.8	153.8	153.8	153.8	153.8	ND	0.1

Note: ND = Not determined

Table 3-6. Hanna III Cavity Water Quality

Parameter	Day 1	2	3	4	5	6	7	8[a]	9[a]
TDS, mg/L	7600	7600	7700	7640	7560	7610	5310	6000	6720
Sulfate, mg/L	5200	5300	5200	4700	4700	4800	2870	3560	4150
pH	7.3	7.4	7.5	7.7	7.6	7.6	7.4	ND[b]	ND
eH	7.6	6.8	7.7	7.7	7.7	7.6	6.0	ND	ND

[a] Pumping was completed at day 7.

[b] ND = not determined

Phase two, treatment of Hanna cavity I, began with the installation of a new well into the cavity. The original well, I-3 (Figure 3-7), was a process well that had degraded to the point that the submersible pump required for the carbon adsorption system would not go to the bottom of the cavity. So, a new well was placed next to I-3. The cavity water was pumped through the carbon adsorption system and injected into Hanna cavity III.

Phenols were not detected in the cavity water from the new well (Table 3-7). It is speculated that since well I-3 was a process well, tars accumulated on the casing and these are leached during sampling.

Table 3-7. Hanna I Cavity Water Quality (Wellhead Samples)

Parameter	Day 1	2	3	4	5
Phenols, µg/L	<20	<20	<20	<20	<20
TOC, mg/L	13	15	<10	33	21
pH	7.7	7.7	7.9	8.0	8.1
eH	2400	2540	2440	3190	2440

The cavity water was pumped through the system to allow for injection of the water into Hanna III to maintain permit compliance. On September 17, 1987, after 122,284 gallons had been treated and injected into the Hanna III cavity, WRI was notified to stop operations and injection into the Hanna III cavity.

The Hanna III cavity water has not been tested since the water injection. The last water quality sample taken before injection contained parameters above target levels. Since the water quality did not change during the initial removal, the addition of clean water should have reduced the levels. To what extent has not yet been determined.

There is approximately 85,000 gallons less than the starting water volume in the cavity. It is difficult to determine the volume of the cavity; however, it is estimated that 80% of the water volume was removed. Injection replenished the cavity to approximately 60% of the starting volume. It will take approximately five years to recharge the cavity to initial levels.

The Hanna I cavity appears to have no contaminants above regulatory limits. It is estimated that 60% of the initial water remains in cavity I with complete charge expected to occur in three years.

WRI recommends that water quality and levels in both cavities be monitored at quarterly intervals. If water quality in the cavities are below regulatory limits for four sampling periods, the WDEQ should be petitioned to permit site abandonment.

It is also recommended that only wells that were installed as monitoring wells be used to determined groundwater quality. Process wells should not be used as they may give false conditions as shown in Hanna cavity I.

Hoe Creek Groundwater Restoration. The Wyoming Department of Environmental Quality (WDEQ) has directed that phenol levels in groundwater from wells WS-22 and WS-10 at the Hoe Creek site should be less than 20 parts per billion (ppb) before the U.S. Department of Energy can be released from further obligation at the site. The Western Research Institute conducted treatment tests to determine the effectiveness of treating 2 million gallons of contaminated groundwater. Wells WS-22 and WS-10 contained the highest phenol concentrations of the monitoring wells at the Hoe Creek site and, therefore, were used for evaluating groundwater restoration.

A groundwater treatment demonstration test was completed at the Hoe Creek underground coal gasification site from August to October 1986. The treatment system consisted of cartridge filter vessels, granular activated carbon adsorbers, and ancillary equipment. Concentrations of phenols in well WS-10 initially decreased but then increased significantly during the test. Concentrations of phenols in well WS-10 and WS-22 were 960 ppb and 260 ppb, respectively, at the conclusion of the test. A total of 129,000 gallons of groundwater was treated.

A new treatment system was assembled and placed in service on July 2, 1987. The treatment system, illustrated by Figure 3-8, was sized to treat approximately 25 gallons per minute, the maximum water flow that could be pumped from wells WS-10 and WS-22. The treatment system consisted of cartridge filters or diatomaceous earth filter vessels, three granular activated carbon adsorbers in series, and

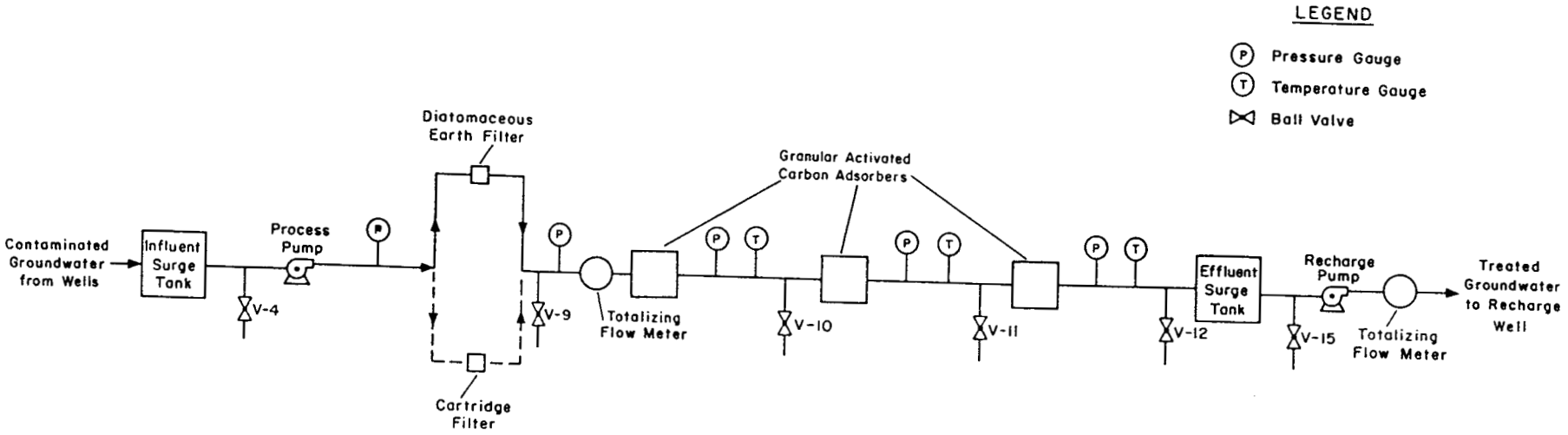

Figure 3-8. Groundwater Restoration Treatment System

auxiliary equipment. Each adsorber contained 60 cubic feet (1500 lbs) of Calgon Filtrasorb 300 carbon. In wells WS-10 and WS-22 the average flow rates of 18.0 and 6.0 gallons per minute (gpm), respectively, were maintained throughout the test period, which was terminated August 29 after 2 million gallons were treated. The system was operated 24 hours a day for 7 days a week. The treated water was reinjected into the Hoe Creek II cavity.

Following shutdown, wells WS-10 and WS-22 were monitored for phenols. Then the treatment system was restarted September 9. For this test the treated water was discharged on the surface 110 feet NNW of the injection port for the gasification cavity. After processing about 20,000 gallons of groundwater, the water treatment system was shut down and removed from the site.

Several water quality parameters were monitored, but phenol concentration proved to be the easiest to measure and most reliable indicator of contamination. Phenol was determined by the distillation colorimetric method. All water samples were delivered to Western Research Institute for analysis by appropriate QA/QC procedures.

The treatment system removed phenols to below detectable limits (less than 20 ppb) as determined in effluent samples collected four times a week. Samples collected after the first and second adsorber also showed phenols less than 20 ppb, indicating that one adsorber was sufficient to treat 2 million gallons. However, the first carbon adsorber was taken off line during the last few days of the test because of excessive pressure buildup from suspended solids that escaped the pretreatment system. Particle-size analyses of well water samples showed that a significant fraction of the suspended solids consisted of particles 5 microns or less in diameter. Five-micron cartridge filters were used to remove suspended solids.

Well WS-10 phenol concentration decreased from 974 ppb on July 2 to the 218-to-251 ppb range by August 29. After shutdown, phenol concentrations decreased to the 97-to-155 ppm range. Upon startup on September 9 phenol concentrations increased and leveled off to the same level that occurred before the first shutdown on August 29, about 218 to 251 ppb. Phenol concentration data are given in Figure 3-9.

Well WS-22 phenol concentrations increased slightly after startup on July 2, and then decreased to the 144-to-189 ppb level by August 29. After shutdown, phenol concentrations increased slightly, and then decreased after startup September 9 (Figure 3-9).

When the treated water was injected into the gasification cavity, which is upgradient of wells WS-10 and WS-22, the water level in the cavity rose about 3 feet. Water levels in groundwater monitoring wells upgradient (north and west) of the cavity increased, and water levels in monitoring wells in the contaminated aquifer downgradient (east) of the cavity decreased. The water level in wells penetrating the Felix II coal seam (the lower, thicker seam separated from the Felix I coal seam by 10 to 54 feet of siltstone and mudstone) was unaffected.

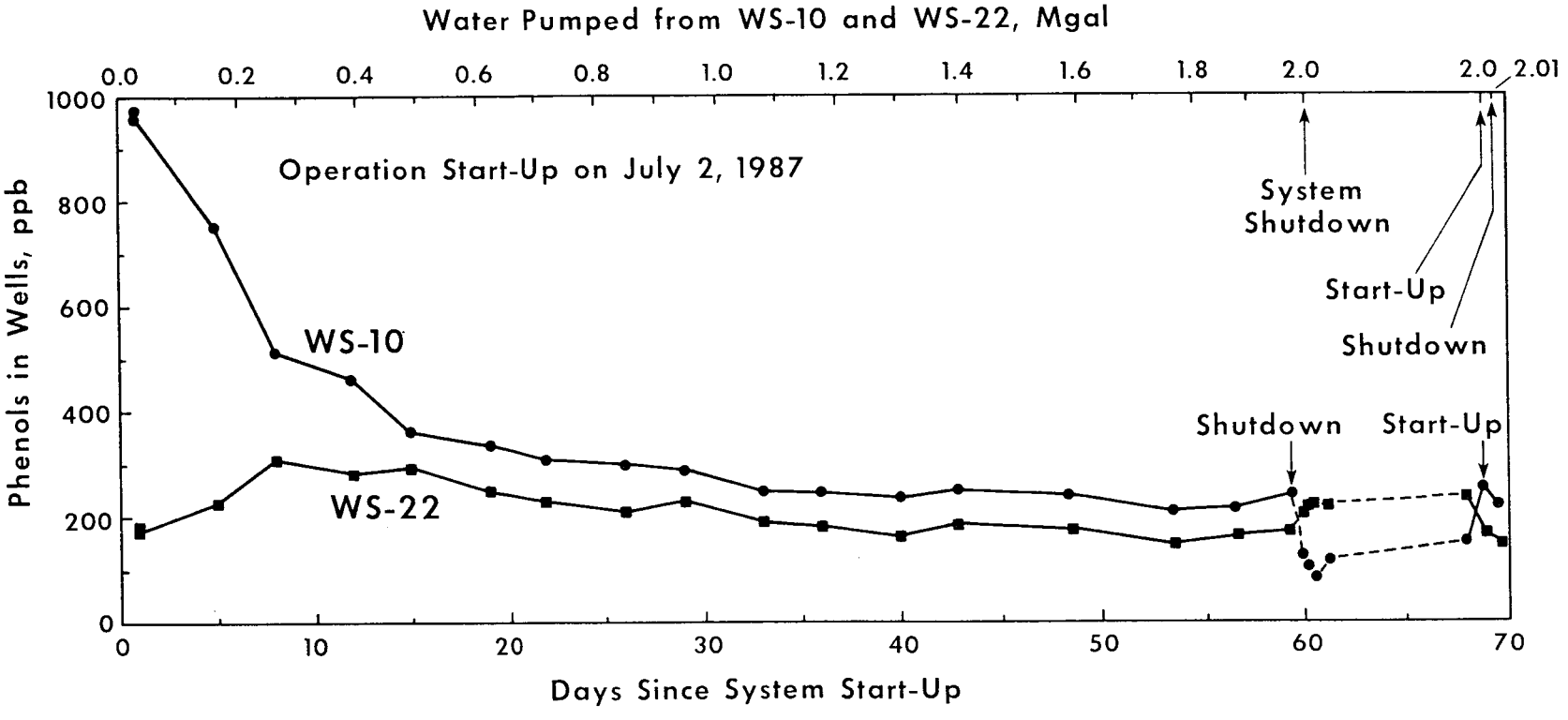

Figure 3-9. Concentration of Phenols in Wells During Groundwater Restoration Program

Water level measurements taken over the July-September period indicated that pumping from wells WS-22 and WS-10 withdrew water from the Felix I coal seam downgradient from the cavity and induced leakage into the coal seam from the overburden aquifer. The Felix II coal seam was unaffected. Concentrations of phenol in water pumped from WS-10 generally remained low after shutdown and again after startup on September 9. There may be a pocket of higher phenol concentrations between WS-10 and WS-22 or between WS-10 and the gasification cavity. This pocket may have been leached progressively during continuous withdrawal of water from WS-10. Different flow regimes in relation to this hypothesized pocket of higher phenol concentration may account for the decrease in WS-10 phenol concentration when operation ceased August 29, and a corresponding increase when operation resumed September 9.

While the treatment operation significantly reduced groundwater phenol concentrations, they were still almost an order of magnitude higher than the target of 20 ppb. The very slow rate of phenol decrease (Figure 3-9) shows that it would be very difficult to reach the target concentration (20 ppb) by groundwater treatment with surface treatment alone.

The following are recommended:

1. Groundwater contamination should be minimized by proper control of underground coal gasification burn parameters. This includes controlling the burn at pressures less than the groundwater pressure and by treatment of groundwater entering the cavity shortly after the burn.

2. Further groundwater treatment by carbon adsorption is not recommended because of the difficulty in reaching the target phenol value.

3. In situ biodegradation of phenols should be explored. Biological agents have been discovered in UCG-affected groundwaters that degrade phenols.

4. The groundwater should continue to be monitored for phenols. Initial phenol concentrations after the last burn in 1979 were in the range of 10 to 40 parts per million. The phenols decreased in WS-10 to about one part per million by late 1986, and 0.2 ppm by September 1987. They should continue to decrease over time.

PUBLICATIONS AND PRESENTATIONS

Publications

Barker, F. P. "Review of Toxicity Studies Performed on an Underground Coal Gasification Condensate Water," September 1987, DOE/FE/60177-2432.

Boysen, J. E., C. G. Mones, and R. R. Glaser. "Laboratory Simulation of Postburn UCG Contaminant Production," 14th Biennial Lignite Symposium Proceedings, Dallas, TX, May 1987.

Contractor, D. N., and J. D. Schreiber. "Field Applications of Multiple-Aquifer, Ground Water Models for Flow and Transport to Underground Coal Gasification Sites," National Water Well Association Conference on Solving Ground Water Problems with Models Proceedings, Denver, CO, February 1987.

Hill, S. L., and D. J. Kocornik. "Final Report on the Toxicological Testing of Groundwaters Affected by Underground Coal Gasification," September 1986, DOE/FE/60177-2428.

Miknis, F. P., T. F. Turner, and L. W. Ennen. "Low Temperature Isothermal Pyrolysis of Illinois No. 6 and Wyodak Coal," Amer. Chem. Soc., Div. of Fuel Chem., August 1987, 32(3), 148-157.

Oliver, R. L. "Geologic Evaluation of the Proposed Rocky Mountain 1 Underground Coal Gasification Test Site, Hanna, Wyoming," February 1987, DOE/MC/11076-2312.

Oliver, R. L., G. M. Mason, and T. E. Owen. "Correlation of Coal and Overburden Mineralogy with Inorganic Constituents in UCG Process Effluents," Fuel Science and Technology International, June 1987, 5(3), 329-355.

Papers in Preparation

Barrash, W., R. S. Schowengerdt, and P. Smith. "Hydrogeology of the Hoe Creek Underground Coal Gasification Site, Powder River Basin, Wyoming," October 1987, DOE report in review.

Berdan, G. L., B. T. Nolan, W. L. Barteaux, and W. Barrash. "Status Report for the Hanna and Hoe Creek Underground Coal Gasification Test Sites," June 1987, DOE report in review.

Boysen, J. E., C. G. Mones, J. R. Covell, S. Sullivan, and R. R. Glaser. "Investigation of UCG Contaminant Production," 13th Underground Coal Gasification Proceedings, Laramie, WY, August 1987, in review.

Glaser, R. R., and J. E. Boysen. "The Importance of Fluid Flow in the UCG Cavity Sidewall for Controlling Groundwater Contaminants Following Shutdown of Underground Coal Gasification Processes," Laramie, WY, September 1987, DOE report in review.

Mason, J. M., R. L. Oliver, and C. G. Moody. "Geology and Groundwater Hydrology of the Proposed Rocky Mountain 1 Underground Coal Gasification Site, Hanna, Wyoming," 13th Annual Underground Coal Gasification Proceedings, Laramie, WY, August 1987, DOE report in press.

Mason, J. M., R. L. Oliver, J. D. Schreiber, C. G. Moody, P. Smith, and M. J. Healy. "Volume I: Geohydrology of the Proposed Rocky Mountain 1 Underground Coal Gasification Site, Hanna, Wyoming," April 1987, DOE report in press.

Nolan, B. T. "Results of the Groundwater Treatment Demonstration at the Hoe Creek Underground Coal Gasification Site," January 1987, DOE report in press.

Oliver, R. L. "Handbook for Selection and Characterization of Potential UCG Sites," June 1987, DOE report in review.

Oliver, R. L., G. M. Mason, and L. K. Spackman. "Results of Environmental Laboratory Studies Conducted on Samples from the Tono I UCG Cavity Excavation Project," 13th Annual Underground Coal Gasification Symposium Proceedings, Laramie, WY, August 1987, in press.

Oliver, R. L., and L. K. Spackman. "Results of Leaching Experiments Conducted on Samples from the Tono I UCG Cavity," June 1987, DOE report in press.

Sullivan, S., and P. Vaughn. "Status Report on Development of a Cavity Growth Coal Gasification Model for Simulation of Laboratory Tests," September 1987, DOE report in review.

Suthersan, S. "Laboratory Studies on In Situ Biodegradation at the Hoe Creek Underground Coal Gasification Site," September 1987, DOE report in review.

Presentations

Boysen, J. E., C. G. Mones, J. R. Covell, S. Sullivan, and R. R. Glaser. "Investigation of UCG Contaminant Production," presented at the 13th Annual Underground Coal Gasification Symposium, Laramie, WY, August 1987.

Covell, J. R., J. E. Boysen, and R. R. Glaser. "Evaluation of Potential Hydrologic Impacts on the UCG Process and the Environments," 13th Annual Underground Coal Gasification Symposium, Laramie, WY, August 1987.

Mason, J. M., and R. L. Oliver. "Geology and Groundwater Hydrology of the Proposed Rocky Mountain 1 Underground Coal Gasification Site, Hanna, Wyoming," 13th Annual Underground Coal Gasification Symposium, Laramie, WY, August 1987.

Nordin, J. S., W. Barrash, W. Barteaux, and T. Nolan. "Groundwater Treatment at the Hoe Creek Underground Coal Gasification Site," 13th Annual Underground Coal Gasification Symposium, Laramie, WY, August 1987.

Oliver, R. L. "Results from the Controlled Excavation of the Tono I UCG Cavity, Centralia, Washington," 13th Annual Underground Coal Gasification Symposium, Laramie, WY, August 1987.

Oliver, R. L., G. M. Mason, and L. K. Spackman. "Results of Environmental Laboratory Studies Conducted on Samples from the Tono I UCG Cavity Excavation Project," 13th Annual Underground Coal Gasification Symposium, Laramie, WY, August 1987.

WESTERN RESEARCH INSTITUTE

ANNUAL TECHNICAL PROGRESS REPORT

OCTOBER 1986 - SEPTEMBER 1987

ADVANCED PROCESS TECHNOLOGY

4.0 ADVANCED PROCESS TECHNOLOGY

TABLE OF CONTENTS

4.0 ADVANCED PROCESS TECHNOLOGY

4.1 Advanced Process Analysis

Extraction research has involved contaminant control and new technology projects. Contaminant control projects have been designed to investigate concepts for the reduction of pyrolysis contaminants from in situ thermal extraction processes. The fossil energy resources of focus have been unconventional gas, oil shale, tar sand, and heavy oil.

An underground coal gasification test was the first in a planned series of experiments with special apparatus to simulate in situ conditions. Companion research on the geochemistry of in situ pyrolysis products in the environment was designed to determine the rate of pollutant formation from these experiments as well as the chemical and physical properties of the products and the development of a geochemical and hydrologic model. Contaminant control extraction projects have been delayed because of budget, however. New technology and geochemical research projects are the focus of current work.

4.1.1 Contaminant Control

The contaminant control research activity was initiated in 1986 at the Western Research Institute (WRI) to investigate the production and control of groundwater contaminants following in situ thermal extraction and recovery experiments. Although this research applies to oil shale and tar sand extraction, the initial focus has been postburn pyrolysis following the shutdown of advanced underground coal gasification (UCG) projects.

Results of the initial research experiments were reported in "Physical and Numerical Modeling Results for Controlling Groundwater Contaminants Following Shutdown of Underground Coal Gasification" by J. E. Boysen, C. G. Mones, R. R. Glaser, and S. Sullivan, and presented to a DOE peer review held in Tulsa, OK, in March 1987.

The UCG contaminant control research program at WRI was initiated after evaluation of literature describing postburn UCG field test conditions. The initial definition of the numerical simulation element was completed by February and a development of a simplified model was begun.

Design of the physical simulator began in March 1986 using the simulation element and preliminary results from the simplified numerical model. The construction, installation, and shakedown of the physical simulator were completed in August 1986.

An initial series of six physical simulations, designed to determine the effects of three variables on postburn coal pyrolysis and subsequent contaminant generation and migration, was completed in September 1986. The direction of the pressure gradient between the underground production cavity and the coal seam, the rate of water influx through the coal seam, and the rate of water injection into the coal gasification cavity were investigated.

The simulations show that the mobile products of coal pyrolysis (gaseous and liquid) are the source of most contaminants associated with UCG operations and the pressure gradient between the cavity and the coal seam must induce flow into the cavity to prevent introduction of these contaminants into the groundwater.

Phenol levels after pyrolysis and phenol distribution in coal were analyzed from the liquids produced during physical simulations. Other contaminant species produced during gasification were also identified. A transient model has been written and results from the model can be used as a first approximation to estimate pollutant production from pyrolysis reactions during the production of gas and with underground production zone cooldown.

Results from these experiments show that injection of water into the UCG cavity can limit postburn coal pyrolysis and reduce the production of contaminants by cooling the masses of rubble and coal ash in the cavity. However, if the injected water forms channels as it flows through the cavity, the cooling effect is localized and the benefit of the water injection in limiting postburn coal pyrolysis is greatly reduced. Also, water flow through the coal limits postburn pyrolysis and subsequent contaminant generation although steam generated in the hot portions of the coal limits the rate of water flow.

UCG field tests should be operated so that the flow of pyrolysis liquids and gases into the formation is prevented, and the natural influx of water into the cavity is allowed. This can be accomplished by minimizing gas leakage to the formation during gasification, venting the cavity when the gasification process is complete, and being sure water injection into the cavity does not cause the steam generated to create too much pressure in the cavity. The Gas Research Institute has funded more work on this advanced process to analyze operational conditions for the Rocky Mountain 1 UCG field test to be conducted this year in Wyoming.

Advanced processes research for oil shale and tar sand extraction progressed to the point of experimental design when it was determined that because of budget its value was limited to the identification of research needs for programs. Remaining funds and effort have been directed toward the new technology concepts, 4.1.2, for heavy oil and tar sand reactions and the generic geochemical model development, 4.2.2, for thermal extraction and recovery.

4.1.2 New Technology

Novel Concepts--TREE^{SM}. Advanced exploratory research at WRI was begun in 1985 to develop new ideas for extraction and recovery of oil and gas. These novel concepts usually involve problems and technologies that affect multiple domestic resources. The goal of this research is to find significant increases in energy efficiency, favorable economics, and environmental benefits.

Earlier project research is summarized here to provide continuity with experiments and data. Research experiments were completed in 1986

to explore the recovery of shale oil using coal conversion to fuel the in situ thermal recovery process. Gasification and shale oil retorting efficiency were determined from preliminary data obtained in simulations of combined coal conversion and extraction, and recovery of shale oil.

The total resource energy extraction (TREE^{sm}) process, which involves the retorting of oil shale with UCG product gas, has been studied and demonstrated using computer and laboratory simulations. Results of the research have been reported in "In Situ Shale Oil Recovery Using the TREE^{sm} Process" by R. R. Glaser, B. C. Sudduth, J. R. Covell, L. J. Fahy, J. D. Schreiber, C. G. Mones, and L. G. Trudell, in April 1987.

Coal seams are frequently encountered in association with oil shale, tar sand, and heavy oil deposits. Ideally, the coal lies underneath the primary resource for oil production, but the coal gas can also be produced within a few miles of the primary resource. Steeply dipping or horizontal bed UCG technologies can be exploited. The coal seam lying beneath the resource can produce the chemical energy in the coal gas and some of the gas-sensible heat available for thermal extraction and recovery of shale oil.

This process is especially beneficial because energy efficiency and environmental benefits are significantly increased by the synergisms between the recovery operations. None of the shale oil is combusted in the reducing atmosphere of the hot flue gases; therefore, less expensive rubblization techniques can be used to enhance permeability. Using only air, UCG gas is produced from coals that would otherwise be uneconomical to use. The gas is consumed as it is produced, eliminating the need for steam and oxygen gasification. The low Btu gas is burned in situ, reducing gas processing experiments.

In this process the permeability of a single continuous section of oil shale can be enhanced by conventional techniques such as surface uplift, hydraulic fractures or modified in situ blasting. These techniques, however, do not provide uniform particle sizes or flow distribution. One advantage of the TREE^{sm} concept is that nonuniformities are much less detrimental because indirect retorting is used with a hot reducing flue gas, eliminating oil combustion losses. The advantages of retorting with a reducing gas are retained because the oxidizing front moves much more slowly than the retorting front. As the gases cool from direct contact with oil shale in advance of the retorting zone, the products are swept to production wells for recovery in surface facilities.

Portions of the oil shale in Wyoming, Utah, and Colorado overlie seams of subbituminous coal, and similar occurrences of oil shale with bituminous coals are apparent in the west central Appalachian states. There are also numerous instances of coal mining operations in close geographic proximity to oil shale, tar sand, and heavy oil deposits. Coal mines are abundant along the edges of the major oil shale deposits. Some mining of coal also occurs near the tar sand deposits in Utah and the heavy oil reservoirs in Texas. The locations of oil shale, tar sands, and heavy oils in the United States are shown in Figure 4-1. Coal occurrences are associated with the majority of these areas.

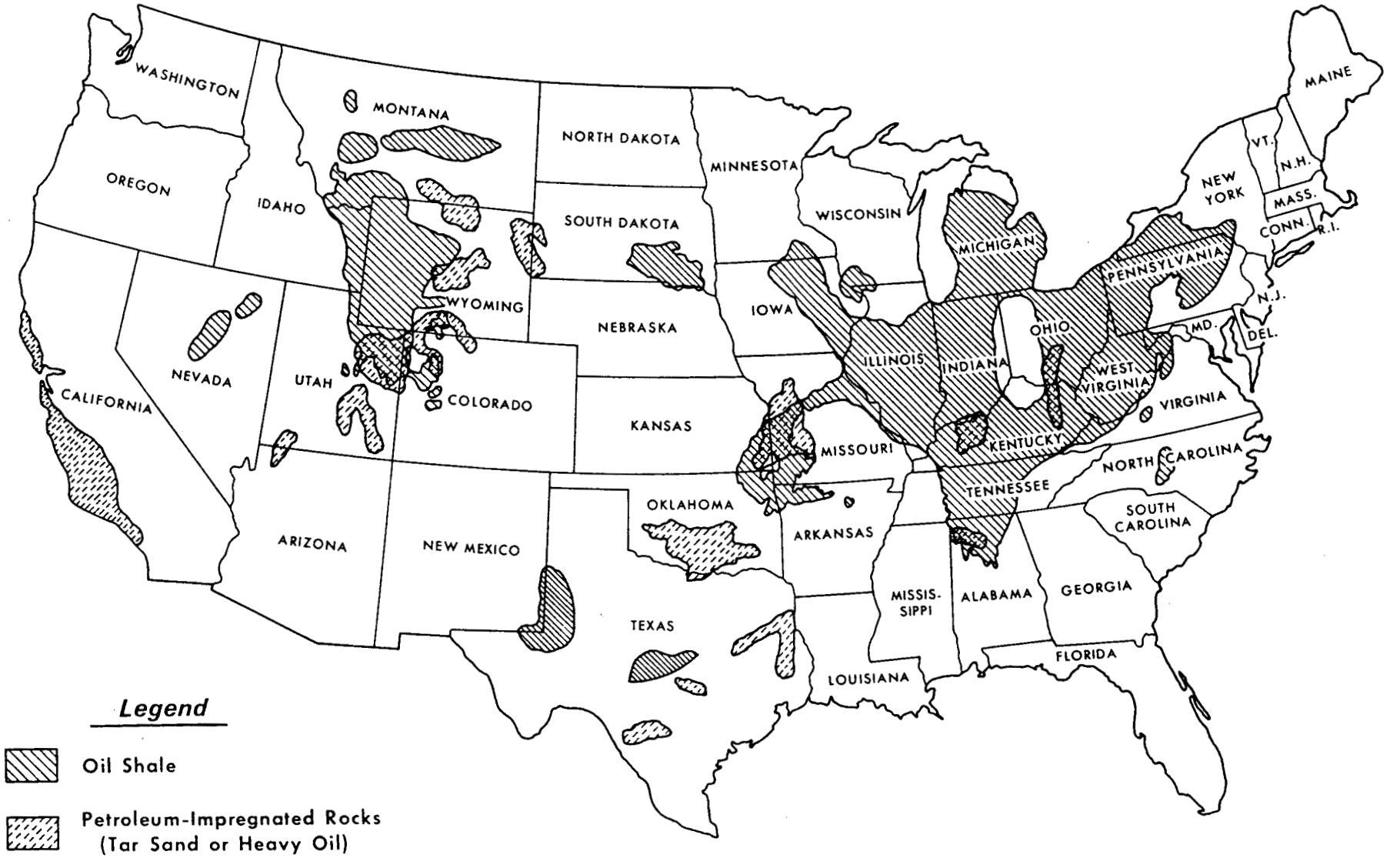

Figure 4-1. Domestic Occurrences of Oil Shale, Tar Sand, and Heavy Oil

Significant joint occurrences of oil shale and coal have been identified at five separate locations in south central and southwestern Wyoming. At each of these locations, greater than 10-meter thicknesses of continuous shale deposits in the Tipton and Laney members of the Green River Formation have average assays of more than 42 liters of oil per ton. Associated coal seams in the Fort Union, Mesa Verde, Niland Tongue, and Wasatch formations underlie the oil shale at depths of less than 3000 feet beneath the surface or exist within 10 miles of the oil shale. The oil shale resources at the five sites in the Green River and Washakie Basins total over 17 billion barrels of oil in place.

Three TREE^{sm} experiments were run to determine the feasibility of the TREE^{sm} process. The objectives of the TREE^{sm} experiments were (1) to estimate the oil yield and coking losses and determine the product quality of shale oil produced by indirect heating with a simulated UCG product gas, (2) to evaluate the effects of sulfur species on the produced oil and the ability of the spent shale to remove sulfur from the produced gas, and (3) to demonstrate laboratory-scale TREE^{sm} processing with coal gasification and oil shale retorting unit operations connected and operating concurrently.

The studies have demonstrated that a gas generated from the combustion of UCG gas is suitable for oil shale retorting. Oil yields range from 65 to 77% of shale Fischer assay. The sulfur contained in the coal gas is absorbed by spent shale most efficiently if the sulfur species are oxidized to sulfur dioxide in the coal gas burner. The oil combustion losses typical of in situ shale combustion are eliminated by TREE^{sm} processing. Coking and cracking losses are not eliminated, but can be minimized. To further develop this research, simulation of coal gas combustion in the presence of nonuniform spent shale and a field demonstration study are suggested.

Solid Fossil and Heavy Oil Reactions. Isothermal and nonisothermal experiments were conducted on solid fossil fuel and heavy oil pairs to determine the effects of coprocessing on conversion. Three solid fossil fuels (eastern reference shale, Asphalt Ridge tar sand, and Wyodak coal) were tested. The heavy oils were SAE-50 nondetergent oil, eastern shale recycle oil from the WRI hot oil process, tar sand recycle oil also from WRI's hot oil process, and pyrene, a purely aromatic "oil." Mixtures (50/50) were reacted isothermally for three different reaction durations at 375°C (707°F). Solid, liquid, gaseous, and solvent extractable products were examined.

Nonisothermal tests were conducted with eastern reference shale and eastern reference shale mixed with SAE-50 oil. Product gas evolution profiles were produced.

Coprocessing enhanced the yields of solvent extracts and liquids from eastern reference shale and Asphalt Ridge tar sand. The best coprocessing oil for the eastern shale was SAE-50 oil, but pyrene was apparently best for converting the more aliphatic tar sand. For coal, the SAE-50 oil speeded conversion but did not increase conversion at a 240-minute reaction time. During the reactions, the extractable materials usually become more aromatic; this is not true for experiments

involving pyrene. The yields of most hydrocarbon gases and hydrogen were higher in coprocessing experiments than in experiments without coprocessing. Carbon monoxide and carbon dioxide yields were less in coprocessing than in experiments without coprocessing.

In nonisothermal experiments, the evolution profiles of ethylene and hydrogen sulfide occurred at a lower temperature when SAE-50 oil was added to eastern reference shale.

This work demonstrates that conversion of solid fossil fuels to gaseous and liquid products is enhanced through coprocessing. However, the type of heavy oil must be carefully selected for the coprocessing of each solid fossil fuel to achieve maximum product yield.

The results of this research are discussed in a report to DOE entitled "Novel Concepts: Low Severity Coprocessing Technology for Improving Fossil Fuel Conversion," September 1987.

Isothermal coprocessing experiments during this year have been conducted on mixtures of Wyodak coal and SAE-50 oil at three temperatures (350°, 375°, and 400°C [662°, 707°, and 752°F]). These experiments were part of an extension of the work done under 4.1.2 of the cooperative agreement extension, DE-FC21-83FE60177. Five tests of differing reaction durations were performed at each of the temperatures. The average material balance for the 15 tests was 98.7 ± 0.8%, indicating that a small amount of material was systematically lost during the experiments. Detailed analyses of the data are under study and will be reported.

4.2 Advanced Mitigation Concepts

The objective of advanced mitigation research is to characterize and measure fossil fuel materials that inhibit new product utilization or complicate environmental controls. It parallels research in advanced extraction technology and exploration. Advanced mitigation research complements the process analysis activity with fundamental studies of fossil energy materials and environments in terms of chemical properties of products as they become available from advanced extraction research.

Subtasks in this research area are impacts of porphyrins, geochemistry of pyrolysis products, and an extension of 1986 advanced instrumentation research to explore methods to characterize heteroatom compounds.

4.2.1 Impact of Porphyrins

The study of the nature of metal complexes in eastern oil shales and the fate of these compounds during extraction supports research in concept development. Information obtained pertains to geochemical, environmental, and processing research.

Oil shales from the eastern U.S. have been suggested as a source of transport fuels together with heavy crudes and tar sand. Substantial quantities of metals are associated with the organic portion of many of

these shales. Detailed knowledge of metal chelates in oil shales is limited, partly because only a small fraction of the organic matter of the shales is soluble in common solvents, and most of the techniques used to concentrate and identify metal chelates require solubility. These metal complexes will affect processing of the shales, particularly hydrotreating. For in situ recovery methods, little is known of the fate of the metal chelates.

The objective of this project is to study metal chelates in certain vanadium-rich Devonian shales. In earlier projects, two overview articles were prepared; "The Influence of Metal Complexes in Fossil Fuels in Industrial Operations" by J. F. Branthaver, and "Application of Metal Complexes in Petroleum to Exploration Geochemistry" by J. F. Branthaver and R. H. Filby. A preceding AER research project produced "Impacts of Porphyrins and Other Metal Chelates on Utilization of Fossil Fuels." This report lays a foundation for research recommendations from which this novel approach to the study of metal complexes has developed

A laboratory procedure, involving strong base extraction, was investigated this year for characterization of metal chelates in a vanadium-rich eastern New Albany shale (Branthaver and Miyake 1987).

Distillation fractions of shale oil obtained by retorting the shale are known to contain porphyrins, but these porphyrin structures may have been modified by thermal treatment. The base extraction procedure does not expose porphyrins to severe thermal stress. It is of interest in exploration geochemistry to compare the exact structure of the porphyrin complexes obtained from the kerogen with those found in the bitumen.

A vanadium-rich New Albany oil shale was extracted with benzene-methanol 3:2 in a Soxhlet extractor to obtain bitumens A. The unextracted shale was decarbonated with 6 N hydrochloric acid to remove carbonate and other soluble minerals. The residual material again was extracted with benzene-methanol 3:2 to obtain bitumens B. The debitumenized-decarbonated shale was treated with 70% hydrofluoric acid to dissolve silica and clay minerals. The residual kerogen-pyrite mixture then was treated with ferric chloride solution to dissolve pyrite. All fractions obtained during the operation of this separation scheme were analyzed for 10 metallic elements.

The debitumenized-decarbonated shale was treated with strong base to solubilize about 20% of residual kerogen. Vanadyl and nickel porphyrins obtained from this procedure and from bitumen A were analyzed by ultraviolet-visible spectrometry and high-resolution mass spectrometry.

The raw New Albany shale also was subjected to Fischer assay. The Fischer assay retorted shale oil and spent shale were analyzed for metallic elements, as were acid leachates from the spent shale.

Large quantities of nickel and vanadyl porphyrins were found in bitumen A, but not bitumen B. Bitumen B is largely inorganic, although soluble in organic solvents after treatment with hydrochloric acid. Porphyrins in bitumen A are of the desoxophylloerythroetioporphyrin

(DPEP) and etio type, both chelated with nickel and vanadium. Bitumen A also appears to contain large amounts of nonporphyrinic nickel and vanadium complexes.

When residual kerogen is solubilized partially by strong base, small amounts of nickel and vanadyl porphyrins are solubilized. These porphyrins are largely of the etio type and are of lower average carbon number than those in bitumen A.

Hydrochloric acid treatment of the New Albany shale removes much of the chromium, manganese, vanadium, and zinc in the shale. Other elements are also readily removed by hydrochloric acid from spent shale obtained by Fischer assay of the shale. The relatively easy solubilization of these strategic and toxic metals must be considered if the shale is to be utilized as a fossil fuel resource.

The procedures employed in this research have provided data that suggest that metals in the shale are bonded to organic species other than porphyrins. Some of these nonporphyrinic compounds probably are metal salts of carboxylic acids. Other, as yet unidentified, metal-organic compounds probably are present. Such compounds probably exist in all fossil fuels. Their identification is important to advanced mitigation studies because of the probable environmental, processing, and geochemical impacts of nonporphyrin metal compounds. These impacts would be expected to differ from those of porphyrins.

4.2.2 Geochemistry of In Situ Pyrolysis Products in the Environment

UCG contaminants have been studied in earlier experiments that served as companion projects to computer and laboratory simulations of contaminant control of in situ thermal extraction processes. First approximations have been made to estimate pollutant production. These research projects will help determine the creation of pyrolysis products from heavy oil, oil shale, and tar sand extraction processes. The evaluation and selection of available geochemical and hydrologic solute transport models and UCG organic contaminants has been reported in "Geochemistry of In Situ Pyrolysis Products in the Environment" by Schreiber et al., in September 1987.

The contaminants produced during in situ thermal extraction of oil shale and tar sand by pyrolysis are under study. The experimental design and schedules for the research are being modified and the computer and laboratory simulation of thermal extraction has been delayed. An organic data base on contaminants generated during in situ extraction of oil shale, tar sands, and coal is being developed so that the reliability of the thermodynamic data base in the model is improved. Microbial transformations are being studied to determine the mobility of model pollutants in natural in situ environments. Laboratory experiments have begun on equilibrium and nonequilibrium adsorption and microbial organic solution chemistry. The research is generic and complementary for these domestic oil, gas, and shale resources.

The development of compatible subroutines in the solute transport model has been significant for laboratory definitions and experimental design that account for organic sorption and microbial removal of contaminants. The generation of organic and inorganic contaminants during in situ thermal extraction processes is known to occur. The types and concentrations of such contaminants have been shown to be functions of the extraction processes employed. Consequently, contaminant control is ultimately dependent on process control, while contaminant remediation is determined by fundamental chemical, physical, and biological processes that modify contaminant concentration and mobility in subsurface environments.

For example, the technical feasibility and commercial potential of UCG are being demonstrated, but the contamination of groundwater both during and after the burn is a major environmental concern. When UCG operations are terminated, thermal energy is stored in the rock and coal ash surrounding the burn cavity, which results in the continued pyrolysis and partial pyrolysis of adjacent coal. The by-products of postburn thermal activities are believed to be one of the major sources of groundwater contamination from UCG.

Efforts to predict the generic behavior of contaminants in groundwater have resulted in the development of numerous geochemical and hydrologic solute transport models. Geochemical models are used to predict the distribution of chemical constituents in a given system and are based on the assumption that important chemical reactions and interactions occur among the solid, aqueous, and gaseous phases. Hydrologic models are used to predict both the flow of water and the mobility of chemical solutes in porous media. Such models rely on the assumption that the physical properties of porous media that influence water flow and solute transport are known, quantifiable, and may be utilized in differential equations to describe chemical mobility.

The primary objective of this research task is to modify existing geochemical and solute transport models in an effort to predict more accurately both the short- and long-term fate of organic contaminants generated in subsurface environments during in situ thermal extraction processes. Contaminant sorption and microbial transformations will be accounted for in the novel subroutines of the transport model.

Several geochemical models were evaluated (WATEQ family, GEOCHEM, MINTEQ, EQ3/6, and PHREEQE) as were three hydrologic solute transport models (BIOPLUME, SWIFT, MAQFLO/MAWUAL). After an exhaustive review of available codes, the EQ3/6 and MAQFLO/MAWUAL models were selected for further development. While initial model development has focused on organic contaminants released during UCG, this research complements other research projects. The principles of contaminant movement as well as the biogeochemical reactions affecting their fate are applicable to other energy-related extraction technologies (e.g., oil shale, tar sands) as well as to other types of groundwater contamination. Interim model development is under way on the formulation and incorporation of compatible subroutines in the solute transport model that will account for organic sorption and microbial removal of contaminants.

4.2.3 Advanced Instrumentation to Identify Heteroatom Compounds in Liquid Products from Advanced Processes

Advanced instrumentation was begun in 1986 with an NMR and GC/MS investigation of the saturate and distillate fractions of the Cerro Negro heavy petroleum crude from the Orinoco oil belt of Venezuela. The overall objectives of this research were to perform fundamental method development through characterization of substitute and new petroleum feedstocks, and to modify existing methods or to develop new methods for the analysis of heavy oils. This research should affect heavy oil processing technology. Conventional methods of petroleum analysis and refinery processing are questionable for an unconventional, biodegraded petroleum like the Cerro Negro petroleum.

The report describing the results of applying nuclear magnetic resonance (NMR) and gas chromatography/mass spectrometric (GC/MS) instrumentation techniques to these fractions to determine the presence of cyclic and acyclic alkanes was prepared by D. A. Netzel and F. D. Guffey in August 1987.

It was concluded from the NMR and GC/MS studies that the Cerro Negro heavy petroleum crude saturate fractions are composed mainly of cycloalkanes with straight carbon chain length and branched alkane substituents. The ASTM mass spectrometric method, D-2786, does not provide an accurate analysis of the normal and branched alkanes but appears to give a reasonably good weight percentage distribution of cycloalkanes when they are compared with NMR average molecular structural parameter calculations.

The presence of normal and branched alkanes in biodegraded petroleum is important. Biodegraded petroleums normally have significantly lower concentrations of acyclic alkanes than do non-biodegraded petroleums. However, previous analyses of two of the saturate hydrocarbon fractions using the ASTM mass spectroscopic method D-2786 determined that these fractions contained significant amounts of acyclic alkanes. Therefore, if the ASTM method is used, the results should be confirmed by other independent methods of analysis to avoid problems of interpretation.

The potential errors that may arise when analyzing unconventional petroleums would stem from the assumptions used in the initial development of the ASTM method D-2786. It was developed for data obtained from more conventional, mid-continent petroleums and to account for various interferences. The off-diagonal matrix elements associated with the mathematical reduction of the mass spectrometric data may not be adequate for unconventional petroleums like the biodegraded Cerro Negro heavy petroleum crude. For this reason, the analysis of an unconventional crude using the standard ASTM method of analyses may not accurately reflect the concentration of hydrocarbon types present. If there is an error in the analysis, it is likely to have an adverse effect on petroleum processing because it will bias the engineering correlations used to determine process operating conditions.

Multinuclear nuclear magnetic resonance spectroscopy is a potential technique that, when fully developed, can be rapid and can provide quantitative results for the most dominant types of heteroatomic functionalities in fossil fuels. It is not always necessary to determine the individual components in fossil fuels to evaluate the characterization of extraction and utilization processes. It is necessary to establish the nature of bonding (the heteroatomic functionality from chemical shift data) and the quantity of the heteroatomic functionality from the integration of the NMR spectrum.

Some preliminary work has been reported recently involving oxygen-17 NMR of coal-derived liquids. However, no one has yet reported any direct nitrogen-15 or sulfur-33 NMR studies for determining the bonding nature and/or quantity of significant heteroatomic functionalities in oil, gas, and coal liquids.

There are several reasons for the lack of direct NMR detection of these nuclei and complex mixtures such as fossil fuel liquids: (1) low isotopic natural abundance, (2) small magnetogyric ratio, (3) line broadening for the quadrupolar nuclei, (4) inadequate instrumentation and methodology, and (5) low weight percentage of heteroatoms in the samples.

Detailed knowledge of the nitrogen fraction(s) will be necessary to provide a comparison of the qualitative and quantitative information obtained from the ^{15}N NMR spectra. To obtain this information, ^{1}H and ^{13}C spectra will be obtained as well as gas chromatography/high-resolution mass spectrometry (GC/HRMS) or stand-alone HRMS. Characterization of the nitrogen fraction(s) using high-resolution mass spectral techniques will be done at WRI using a VG-micromass ZAB-1F high-resolution mass spectrometer.

Initial nitrogen-15 heteronuclear NMR experiments will be performed using the JEOL FX-270 SCM spectrometer at the University of Wyoming. The nitrogen-15 frequency for this spectrometer is 27.36 MHz. For increased sensitivity, the Bruker AM-500 spectrometer at the NMR regional facility located at Colorado State University can also be used.

Once the instrument parameters have been optimized and the different polarization pulse sequences have been evaluated, the natural abundance nitrogen-15 NMR spectra will be obtained for samples of concentrated nitrogen fractions obtained from shale oil.

PUBLICATIONS AND PRESENTATIONS

Papers in Preparation

Boysen, J. E., C. G. Mones, R. R. Glaser, and S. Sullivan. "Physical and Numerical Results for Controlling Groundwater Contaminants Following Shutdown of Underground Coal Gasification Processes," March 1987, DOE report in press.

Branthaver, J. F. "Impacts of Porphyrins and Other Metal Chelates on Utilization of Fossil Fuels," March 1987, DOE report in review.

Branthaver, J. F., and G. Miyake. "Porphyrins and Other Metal Containing Compounds in an Eastern U.S. Oil Shale," September 1987, DOE report in review.

Glaser, R. R., B. C. Sudduth, J. R. Covell, L. J. Fahy, J. D. Schreiber, C. G. Mones, and L. G. Trudell. "In Situ Shale Oil Recovery Using the TREE^{SM} Process," April 1987, DOE report in review.

Netzel, D. A., and F. D. Guffey. "NMR and GC/MS Investigations of the Saturate and Distillation Fractions from the Cerro Negro Heavy Petroleum Crude," August 1987, DOE report in review.

Schreiber, J. D., J. Bowen, K. J. Reddy, R. Wills, and P. J. Colberg. "Geochemistry of In Situ Pyrolysis Products in the Environment," September 1987, DOE report in review.

Turner, T. F., and L. W. Ennen. "Novel Concepts: Low Severity Coprocessing for Improving Fossil Fuel Conversion," September 1987, DOE report in review.

WESTERN RESEARCH INSTITUTE

ANNUAL TECHNICAL PROGRESS REPORT

OCTOBER 1986 - SEPTEMBER 1987

ADVANCED FUELS RESEARCH

5.0 ADVANCED FUELS RESEARCH

TABLE OF CONTENTS

5.0 ADVANCED FUELS RESEARCH

5.1 Development of Fuels from Shale Oil, Tar Sand Oil, Coal Liquids, and Petrochemical By-Products

5.1.1 Jet Fuels from Coal

The Great Plains Gasification Plant, near Beulah, ND, produces three liquid by-products from lignite gasification in addition to its primary product, synthetic natural gas. These products are tar oil, about 3,300 barrels per day (bpd), crude phenols, 900 bpd, and naphtha, 750 bpd. Although these by-product liquids are currently burned to generate process steam, the Department of Energy, which owns the plant, is interested in finding other uses for them that might prove to be more profitable to the plant. This interest is shared by the U.S. Air Force, which regards the by-products as a possible future domestic source of jet fuel for nearby Minot Air Force Base. Fuel for the base, about 2,400 barrels per day of grade JP-4, is currently delivered by truck from Canada.

To explore the jet fuel potential of the by-products, the Department of Energy and the Air Force have cosponsored an investigation at WRI to evaluate them as sources for three grades of military jet fuel--JP-4, JP-8, and a high density JP-8 designated JP-8X. This report describes the by-products, the processing experiments, and summarizes results of work conducted during the past year.

Bulk properties of the by-products (Table 5-1) are specific for the drum samples used in all WRI experiments. All the by-products have significant heteroatom contents and are deficient in hydrogen compared with the target fuel types for which minimum hydrogen contents of 12.5 wt % (JP-8X), 13.5 wt % (JP-8), and 13.6 wt % (JP-4) are specified. This and other elements of fuels specifications are satisfied only by highly stable hydrocarbon fuel mixtures. As a first evaluation, data in Table 5-1 indicate that much hydrogen must be added, and the heteroatoms removed, to transform the by-products into jet fuels.

Some of the more critical elements of the fuel specifications are found in Table 5-2. Typical boiling ranges for JP-4 and JP-8 are 38-293°C (100-560°F) and 110-316°C (230-600°F), respectively, based on ASTM D-2887 (simulated distillation) data obtained at WRI for specification-grade samples provided by Air Force Wright Aeronautical Laboratories. Since JP-8X is in the development stage, its specification values are still tentative, but the target boiling range is about the same as that of JP-8. Aromatics contents are limited to a maximum of 25 vol %, but commercially produced fuels from petroleum usually contain considerably less than this amount in order to exceed minimum hydrogen content requirements. Analysis of the by-products by various chromatographic methods and by mass spectrometry showed that all three are highly aromatic mixtures, as expected for coal-derived liquids.

Table 5-1. Bulk Properties of Liquid By-Products from Great Plains Gasification Project

Properties	Tar Oil REF 86-72A	Crude Phenols REF 86-73A	Naphtha REF 86-74
Specific gravity, 60/60°F	1.018	1.066	0.821
API gravity	7.5	1.2	40.9
Water content, wt %	1.5	5.5	0.3
Distillation (ASTM D-2887)			
IBP, °F	200	233	62
10/20	354/396	341/350	126/161
30/50	423/513	358/382	169/177
70/80	617/686	401/424	221/228
90/95	774/834	476/518	242/276
FBP	930	766	364
Elemental composition, wt % dry basis			
Carbon	83.5	75.5	85.0
Hydrogen	8.6	7.2	9.8
Nitrogen	0.8	0.5	0.2
Sulfur	0.5	0.2	1.8
Oxygen (difference)	6.6	16.6	3.2
[H/C]	1.23	1.14	1.37

Table 5-2. Critical Properties of USAF Turbine Fuels

Property	JP-4[a]	JP-8[a]	Near-Term JP-8X
Specific gravity, 60/60°F	0.710-0.802	0.788-0.845	0.850 min
Hydrogen, wt %	13.6 min	13.5 min	13.0 min
Boiling range, °F (ASTM D-2887)	Report-608	Report-626	Report-626
ΔH_c, net Btu/gal x 10^{-3}	not specified	120.9 min	130 min
Freezing point, °F	-72 max	-58 max	-53 max
Aromatics, vol %	25.0 max	25.0 max	25.0 max
Paraffins, vol %	not specified	not specified	0-10

[a] Specification properties from "Handbook of Aviation Fuel Properties," CRC Report No. 530, Coordinating Research Council, Inc., Atlanta, GA, 1983

Tar oil was shown to contain about 5 wt % tar bases, mostly pyridines, about 10 wt % tar acids, mostly phenol and cresols, up to 10 wt % of other hydroxyaromatics, 60-65 wt % aromatic hydrocarbons, and about 6 wt % saturated hydrocarbons. The saturates are almost entirely made up of n-alkanes with carbon numbers from 11 to 27. The data demonstrate that tar oil is more than 90 wt % aromatics.

The crude phenols by-product, extracted from process water by diisopropyl ether, consists almost entirely of hydroxyaromatics. Analysis by GC/MS showed it contains 78 wt % phenol plus alkylphenols, 18 wt % dihydric phenols/alkyl-substituted dihydric phenols, and about 2 wt % naphthol/alkylnaphthols based on the percentage of total ionization in the mass spectrum. The dihydric phenols include guaiacol (o-methoxyphenol), estimated at 1.5 wt % of the whole product, and 4.3 wt % resorcinol (m-dihydroxybenzene). The three major components are phenol, cresols, and xylenol/ethylphenol estimated at 35 wt %, 30 wt %, and 13 wt %, respectively.

The naphtha by-product is a low-boiling mixture extracted from the syngas with cold methanol by a patented Lurgi process. The product has a high sulfur content and a noxious odor attributed to thiols. Extraction with a caustic solution reduced the sulfur content to less than half its original value. This result indicates the stream contains thiols and demonstrates a relatively simple desulfurization method. As the properties shown in Table 5-1 and the GC/MS analysis indicate, the naphtha is composed of about 90 wt % monoaromatics, 1 wt % nitrogen compounds, 4-5 wt % sulfur compounds, and the balance oxygen compounds. According to data provided by American Natural Gas (operators of the plant), oxygen compounds in the naphtha include methanol, acetone, and methylethylketone. These data indicate that hydrogen processing to remove sulfur, nitrogen, and oxygen compounds could yield a highly aromatic light gasoline component that would be too low-boiling for jet fuel.

The method selected for processing experiments was catalytic hydrogenation, since this is the process most widely used in the petroleum refining industry for heteroatom removal and aromatics saturation. A series of hydrogenation screening experiments were performed on each by-product at conditions that experience had shown to be appropriate for processing heteroaromatic shale oils and highly aromatic petroleum process intermediates.

The catalyst chosen for this work was Shell 424, a nickel-molybdenum tri-lobe type in which the metals are deposited on silica-improved alumina acidified with phosphoric acid. This catalyst was selected because it is a well-known and widely used commercially available catalyst with good resistance to nitrogen deactivation and good saturation activity. The bed was prepared with either 60 cc or 120 cc of catalyst particles in a stainless steel reactor tube, packed in three sections of equal length, separated by about 1 inch of 100-mesh Berkshire sand, each section supported by stainless-steel mesh. Sand was also dispersed in each catalyst section to partially fill interstitial spaces. This packing method was designed to minimize the possibility of channeling and to make the catalyst bed volume sufficient to fill that part of the reactor tube directly heated by the furnace

elements. The reactor tube extending above the top furnace element was packed with 20-mesh inert particles to act as a preheat section. Before each experiment, the catalyst was presulfided with 5% H_2S in hydrogen, pressurized and heated to the starting pressure and temperature. Then hydrogen and liquid were passed downward through the catalyst bed. The liquid feed rate was controlled by a Hruska positive-displacement pump, and hydrogen feed rate was regulated by a mass-flow controller. The reactor tube was enclosed by a copper jacket heated by a four-section clamshell furnace, each section controlled to within ± 0.6°C (± 1°F).

Each experimental series was conducted for one to two weeks of once-through continuous operation with the first 24-36 hours of production discarded. Thereafter, liquid product representing the initial set of operating conditions was collected for analysis. Conditions were then changed, the next 16-20 hours of product discarded, another analytical sample collected, and the sequence was repeated. Analytical samples were washed with cold water to remove ammonia and hydrogen sulfide, dried by stirring in a sealed Pyrex container with anhydrous barium sulfate, and submitted for analysis.

Process intermediates generated in seven experimental series included 9 from whole tar oil, 16 from tar oil distillates, 14 from crude phenols, and 6 from naphtha. Experimental emphasis was placed on tar oil processing, because it represents the largest potential source of jet fuel both in production volume and by boiling range.

Whole tar oil was the feedstock for the first experimental series conducted at a pressure of 2,000 psig, liquid hourly space velocity (LHSV) of 1.0, and hydrogen feed ratio of 6,000 standard cubic feet per barrel (scfb) of liquid feed. Reactor temperatures were 343°C (650°F), 357°C (675°F), and 371°C (700°F). Within 36 hours of the start of operation, hydrogen flow, pump pressure, and reactor back-pressure began to vary unpredictably, indicating plugging of the catalyst bed. This forced termination of the experiment after four days. Analyses of the three process intermediates from this first period of operation showed that their compositions varied widely, demonstrating no consistent change in composition with change in reactor temperature. This indicates that the catalyst system did not reach steady-state conditions.

After the residual carbon was burned off the catalyst in a stream of air, the bed was unpacked by sections. The top of the bed was plugged by fine particulates lodged in the inert zone and in the top of the first catalyst section. These particulates were screened from the coarser particles and submitted for metals analysis by inductively coupled argon plasma (ICAP) scan. A 5-gallon sample of tar oil was passed through a filter cartridge and a sample of the semisolid matter retained in the cartridge was also submitted for ICAP scan. Results of the analyses of these materials are found in Table 5-3.

The most abundant components are silicon, iron, calcium, aluminum, magnesium, sodium, and barium, elements typically found in dirt or coal ash. Arsenic, lead, bismuth, nickel, and strontium were also found in significant quantities. Many of the metals have significance both from the processing and environmental protection viewpoints, since they must

Table 5-3. Metals Found in Great Plains Tar Oil Solids by ICAP Scan (Metals Content in mg/kg)

	Filter Resid. 86-03-4	Reactor Fines 86-03-5
Aluminum	1,800	40,500
Arsenic	<21	1,390
Boron	38.2	112
Barium	640	12,500
Calcium	8,200	86,400
Bismuth	67.3	1,330
Cadmium	75.0	1,490
Cobalt	<2.1	56.5
Chromium	8.9	383
Copper	29.1	824
Sodium	1,720	16,200
Iron	2,860	125,000
Potassium	<1,040	2,260
Lithium	<2.1	64.2
Magnesium	1,850	26,800
Manganese	52.5	506
Molybdenum	<4.2	595
Nickel	11	2,200
Phosphorus	<208	1,750
Lead	206	3,920
Selenium	<21	568
Silicon	32,200	180,000
Strontium	314	4,790
Zinc	87.4	992

be removed from the oil, and concentrated at some point in processing and disposed of. Aside from the demonstrated ability of the particulates to plug a fixed catalyst bed, many of the associated metal components poison catalysts irreversibly and several are recognized environmental hazards.

A second experimental series was conducted with filtered tar oil with somewhat better results. The first and only evidence of plugging occurred near the end of a one-week run. Fine particulate matter was again found at the top of the catalyst bed, demonstrating that some of the inorganic solids could pass a 10-micron filter element. Hydrogen consumption values and properties of intermediates collected at reactor temperatures of 371°C (700°F), 382°C (720°F), and 399°C (750°F) are listed in Table 5-4. The last column in the table represents the calculated average composition of the 79-316°C (175-600°F) jet fuel distillate from each of the intermediates. The data show that most of the heteroatoms were removed, and that aromatic contents are reduced to about 30 wt %. The calculated average composition of the distillate indicates that aromatics would be concentrated to an unacceptably high level in the jet fuel boiling range.

Table 5-4. Properties of Three Hydrogenated[a] Products and a Hypothetical Jet Fuel Distillate from Great Plains Tar Oil, REF 86-72A

Property	Product Number 86-02-1	86-02-2	86-02-3	Average Distillate[b] (175-600°F)
Specific gravity, 60/60°F	0.870	0.865	0.861	
Reactor temp., °F	700	725	750	
Average H_2 consumption, scfb	3,127	2,935	2,895	
Elemental composition, wt % (ppm)				
Carbon	87.1	87.2	86.7	
Hydrogen	12.8	12.5	12.7	
Nitrogen	(20)	(<10)	(<10)	
Sulfur	(<20)	(<20)	(<20)	
Oxygen (difference)	~ 0.1	~ 0.2	~ 0.5	
Distillation (ASTM D-2887), °F				
IBP	155	136	135	175
5%	209	205	193	
10%	227	222	218	
20%	289	284	277	
30%	346	341	334	
50%	435	428	418	
70%	525	518	505	
80%	589	581	568	
90%	683	675	658	
95%	762	752	738	
FBP	885	883	867	600
Compound class by GC/MS, wt %				
Paraffins	29.9	29.7	24.6	17.1
Monocycloalkanes	32.5	26.6	34.1	31.9
Dicycloalkanes	5.4	5.3	7.2	8.0
Total saturates	67.8	61.6	65.9	57.0
Alkylbenzenes	5.7	8.3	8.3	7.9
Indanes/Tetralins	18.7	21.4	15.3	24.7
Naphthalenes	3.4	1.3	2.8	3.0
Dihydrofluorenes	0.7	1.1	0.9	1.0
Fluorenes	0.6	0.8	0.2	0.3
Phenanthrenes/Anthracenes	0.3	0.4	0.4	0.3
Dihydropyrenes	0.1	0.3	0.0	0.2
Fluoranthenes	0.0	0.2	0.3	0.0
Total aromatics	29.5	33.6	28.2	37.4

Table 5-4. Properties of Three Hydrogenated[a] Products and a Hypothetical Jet Fuel Distillate from Great Plains Tar Oil, REF 86-72A (continued)

Property	Product Number 86-02-1	86-02-2	86-02-3	Average Distillate (175-600°F)[b]
Phenols	ND[c]	0.7	ND	0.2
Naphthols	2.7	4.1	5.9	5.4
Wt % of product	100	100	100	75.2

[a] Shell 424 Catalyst, 2,000 psig, 1.0 LHSV, H_2 feed rate 6,000 scfb

[b] Calculated composition of a blend of 175-600°F true boiling point distillates prepared by blending equal volumes of distillate from 86-02-1, 86-02-2, and 86-02-3

[c] Not detected

Based on tar oil composition data, the calculated chemical hydrogen requirement to remove all heteroatoms and to reduce aromatics content to 30 wt % is about 2,700 scfb. The calculation assumes that only heteroatom-containing rings are opened and that no other carbon-carbon bond cleavage occurs. However, the high paraffin values for the intermediates, ranging from 25 to 30 wt %, contrasted with only 6 wt % in the feedstock, is indirect evidence that other rings must have opened, increasing hydrogen consumption. The measured hydrogen consumption values also include hydrogen lost in solution in the liquid products. For these reasons, the measured values are expectedly higher than the calculated value, indicating that measured hydrogen consumption values are reasonable.

Experiments with whole tar oil demonstrated processing difficulties caused by inorganic particulate matter and indicated high hydrogen consumption (above 3,000 scfb) would be necessary to yield an acceptable jet fuel intermediate. All further tar oil experiments were conducted with tar oil distillates.

Tar oil was distilled in a continuous-feed flash distillation unit to reject the particulates in a high-boiling residue. The distillate was collected in two fractions--a light distillate boiling from the initial boiling point (IBP) to 233°C (IBP-450°F) and a heavy distillate boiling from 233-399°C (450-750°F). The light distillate was collected at 585 torr, which is Laramie atmospheric pressure. The heavy distillate was collected at 10 torr. A total of 93.4 liters of tar oil was fed to the first-pass distillation, which yielded 25 liters of light distillate. The second pass yielded 51.5 liters of heavy distillate. The residue totaled 16 wt % of the initial charge, and 3 wt % of the charge was lost by evaporation and handling. The light distillate was extracted three times with 12-liter portions of 30% sodium hydroxide

solution, and the raffinate was washed with water to remove residual caustic. A portion of the raffinate was mixed with twice its volume of heavy distillate to form a partially upgraded blend. Both the heavy distillate and the raffinate-distillate blend were used as feedstocks for further hydrogenation experiments.

The rationale for these experiments was based on two alternative refining schemes. One scheme anticipated that the light distillate, containing most of the monohydric phenols from tar oil, could be allocated with the crude phenols to cresylic acids production, leaving only the heavy tar oil distillate for jet fuels production. The second scheme anticipated that phenols might be extracted from the light distillate, and the extract diverted to cresylic acids production. This scheme would permit reblending of the raffinate with heavy distillate to form a hydrogenation feedstock that should be lighter in gravity and lower in oxygen content than either the original tar oil or the heavy distillate. Table 5-5 lists selected properties of the tar oil, the distillates, and the caustic-extracted distillate blend for comparison. The data show that oxygen compounds are more concentrated in the light distillate, and that the caustic extracted blend is substantially lower in oxygen content and lighter in gravity than either the heavy distillate or the tar oil. It was predicted that this partial upgrading should make the blend more amenable to hydrogenation.

Table 5-5. Characteristics of Tar Oil, Flash Distillates, and Raffinate-Distillate Blend

Property	REF 86-72A Tar Oil	87-08-3 IBP-450°F	87-08-4 450-750°F	87-08-9 Dist. Blend
Specific gravity, 60/60°F	1.018	0.953	1.028	0.982
Carbon	83.5	80.6	81.7	84.2
Hydrogen	8.6	9.2	8.3	9.0
Nitrogen	0.8	0.6	0.7	0.7
Sulfur	0.5	0.5	0.6	0.6
Oxygen (difference)	6.6	9.1	8.7	5.5
Distillation (ASTM D-2887)				
IBP	200	171	278	223
5/10	318/354	235/284	368/397	294/342
20/30	396/423	337/364	438/483	395/422
40/50	469/513	384/401	522/577	459/497
60/70	559/617	412/432	597/644	534/583
80/90	686/774	458/506	695/762	647/731
95	834	543	813	791
FBP	930	674	908	908
Vol % of tar oil	100	27	55	74

Hydrogenation of the heavy distillate at 2,000 psig, LHSV 0.5 and 1.0, hydrogenation feed ratio of 6,000 scfb, and at temperatures from 316-371°C (600-700°F) showed that the distillate was even more resistant to saturation than the tar oil. At LHSV = 1.0, oxygen was still present in measurable quantities in intermediates produced at reactor temperatures below 371°C (700°F). At 0.5 space velocity, equivalent to longer reactor residence times, intermediates produced at temperatures lower than 357°C (675°F) contained oxygen at concentrations of 0.8 wt % or higher and more than 700 ppm nitrogen. Hydrogenation process data and properties for the two best products are found in Table 5-6.

Both products contain less than 13 wt % hydrogen, more than 60 wt % aromatics, and measurable amounts of residual naphthalenes and fluorenes. However, no plugging problems or evidence of erratic flow were encountered in two weeks of continuous operation. Some evidence of sustained catalyst activity was provided by comparing the characteristics of the product collected at 343°C (650°F) and LHSV = 1.0 after 42 hours on stream with those of a product collected under identical conditions after 200 hours on stream. Product densities, elemental compositions, and boiling range characteristics of the products are identical within the limits of analytical error. This smooth, reproducible hydrogenation behavior indicates that steady-state operation and sustained catalyst activity were achieved, probably as a consequence of removing particulates and high-boiling components from the feedstock. However, data in Table 5-6 demonstrate that the products were not sufficiently hydrogenated to serve as intermediates for jet fuel production.

Hydrogenation of the raffinate-distillate blend yielded a more promising set of products and led to preparation of JP-8 and JP-8X test-fuel distillates. The catalyst volume for the experimental series was 120 cc, and intermediate products were collected in a continuous 2-week run at two sets of conditions. For the first set, conditions were LHSV = 0.5, hydrogen feed ratio 10,750 scfb with products collected at 357°C (675°F), 371°C (700°F), and 382°C (720°F). For the second set, conditions were LHSV = 0.33, hydrogen feed ratio was increased to 16,000 scfb, and products were collected at 311°C (700°F) and 399°C (750°F). These were the most severe conditions employed, aimed at achieving at least 13 wt % hydrogen in the products and at reducing aromatic contents to 30 wt % or less. The principal objective was to make sufficient intermediate products of acceptable quality that could yield up to a gallon of either JP-8 or JP-8X distillate meeting the critical elements of the applicable specification. Hydrogenation conditions, hydrogen consumption values, and product characteristics are listed for the best four products in Table 5-7 (two pages).

Oxygen was not detectable in the products, nitrogen and sulfur contents were found to be less than 30 ppm, and the intermediates represent the highest level of saturation achieved with tar oil feedstock. Residual naphthalenes and indanes/tetralins are at acceptably low levels in three products. The comparatively high levels of dicycloalkanes appeared to offer good prospects for obtaining a high density jet fuel from the right blend of these products, although the paraffin contents are considerably higher than the JP-8X specification

Table 5-6. Hydrogenation of Tar Oil Heavy Distillate, 123-87-87-08-4, on Shell 424 Catalyst

	Product Number	
	123-93-87-09-7	123-93-87-09-9
Hydrogenation Conditions		
Pressure, psig	2,000	2,000
LHSV	1.0	0.5
Temperature, °F	700	675
Hydrogen feed, scfb	6,000	6,000
Time on stream, hr	80	245
Hydrogen Consumption, scfb	3,032	3,131
Product Characteristics		
Specific gravity, 60/60°F	0.865	0.865
Elemental composition, wt % (ppm)		
Carbon	87.4	87.2
Hydrogen	12.7	12.9
Nitrogen	<25	<35
Sulfur	<35	<25
Distillation (ASTM D-2887)		
IBP/5	133/210	164/213
10/20	249/329	264/346
30/40	462/499	392/436
50/60	535/587	472/504
70/80	663/740	541/592
90/95	735/790	670/747
FBP	864	866
Hydrocarbon Class, wt %		
Paraffins	7.7	8.8
Monocycloalkanes	10.7	14.2
Dicycloalkanes	8.8	12.9
Tricycloalkanes	1.2	2.5
Total saturates	28.4	38.4
Alkylbenzenes	13.5	10.3
Indanes/Tetralins	56.2	50.6
Naphthalenes	1.3	0.6
Fluorenes	0.5	0.1
Anthracenes/Phenanthrenes	0.1	0.0
Total aromatics	71.6	61.6

Table 5-7. Hydrogenation of Caustic-Extracted Distilled Tar Tar Oil on Shell 424 Ni-Mo Catalyst at 2,000 psig

	Product Number	
	367-8-87-11-3	367-8-87-11-5
Reactor temperature, °F	700	720
LHSV, V_o/V_c/hr	0.5	0.5
H_2 feed ratio, scfb	10,750	10,750
H_2 consumption, scfb	3,250	3,468
Product Characteristics		
Specific gravity, 60/60°F	0.837	0.834
Hydrogen, wt %	13.4	13.5
Paraffins, wt %	20.8	23.1
Monocycloalkanes	17.4	17.1
Dicycloalkanes	29.0	27.6
Tricycloalkanes	2.0	2.0
Total saturates	69.2	69.8
Alkylbenzenes	18.1	17.1
Indanes/Tetralins	12.7	13.1
Naphthalenes	0.1	trace
Total aromatics	30.8	30.2
Distillation (ASTM D-2887)		
IBP, °F	141	130
5/10	209/240	207/238
20/30	299/347	296/346
40/50	373/400	372/399
60/70	439/478	436/475
80/90	523/603	521/601
95	683	680
FBP	844	843

Table 5-7. Hydrogenation of Caustic-Extracted Distilled Tar Oil on Shell 424 Ni-Mo Catalyst at 2,000 psig (continued)

	Product Number	
	367-8-87-11-6	367-8-87-11-7
Reactor temperature, °F	700	750
LHSV, V_O/V_C/hr	0.33	0.33
H_2 feed ratio, scfb	16,000	16,000
H_2 consumption, scfb	3,533	3,780
Product Characteristics		
Specific gravity, 60/60°F	0.839	0.829
Hydrogen, wt %	13.4	13.7
Paraffins, wt %	21.7	21.6
Monocycloalkanes	16.1	27.5
Dicycloalkanes	31.1	30.5
Tricycloalkanes	2.3	1.9
Total saturates, wt %	71.2	81.5
Alkylbenzenes, wt %	17.0	9.3
Indanes/Tetralins	11.8	8.8
Naphthalenes	0	0.1
Fluorenes	0	0.0
Total aromatics, wt %	30.5	18.5
Distillation (ASTM D-2887)		
IBP, °F	153	131
5/10	211/248	205/233
20/30	307/351	287/337
40/50	377/406	364/391
60/70	445/484	422/462
80/90	530/611	508/581
95	693	657
FBP	847	827

permits. After calculating the hydrocarbon composition of the 110-316°C (230-600°F) distillate from each product, two products were blended in the proportions that would yield a distillate with minimum paraffin content and with about 24 wt % aromatic content. This blend was composed of product 367-8-87-11-7 and product 367-8-87-11-3.

An 8-liter blend was distilled in a distillation unit equipped with a 5 1/2-ft column packed with stainless steel Helipak. A fraction boiling from 110-316°C (230-600°F) at 760 torr was collected, a boiling

range corresponding to the measured true boiling range of a specification grade JP-8 sample. Distillate yield was 6,130 mL (76.6 vol %). Measured and calculated properties of the distillate, which are in good agreement, are found in Table 5-8. The product failed to meet the minimum density requirement or the maximum paraffin requirement for JP-8X, but apparently meets the critical specification requirements for conventional JP-8.

Table 5-8. Measured and Calculated Properties of 230-600°F Distillate from Hydrogenated Blend (23 vol % 367-8-87-11-4, 77 vol % 367-8-87-11-7)

	Measured	Calculated
Bulk Properties		
Specific gravity, 60/60°F	0.838	--
Hydrogen, wt %	13.6	13.4
Freezing point, °F	-60	--
Flash point, °F	102	--
Viscosity at -4°F, cSt	4.11	--
Hydrocarbon Composition		
Paraffins, wt %	20.5	21.1
Monocycloalkanes	15.7	15.2
Dicycloalkanes	38.2	37.4
Tricycloalkanes	2.7	2.3
Total saturates, wt %	77.1	76.0
Alkylbenzenes, wt %	12.2	13.0
Indanes/Tetralins	10.8	11.0
Total aromatics, wt %	23.0	24.0
Distillation (ASTM D-2887)		
IBP, °F	228	
5/10	255/274	
20/30	316/350	
40/50	367/388	
60/70	411/441	
80/90	472/508	
95	531	
FBP	563	
Yield, wt % of charge	82	86
Yield, vol % of charge	77	--

A second attempt was made to prepare JP-8X by reducing the distillate boiling range to 149-316°C (300-600°F), and increasing the aromatics content to 30 vol %. Calculated compositions for 149-316°C (300-600°F) distillates from the intermediates showed that product 367-8-87-11-6 could yield a distillate containing slightly over 30 wt % aromatics, corresponding to slightly less than 30 vol %. A 928-mL charge of the designated product was distilled as previously described. Measured and calculated properties of the distillate are recorded in Table 5-9. The calculated values predict the overall contents of saturates and aromatics quite well, but there are substantial differences in the calculated and measured values for paraffins and dicycloalkanes. In fact, because of the high content of dicycloalkanes the measured composition is somewhat better for a high-density fuel than the predicted composition. The distillate meets the critical target properties for JP-8X except for freezing point, which is much higher than the specified maximum. The high value for freezing point is unexpected, because of the comparatively low paraffin content. We attribute this to the presence of high-boiling n-paraffins in combination with relatively low concentrations of monocycloalkanes and alkylbenzenes needed to keep n-alkanes in solution at low temperature. The higher initial boiling point of this distillate excludes much of the monocyclics in the intermediate.

The crude phenols by-product was hydrogenated in two experimental series conducted in the same fashion as described for tar oil hydrogenation, but at somewhat lower temperatures. In one experimental series, conditions were 2,000 psig, LHSV = 1.0, hydrogen feed ratio 6,000 scfb, and products were collected at 260°C (500°F), at 288-330°C (550-625°F) in 14°C (25°F) increments, and at 310°C (590°F). In a second series at the same pressure and hydrogen feed ratio, LHSV was reduced to 0.5 and products were collected at 288°C (550°F), 302°C (575°F), and 316°C (600°F). The objective of these experiments was to find the least severe conditions sufficient to eliminate oxygen. Of the 14 intermediates collected, only the 4 produced at 316°C (600°F) or higher contained no detectable oxygen. Hydrogenation conditions, hydrogen consumption values, and properties of these four products are found in Table 5-10. Hydrogen consumption values are all in excess of 4,300 scfb, a value unthinkably high in petroleum processing. The total liquid products drained from the receiver contained 20 vol % or more water. The dried products represented in the table contain over 90 vol % hydrocarbons boiling in the gasoline range, mainly cyclohexanes and paraffins. The experiments indicate that the crude phenols could make a minor contribution to JP-4 production, but at a very high investment in hydrogen, much of which is lost to water.

The naphtha by-product was hydrogenated in a single experimental series over a 60-cc catalyst bed. Conditions were 500 psig, LHSV = 1.0, and hydrogen feed ratio 1,500 scfb. Products were collected at temperatures varying from 149-260°C (300-500°F) in 27.8°C (50°F) increments. Hydrogenation conditions, hydrogen consumption values, and product characteristics for three products are found in Table 5-11. The products are equivalent to a light gasoline component composed of cyclohexanes and a mixture of benzene and alkylbenzenes. The experiment demonstrates that the by-product is easily desulfurized to a highly

Table 5-9. Measured and Calculated Properties of 300-600°F Distillate from Hydrogenated Product, 367-8-87-11-6

	Measured	Calculated
Bulk Properties		
Specific gravity, 60/60°F	0.856	--
Hydrogen content, wt %	13.3	--
Freezing point, °F	-22	--
Viscosity at -4°F, cSt	7.36	--
Hydrocarbon Composition		
Paraffins, wt %	6.3	15.3
Monocycloalkanes	7.9	8.4
Dicycloalkanes	46.8	41.0
Tricycloalkanes	5.3	3.0
Total saturates, wt %	66.3	67.7
Alkylbenzenes, wt %	15.3	16.6
Indanes/Tetralins	18.4	15.6
Total aromatics, wt %	33.7	32.3
Distillation (ASTM D-2887)		
IBP, °F	296	
5/10	325/343	
20/30	365/387	
40/50	407/436	
60/70	467/498	
80/90	533/583	
95	599	
FBP	620	
Yield, wt % of charge	76.9	75.7
Yield, vol % of charge	75.4	--

Table 5-10. Hydrogenation of Crude Phenols and Properties of Products

	Sample Number			
	87-07-5	87-06-1	87-07-8	87-06-3
Hydrogenation Conditions				
Pressure, psig	2,000	2,000	2,000	2,000
Temperature, °F	600	600	625	650
LHSV, V_O/V_C/hr	0.5	1.0	1.0	1.0
H_2 feed rate, scfb	6,000	6,000	6,000	6,000
H_2 consumption, scfb	4,983	4,411	4,335	4,352
Specific gravity, 60/60°F	0.793	0.803	0.797	0.800
Elemental composition, wt % (ppm)				
Carbon	85.7	86.2	85.7	86.7
Hydrogen	14.2	13.8	13.9	13.8
Nitrogen	(<25)	(<25)	(<25)	(<25)
Sulfur	(37)	(120)	(35)	(<25)
Distillation (ASTM D-2887)				
IBP	138	135	129	136
5%	165	165	164	165
10%	172	169	170	170
20%	180	179	179	179
30%	195	188	190	187
50%	216	216	216	215
70%	259	257	254	248
80%	289	287	279	276
90%	397	404	368	380
95%	472	490	449	456
FBP	704	771	642	685
Hydrocarbon class, wt %				
Paraffins	13.4	11.0	14.5	11.2
Monocycloalkanes	84.8	80.6	79.8	80.9
Dicycloalkanes	0.1	0.2	0.2	0.2
Tricycloalkanes	0	0	0	0
Total saturates	98.3	91.8	94.5	92.3
Alkylbenzenes	1.5	5.4	4.9	6.7
Indanes/Tetralins	0.2	2.8	0.6	1.0
Naphthalenes	0	0	0	0
Fluorenes	0	0.1	Trace	0
Total aromatics	1.7	8.3	5.5	7.7

Table 5-11. Hydrogenation of Naphtha and Product Composition--Shell 424 Ni-Mo Catalyst, 500 psig, LHSV 1.0, Hydrogen Feed Ratio 1,500 scfb

	Sample Number		
	123-106-87-10-2	123-106-87-10-4	123-106-87-10-6
Hydrogenation Conditions			
Pressure, psig	500	500	500
Temperature, °F	400	450	500
LHSV, V_O/V_C/hr	1.0	1.0	1.0
H_2 feed rate, scfb	1,500	1,500	1,500
H_2 consumption, scfb	273	431	665
Product Properties			
Specific gravity, 60/60°F	0.826	0.816	0.806
Elemental Composition, wt % (ppm)			
Carbon	89.9	89.8	89.5
Hydrogen	9.8	10.1	10.3
Nitrogen	(872)	(114)	(26)
Sulfur	(1,271)	(875)	(551)
Oxygen (difference)	<0.1	<0.1	<0.1
Hydrocarbon Composition, wt %			
Monocycloalkanes	--	--	58.4
Benzene/Alkylbenzenes	--	--	41.6
Distillation (ASTM-D2887)			
IBP	74	67	66
5/10	126/156	106/137	91/121
20/30	168/176	164/172	161/169
40/50	186/210	181/195	178/188
60/70	225/231	221/228	214/227
80/90	252/283	237/276	233/273
95	341	302	287
FBP	725	641	597

aromatic gasoline-blending component. However, the low volume of naphtha production and the low boiling range of the hydrogenated products indicate that the naphtha would make no significant contribution to jet fuel production.

In summary, only the tar oil could serve as a significant source of jet fuels. Calculated compositions for distillates boiling in the JP-4 range, IBP-305°C (IBP-580°F), from the most highly hydrogenated tar-oil products (Table 5-7) indicate that one product, 367-8-87-11-7, could have yielded a JP-4 distillate containing less than 19 wt % aromatics. This intermediate product represented a hydrogen consumption level of almost 3,800 standard cubic feet per barrel of distillate feedstock. This is an extremely high hydrogen requirement for jet fuel production compared with jet fuel production from natural petroleum. Neither the crude phenols or the naphtha are desirable sources for jet fuels production.

PUBLICATIONS AND PRESENTATIONS

Presentations

Smith, E. B., F. D. Guffey, and S. A. Holmes. "Silk Purse from Sow's Ear--Engine Fuels from Lurgi Liquids?," presented at Confab '87, Silver Creek, CO, July 28-31, 1987.

Guffey, F. D., S. A. Holmes, and E. B. Smith. "Evaluation of Process Streams from Gasification of Lignite--An Insight to Production of Aviation Turbine Fuels," presented at Confab '87, Silver Creek, CO, July 28-31, 1987.

☆U.S. GOVERNMENT PRINTING OFFICE: 1988-548-122/60042